

POLITECNICO DI MILANO
SCUOLA DI INGEGNERIA INDUSTRIALE E DELL'INFORMAZIONE
Master of Science in Mechanical Engineering



**Development of a device for the
characterization of scissors' cutting
efficiency**

Advisor: Prof. Marco **Tarabini**

Master thesis of:
Davide **Magnani** Matr. 852757

ACADEMIC YEAR 2016-2017

Ringraziamenti

In primis vorrei ringraziare il professori Marco Tarabini per avermi proposto questo progetto e per la sua guida ed il suo sostegno durante questi mesi. Un sentito ringraziamento va anche a Riccardo Ercoli, con cui ho condiviso una parte del lavoro.

Vorrei poi dedicare questo lavoro a tutti coloro che mi hanno accompagnato e supportato, non solo durante il lavoro di tesi, bensí per tutta la durata dei miei faticosi studi universitari, partendo dai miei adorati genitori e mia sorella, primi a gioire con me nei momenti felici o a consolarmi nei momenti tristi. Passando per i miei nonni che, ciascuno a modo suo, non hanno mai fatto mancare il loro amore e la loro fiducia nei miei confronti. Poi i miei cugini, che considero come fratelli, e zii, sempre pronti a darmi i giusti consigli.

Vorrei anche ringraziare Lorenzo, mio piú caro amico che mi ha aiutato agguinzando momenti di leggerezza ai miei anni universitari. I miei colleghi universitari Nicola, compagno sopravvissuto, Alberto, Marco, Alessandro, Matteo e tanti altri senza cui difficilmente sarei arrivato in fondo.

Un ringraziamento va anche ai ragazzi del laboratorio di Lecco con cui ho condiviso gli ultimi mesi di lavoro.

Infine la dedica che piú mi commuove va a mio nonno Piero, che non potrà leggere questi ringraziamenti, ma che spero di aver reso fiero.

Abstract

In this thesis the design of an automatic machine able to test scissors of different dimension and geometries is performed. This design is then validated with an experimental campaign consisting of more than 125000 cuts. The core of the project is the design of both hardware and software of the functional group able to move the scissors.

The complete machine is later obtained by designing additional functional groups that improve the accuracy of the system or increase the detectable parameters.

In order to develop the project, an introductive critical overview of existing machines with the aim of testing scissor and, more generally, cutting tools is done, so that possible improvements and considerations are consistent with the state of the art. From the literature review, also an analysis of factors that may influence the test is done, exploiting the similarities between the different cutting tools. The influence of these parameters is verified in the experimental phase of the project.

Sommario

Obiettivo di questa tesi è la progettazione di una macchina automatica in grado di testare forbici di varie dimensioni e forme. Il prototipo realizzato viene poi validato tramite una campagna sperimentale per cui sono stati effettuati più di 125000 tagli.

Punto focale del progetto è la progettazione del gruppo funzionale atto a muovere le forbici, sia dal punto di vista fisico che da quello di controllo.

L'intero prototipo viene poi completato con l'aggiunta di ulteriori gruppi funzionali volti ad aumentare l'accuratezza del sistema o ad aggiungere ulteriori grandezze misurabili.

Lo sviluppo del progetto viene introdotto da un'analisi critica delle macchine esistenti che sono in grado di testare forbici e, più in generale, strumenti di taglio, di modo che possibili miglioramenti e considerazioni siano consistenti con lo stato dell'arte. Dall'analisi della letteratura vengono anche analizzati parametri di processo che possano influenzare le prove, sfruttando le similitudini tra coltelli e forbici. L'influenza di questi parametri sarà poi verificata nella parte sperimentale del progetto.

Contents

Acknowledgment	2
Abstract	3
Compendio	4
1 Introduction and state of the art	17
1.1 Nature of the problem	17
1.2 ISO 8442-5 and knife testing	18
1.2.1 Testing machines for knives	25
1.3 Testing machines for scissors	26
1.3.1 Analysis of CATRA machine	28
1.3.2 Analysis of PREMAX union testing machine	31
1.4 Literature review	42
1.5 Aim of the project	48
1.6 Scheme of the thesis	48
2 Scissors actuation functional group	49
2.1 Hardware development	49
2.1.1 Overview of the solution	50
2.1.2 Motor-reducer unit selection	52
2.1.3 Main support of the group	60
2.1.4 Torque-meter	62
2.1.5 Beam couplings	65
2.1.6 Ball bearings	66
2.1.7 Oldham coupling	67
2.1.8 Electrical connection	68

2.1.9	Initial positioning sytem	71
2.2	Software development	72
2.2.1	EPOS Studio	72
2.2.2	LabView	77
3	Material feeding functional group	83
3.1	Hardware development	83
3.1.1	Overview of the solution	83
3.1.2	Electric motor	84
3.1.3	Electric connection	87
3.1.4	Final designs	88
3.2	Software development	89
4	Improvements and additional functional groups	91
4.1	Improved material feeding functional group	91
4.2	Tear cut functional group	93
4.3	Hand pressure functional group	94
5	Experimental results	97
5.1	Analysis software development	97
5.1.1	Loading of the data	98
5.1.2	Analysis and plot of the results	101
5.2	Characterizing parameters	102
5.3	Repeatability and reproducibility	103
5.3.1	Repeatability of consecutive cuts	103
5.3.2	Repeatability of consecutive cuts with re-positioning	108
5.4	Influence of process parameters on the cutting torque	112
5.4.1	Influence of pre-tensioning of the material	112
5.4.2	Velocity influence	116
5.4.3	Influence of the resistance of the cut material	118
5.4.4	Influece of nicks on the blade	120
5.4.5	Wear of the scissors, test on cloth	122
5.4.6	Wear of the scissors, test alternated blank/cloth cuts	123
6	Conclusion	131
6.1	Recap of the work	131
6.2	Future development	133

Bibliography	135
AppendixA	139
AppendixB	149

List of Figures

1.1	Cross section of the blade with the centre line	19
1.2	Definition of deviation from straight of a blade along the stroke length	20
1.3	Schematic arrangement of suitable test apparatus	23
1.4	Typical performance of a knife on test	24
1.5	Machine for field measurement of knife sharpness	25
1.6	Newell and Scott Vogel machine	27
1.7	Scissors cutting performance test machine, CATRA	29
1.8	Clamping of the scissors	29
1.9	Mechanism transmitting the force	30
1.10	PREMAX union machine	31
1.11	Scissors clamping and actuation mechanism	32
1.12	Mechanical jig for initial positioning	33
1.13	Tear closure mechanism	33
1.14	Cloth holder	34
1.15	Switch controlling the electric motor	34
1.16	Tensioning pneumatic actuators	35
1.17	Representation of the mechanism moving the cloth	36
1.18	Example of limits of acceptability	38
1.19	Two not compliant tests, force against actuator displacement	40
1.20	Not compliant test, derivative of the force against actuator displacement	41
1.21	Two compliant tests, force against actuator displacement . .	41
1.22	Compliant tests, derivative of the force against actuator dis- placement	42
1.23	Edge radius and edge angle	44

1.24	Effect of edge roundness on cut energy	45
1.25	Effect of nicks on the force history	46
1.26	Dulling behavior for different number of passages	47
1.27	Effect of pre-tension on the cut yarn	47
2.1	CAD model of the scissors actuation functional group	50
2.2	CAD model of the scissors actuation functional group, detail	51
2.3	First attempt motion law	54
2.4	Static friction evaluation	55
2.5	α vs β for the final selected motor	57
2.6	Range of τ admissible and final selected transmission	58
2.7	Check 1, maximum torque supplied	59
2.8	Harshest motion law	60
2.9	Main support of the actuating functional group	61
2.10	Torque-meter calibration, set up	63
2.11	Torque-meter calibration, linear regression	64
2.12	Model of the arm	64
2.13	Helical coupling	65
2.14	Mounting scheme of the ball bearings	67
2.15	Oldham coupling	68
2.16	Wiring of the system	69
2.17	Torque-meter specification	70
2.18	Scout 55 specification	70
2.19	Initial positioning system for the scissors actuation functional group	72
2.20	Responses of the system to different gain values	75
2.21	Front panel	77
2.22	User interface of DESIGN MOTION LAW	78
2.23	Window that opens the communication with the board	79
2.24	Pausing program for the installation of the cloth	81
3.1	Overview of the functional group	84
3.2	Influence of the thickness of the rolled cloth on the advancement	85
3.3	Electric motor calibration	86
3.4	Electric connection of the material feeding functional group .	87
3.5	Final design of the material feeding functional group	88

4.1	Layout of the improved material feeding functional group . . .	92
4.2	Layout of the tear cut functional group	93
4.3	Layout of the hand pressure functional group	94
5.1	Step in the position due to a problem in the test, the software still finds the start of the operations correctly	99
5.2	Example of search of the opening and closing cycle	100
5.3	Example of superimposed torques as function of the scissors' angle	101
5.4	Example of characterizing parameters	102
5.5	Test 1, RMS(T) with motor unwinding	104
5.6	Test 1, RMS(T) with hand unwinding	105
5.7	Test 1, RMS(T) boxplot comparison	105
5.8	Test 2, RMS(T) with hand unwinding	106
5.9	Test 2, RMS(T) with motor unwinding	107
5.10	Test 2, RMS(T) boxplot comparison	107
5.11	Test 1, RMS(T) boxplot comparison	109
5.12	Test 2, RMS(T) boxplot comparison	111
5.13	Set-up used to analyze the pre-tensioning influence	112
5.14	Test 1, influence of the pre-tensioning	114
5.15	Test 2, influence of the pre-tensioning	114
5.16	Test 3, influence of the pre-tensioning	115
5.17	Test 4, test with higher pre-load	115
5.18	Test 1, influence of the velocity	117
5.19	Test 2, influence of the velocity	117
5.20	Test 1, influence of the resistance of the cut material	119
5.21	Test 2, influence of the resistance of the cut material	119
5.22	Nicked blade	120
5.23	Effect of a nick on the blade	121
5.24	Effect of a nick on more than two cuts	121
5.25	Test fully on cloth	122
5.26	Test 1, type of closure alternated	124
5.27	Loosening of the screw during the wear test	125
5.28	Ring lock system	126
5.29	Test 2, type of closure alternated	127
5.30	Variation of the surface of the blade during the test	127

5.31 Test 3, type of closure alternated	129
5.32 Test 4, type of closure alternated	129

List of Tables

1.1	Cutting test parameters	20
1.2	Performance level	21
1.3	Composition of the silica abrasive	21
1.4	Grain size distribution of silica, C 400	21
2.1	Motion law parameters	52
2.2	Symbols used	53
2.3	Motor catalogue parameters, values of the selected one	55
2.4	Speed reducer catalogue parameters, values of the selected one	56
2.5	Calibration parameters	63
2.6	Linear regression statistical analysis	65
2.7	Linear regression statistical analysis	66
2.8	Electrical connection specifications	69
2.9	Scout 55 parameters	71
2.10	Motor-encoder parameters	73
2.11	Gain values for the current regulator	74
2.12	Gain values for the position regulator	75
2.13	Limits of the motion law	78
3.1	Electric motor parameters	85
3.2	Parameters influencing the advancement	86
3.3	Calibration results	87
3.4	Electrical connection specifications	88
5.1	Comparison between similar cuts	103
5.2	Repeatability of consecutive cuts	108
5.3	Effect of the re-positioning	111

5.4	Linear regression, influence of resistance of the material . . .	119
5.5	Linear regression, influence of resistance of the material . . .	124

Chapter 1

Introduction and state of the art

1.1 Nature of the problem

An issue of paramount importance when dealing with scissors, and cutting tools in general, is the comparison of different tools and the definition of sharpness [1][2].

In fact, both practical [1][3][4][5] and theoretical [2][6][7][8] approaches have been applied to study the dulling process of blades for knives [8] and razors. These studies are needed not only to compare similar tools to determine the one with the best characteristics, but also because these objects are used daily by different categories of workers and an accurate analysis of their behavior in time could grant them benefits on short and long term. For instance, the use of dulled blades may cause increasing in the force exposure of the lower arm and causes muscular pathologies [5][9] or carpal tunnel syndrome; or else the use of a dulled blade would increase the time to perform an operation, reducing productivity [1].

For these reasons, a regulation was devised for cutlery and the ISO 8442-5 (2004) was produced.

On the other hand, even though similar issues are present in the field of scissors, few, or often none, researches have been performed.

The development of a new testing machine and procedure for scissors comparison, could give important information on the behavior of these kind of

instruments and help in facing and solving problems already identified for the other cutting tools, such as the most suitable sharpening schedule. This machine could also help improving the productive cycle of scissors and the monitoring of the constancy of the quality of the product over time.

1.2 ISO 8442-5 and knife testing

The document of most interest when dealing with sharpness of cutting tools such as scissors and knives, is the ISO 8442 (2004) “Material and articles in contact with foodstuffs-Cutlery and table hollower”; the focus is set on part 5 of this norm, which deals with “Specification for sharpness and edge retention test of cutlery”, that gives useful information for the selection of the parameters for a proper development of a testing procedure also in the scissors case.

A description of the contents of the norm is given pointing out parameters and characteristics applicable in the scissors case.

Even though the standard is written considering knives for hand use with blades made of various grade heat treated steel, knives for any type of use and made of any type of material can be tested as long as the test criteria are met.

The principle of the testing is to reproduce a cutting action, by forward and reverse strokes, against a pack of synthetic test medium under controlled parameters [10].

Some definitions are important in the development of a measure procedure for sharpness of cutting tools:

- The *centre line* is defined as ‘line which generally bisects the cross-section of the blade passing through the cutting edge and the back of the blade’ [10] Figure 1.1.
- The *initial cutting performance* (ICP) ‘is the cutting ability to be expected by the user from a knife when supplied “as new” from the factory or point of sale’ [10]; it must be reformulated in the scissors’ case: it has no meaning to select the depth of cut as a control parameter for scissors (being always equivalent to the length of the blade for successful cutting operations), thus the mean RMS of the torque

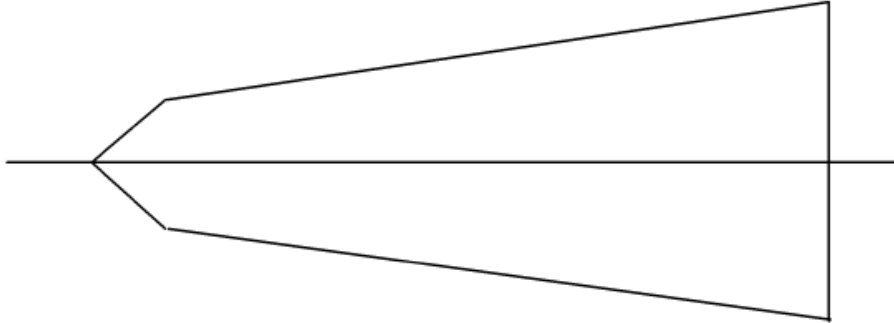


Figure 1.1: Cross section of the blade with the centre line

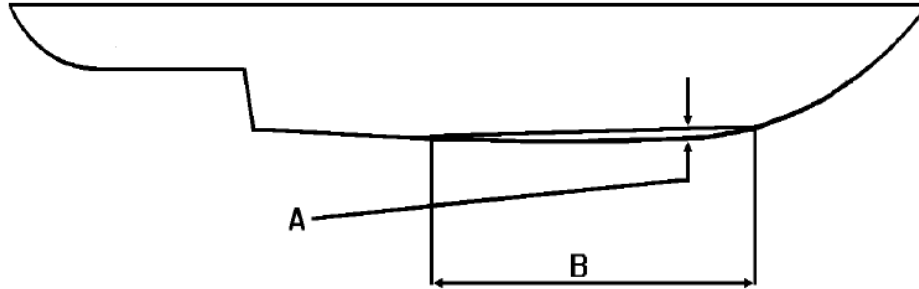
applied to the scissors during the first ten cuts is adopted (see 5.2).

- The *cutting-edge retention* (CER) is the ‘ability of the knife’s blade edge to resist wear throughout its useful life’ [10].
- The *total card cut* (TCC) is the ‘cumulative amount of card cut (measured in millimeters) by the tested knife over the duration of a full test’ [10]. Also this parameter must be reformulated in the scissors’ case: the new parameter that express the lifespan of the scissors is the number of cycles before tearing occurs (that will be called CBT and will be described in the following chapters).
- And finally, the *cutting cycle* is defined as ‘one forward plus one reverse stroke of the designated length of the blade against the medium’ [10] and is redefined for scissors as a closing plus opening operation.

After the definition of the terminology, the test and the parameters that must be used are described.

First the test must be performed on the new object as it is received from the producer, thus the sharpness of the tool is not affected by any previous operation. This characteristic is required also in the scissors case.

It is then required that the edge is straight: a deviation of 1 mm (negative or positive, not both) is allowed along the stroke length Figure 1.2. The test



Key

- A Max. deviation from straight (shown positive)
- B Stroke length

Figure 1.2: Definition of deviation from straight of a blade along the stroke length

conditions are then set depending on whether the blade can be re-sharpened by the user (Type A) or not (Type B) as in Table 1.1.

The level of initial and durability performance that are required from the

Table 1.1: Cutting test parameters

Blade edge Type	Test load [N]	Nominal cutting speed [mm/s]	Stroke length [mm]	N. of cutting cycles [F]
A	50	50	40	60
B	50	50	40	200

cutting edge are then specified as in Table 1.2.

The test is designed so that the rate of wear of the blade is increased as much as possible. This is possible thanks to the selection of the most suitable test medium: a chemical soda pulp is produced in the form of sheets of card containing a controlled amount of abrasive material (quartz). The composition of the material is reported in Table 1.3 and Table 1.4.

Before using the test medium, it shall be conditioned in a controlled atmosphere of $20 \pm 2^\circ C$ and relative humidity at $55 \pm 5\%$ for a period of 24 h.

Table 1.2: Performance level

Blade edge type	Minimum ICP [<i>mm</i>]	Minimum CER (TCC) [<i>mm</i>]
A	50	150
B	50	1500

Table 1.3: Composition of the silica abrasive

Compound	Composition [%]
SiO ₂	99
Fe	0.013
Al ₂ O ₃	0.22
MgO	Nil
Alkalines	Nil

Table 1.4: Grain size distribution of silica, C 400

Grain size [<i>μm</i>]	Composition (in weight) [%]
>50	0.2
>30	4.7
>20	15
>16	2
>12	11
>10	10
>8	7
>6	9
>4	12
>2	29

The card shall be open to this atmosphere and used within 4 *h* of removal from it [10].

The target material selected in the scissors case could be the same: this material has great dulling ability and it is suitable for the purpose. This characteristic allows a sensible reduction in time of each test, with respect to a generic material, thus it could be advantageous in case of test performed fully on the target medium.

The material for the knife tests is cut into strips 10 mm wide with the fibers of the card grain flowing across the strip and then packed.

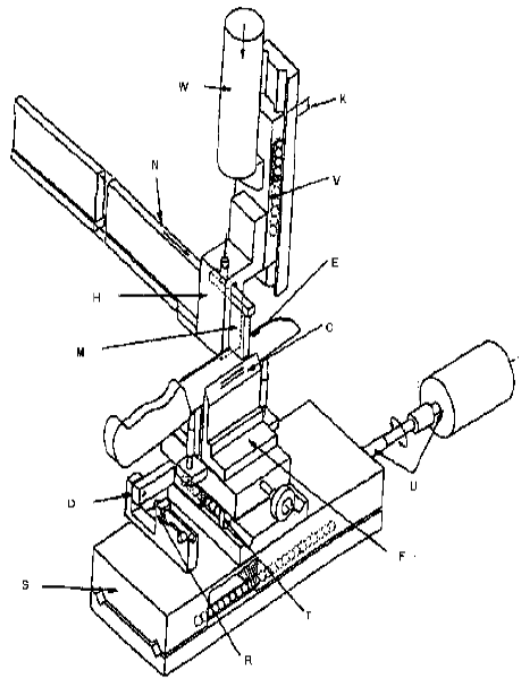
The test medium shall be kept into place by a force of $130 \pm 2.55 N$ on the inboard side of the cutting line. Also, the cut part must be able to fall away freely.

The apparatus used to perform the test must have the schematic structure of Figure 1.3.

Then, the regulation describes the main components of the machine with careful explanation of limits and boundaries for the usage. Since they are not pertinent to the aim of this paper, this part is omitted.

The next relevant part for this paper is the test procedure. First the part of the blade that meets the straightness criterion is selected. The total run is 50 *mm* long (40 *mm* of stroke plus 10 *mm* width of the test card) and it must be marked on the blade. The knife is mounted with the blade facing up and the stroke is leveled (difference between the two ends of the stroke must be 0.5 *mm* at most). Then the test card is set into place and the preload is applied with the addition of weights. At least the first 24 *mm* of the cardboard must be protruding and the blade must be at 3 *mm* from the clamped edge.

At this point the proper test starts with alternated back and forth movements of the blade of 40 *mm* with the blade always in contact with the test material. The depth of cut at each run must be measured. The blade should never reach the metal bar supporting the test medium: when more card is required the blade is lowered out of the material and it is advanced of approximately 3 *mm*. The starting position must be reached once more and the test will continue on a fresh test medium. Also in the scissors test the first part of material is not used for the test (also for technological reasons, since the material must either be connected to the weight that imposes the pre-load or to the roller that drags it) and the advancement of the material



Key

- | | | | |
|---|---------------------------------------|---|-----------------------------------|
| C | Cutting strokes | N | Medium feed forwards |
| D | 1 st cut datum | R | Retaining clamp |
| E | Test blade | S | Longitudinal slide |
| F | Component fixture | T | Transverse slide |
| H | Medium holder | U | Motor & ballscrew drive mechanism |
| K | Depth of cut measured by slide travel | V | Vertical slide |
| M | Medium | W | Additional test weight |

Figure 1.3: Schematic arrangement of suitable test apparatus

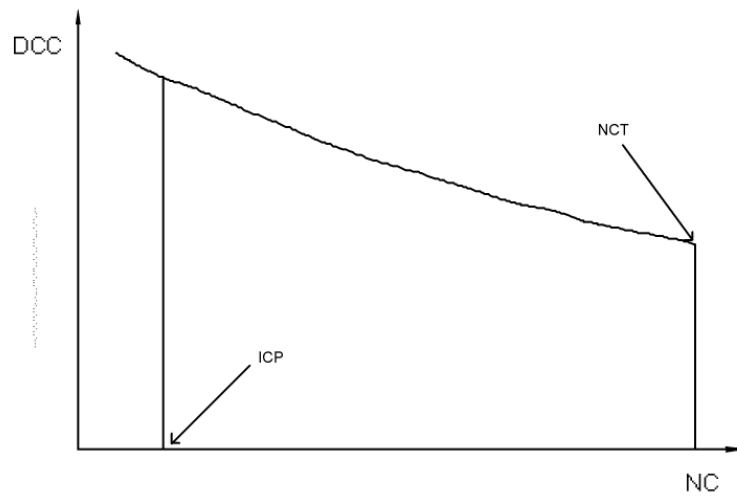
depends on the type of scissors (the longer the blade the higher the advancement will be).

The result should be reported in tables with on each row: the number of the cycle, the depth of the card cut at that cycle and the cumulative card cut up to that cycle.

A graphical representation of the results is not mandatory, but helps giving an intuitive image of the behavior.

The characteristic parameters of the test are calculated as:

- The initial cutting performance ICP is determined by adding together the card cut (in mm) during the initial 3 cycles [10] (Figure 1.4).
- The cutting-edge retention is determined by the total card cut during the complete test [10].



Key	
DCC	Depth of card cut per cycle (mm)
ICP	Initial cutting performance – Cumulative depth of card cut after 3 cycles
NC	Number of cycles
NCT	Limiting number of cycles for test

Figure 1.4: Typical performance of a knife on test

The report of the results should be redesigned in the scissors case, since the definition of the parameters and requirements is different.

To ensure the apparatus performance, it is required to do a calibration performing a test with a standard blade: any difference in the results of the tests should be compensated for. Before this calibration procedure, at first a full test shall be performed with a spare blade to allow the machine parameters to stabilize. This operations are recommended also in the scissors test to grant constancy of the machine performance and the stabilization of its parameters before starting any test.

1.2.1 Testing machines for knives

There exist many different machines used to assess the sharpness of knives. There are simpler examples, like the one described by McGorry and others in [4], up to much more sophisticated one, developed based on [10]. The machine in Figure 1.5, that was developed by McGorry and others

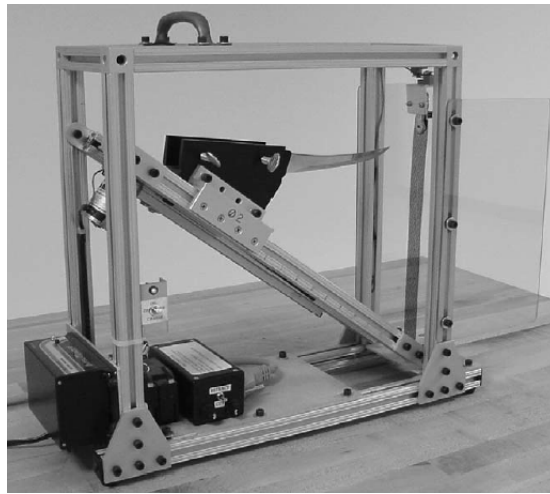


Figure 1.5: Machine for field measurement of knife sharpness

in [4], allows to quantify the force required to perform a reproducible cut with each portion of the blade. By performing the test at different times, the dulling of the blade can be analyzed and the best schedule for sharp-

ening operations can be developed. Even though this machine is small and simple, from test made with it, many useful information can be obtained on the behavior of a dulling blade (see 1.4 and Figure 1.25).

Completely automatic machines that perform tests according to [10] are also present on the market. For example, CATRA association has developed a machine ([11]) able to perform such tests with a large possible range of parameters, but the one proposed by the standard are usually recommended. The most interesting feature of this machine, that is not already specified in the standard, is the possibility of measuring the force applied on the blade during the cutting operation along three directions. This allows to develop knife edges that minimize the cutting forces [11].

Another machine designed to test knives and conforming to [10] is the one developed by Haida International Equipment CO., LTD. and described at [12].

There will not be a more detailed analysis of the technological solutions adopted on testing machine for knives, but a discussion of the results of tests made with those machines will be held in 1.4, that could also be useful in the developing of a testing procedure for scissors and to interpret the results obtained with it.

1.3 Testing machines for scissors

There are already some machines developed with the aim of testing scissors, even though a standardize testing procedure has not yet been developed. These machines could be quite simple, like the one developed by Newell and Scott Vogel in [13] (and depicted in Figure 1.6), or much more sophisticated, like the one developed by CATRA ([14]), that will be described in detail in 1.3.1.

The machine depicted in Figure 1.6 has been developed with the aim of assessing the instantaneous condition of the scissors and compare it with previous tests performed on the same tool. This could be useful to check the instrument directly on the workplace to make the sharpening operation at the best time.

It is a machine able to measure the position of the blades (thanks to a potentiometer mounted below 42 in Figure 1.6 and connected to the moving

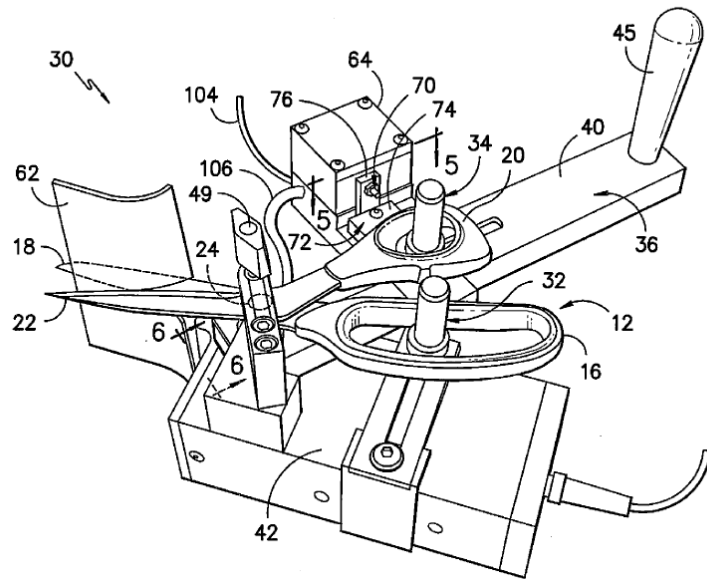


Figure 1.6: Newell and Scott Vogel machine

part close to the pin of the scissors) and the force required to perform the cut as a function of the position (thanks to a load cell connected to the moving part and located inside 64 in Figure 1.6); from the comparison of these data with historical one obtained on the same tool, it is possible to quantify the dulling of the scissors.

This machine presents the limitation of a manual actuation of the scissors: this cause a slow procedure if many cutting repetition are of interest to study the dulling process thoroughly and not just at random instants on an instrument used manually. This type of actuation causes a loss in repetitively and generality.

Also, the clumping device requires a certain amount of time to be regulated on a particular set of scissors and there could be some friction on the clamping devices (at 24 and between 20 and 34 in Figure 1.6).

This machine is thus more limited than the one that would be required for the porpoise of this paper. For this reason, the most sophisticated testing machine that can be found on the market will be discussed in 1.3.1 and a description of an already existing and functioning machine that will be used as a base of this project, will be described in 1.3.2.

1.3.1 Analysis of CATRA machine

The most complete machine to perform tests on scissors present on the market nowadays is the Scissors cutting performance test machine for shears, wire cutters, scissors, secateurs, pruners and snips, developed by CATRA (Cutlery & Allied Trades Research Association) and depicted in Figure 1.7. This machine works by studying the time evolution of the effort required to cut a reference material under set conditions. The clamping method is performed thanks to two regulable spigots that must be adjusted one on each bow. If the product of interest does not present bows, a special clamping device must be used. One spigot is rigidly connected to the machine frame, while the other one is mounted on a crack arm attached to a motor. The pivot of the scissors must be aligned with the center of rotation of the crank arm [14] (Figure 1.8).

A side pressure applicator is present on a bow to simulate the side pressure often applied by the human hand.



Figure 1.7: Scissors cutting performance test machine, CATRA

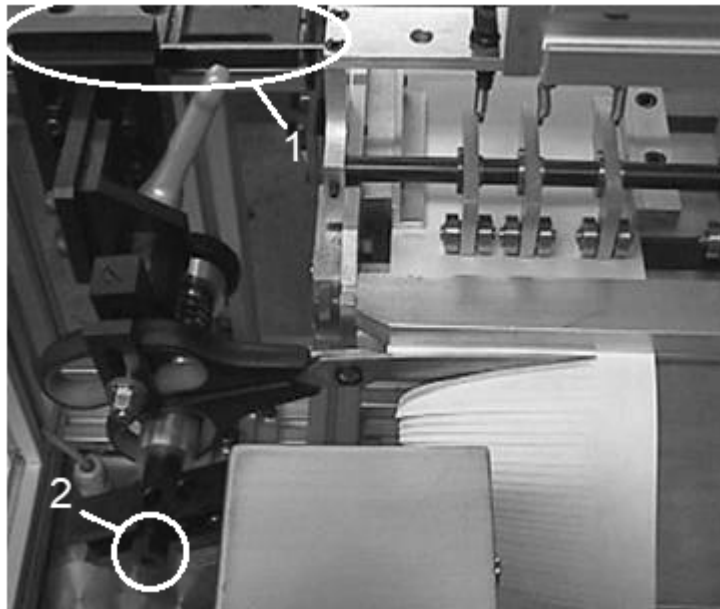


Figure 1.8: Clamping of the scissors

The force sensor is positioned in the crank arm, measuring the force required to guide the scissors through a predetermined arc of programmable speed. Different test material can be chosen, but the standard configuration uses special paper of controlled abrasive properties, as the one specified by [10] for knives. The media is fed from a tension controlled roller system synchronized with the scissors movements.

The pick force is recorded in real time, alternatively the total energy could be selected.

All the defining parameters of the control law can be controlled by the operator.

The test results are stored and can be compared with historical data [14].

The main issues noticed while analyzing this machine are concentrated in the clamping device and procedure. During the mounting operation, the scissors must first be mounted with the pivot aligned with the center of rotation of the crank (as is clearly stated in [14]). This procedure is performed using the slide connected above the upper bow (1 in Figure 1.8). Then the length of the crank arm is set manually to allow the spigot to enter the moved bow thanks to the knob numbered as 2 in Figure 1.8.

When the test starts, the movement is transmitted to the scissors by fric-

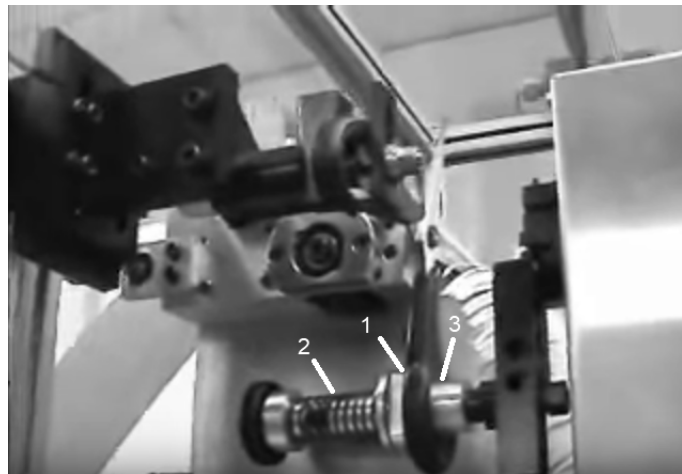


Figure 1.9: Mechanism transmitting the force

tion and geometrical coupling: the friction occurs between the plate pressing

on the rear side of the bow and the bow itself (surface marked as 1 in Figure 1.9) and the contact force is given by a spring (2 in Figure 1.9), while the geometrical contact occurs between the bow and the cylinder passing through it (3 in Figure 1.9).

Friction in the contact points could absorb a part of the energy and thus an overestimation of the force occurs as a result. In particular, this may cause significant errors when scissors with handles made of different material are compared.

Also, the manual mounting operation is critical: a misalignment between the pivot of the scissors and the crank center of rotation or a not exact matching between the crank arm length and the scissors distance between the center of the bow and the pivot, still increase the friction and thus increase the already described effect.

1.3.2 Analysis of PREMAX union testing machine

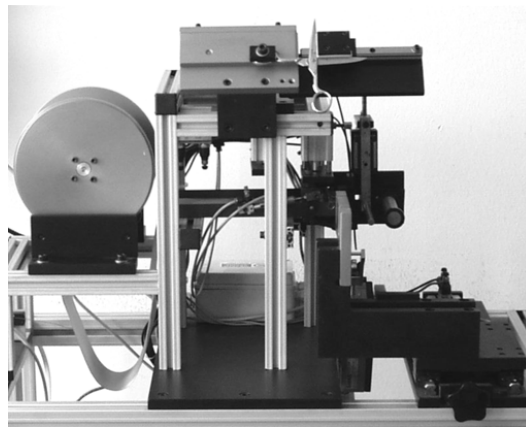


Figure 1.10: PREMAX union machine

The starting point in the development of the new machine is the testing machine designed by Premax and realized by Officina Meccanica e Automazione Giorgio Bevilacqua that is depicted in Figure 1.10. This machine is essentially made of electric and pneumatic actuators controlled by a PLC unit. The scissors are opened and closed by a linear electric actuator, de-

picted in Figure 1.11, which also works as a force and displacement sensor. The displacement measured is the one of the bow to which the actuator is connected through a slider constrain, realized with a ball bearing. The other bow is clamped to the chassis of the machine (Figure 1.11).

The initial positioning of the scissors is done with the use of a mechanical



Figure 1.11: Scissors clamping and actuation mechanism

jig (Figure 1.12) so that even scissors with different geometry are positioned uniformly.

Another actuation mechanism is required to realize the tear closure: a pneumatic actuator (1 in Figure 1.13) is connected to a linear slide (2 in Figure 1.13) on top of which both the rigid clamping part (3 in Figure 1.13) and the linear actuator (4 in Figure 1.13) are mounted.

This movement is performed when the scissors are closed on the cloth to check the correct cut of the target material.

The last functional group is the one required to move the target material and replace the one cut. The cloth is placed on a roller (5 in Figure 1.14) which is unrolled by an electric motor (6 in Figure 1.14).

The cloth is not tensioned by this motor, but a certain amount of it is kept unrolled thanks to the switch (7 in Figure 1.15), that governs the motor. The advancement of the cloth is regulated by three synchronized pneumatic

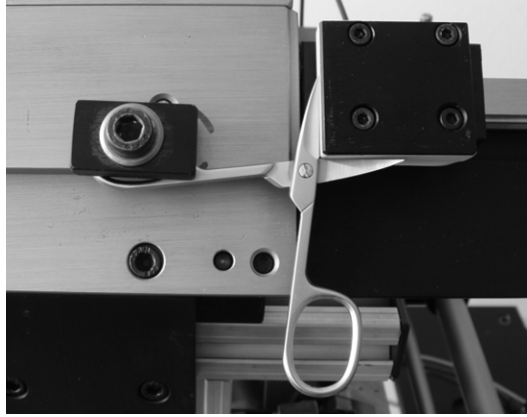


Figure 1.12: Mechanical jig for initial positioning

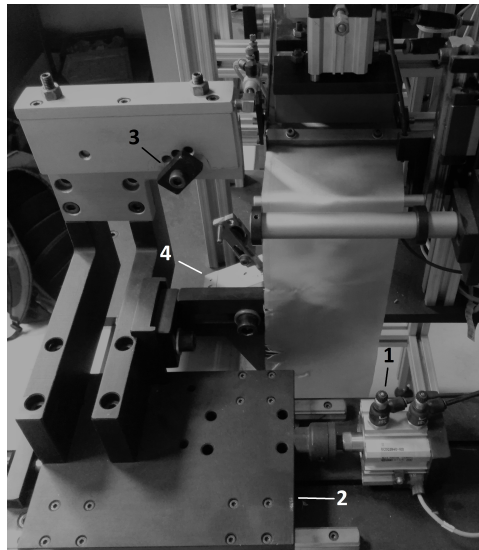


Figure 1.13: Tear closure mechanism

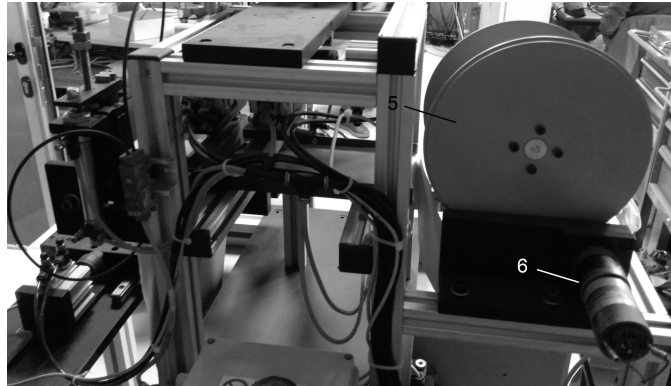


Figure 1.14: Cloth holder



Figure 1.15: Switch controlling the electric motor

actuators (8, 9 and 10 in Figure 1.16).

In Figure 1.17 there is a schematic representation of the procedure used to

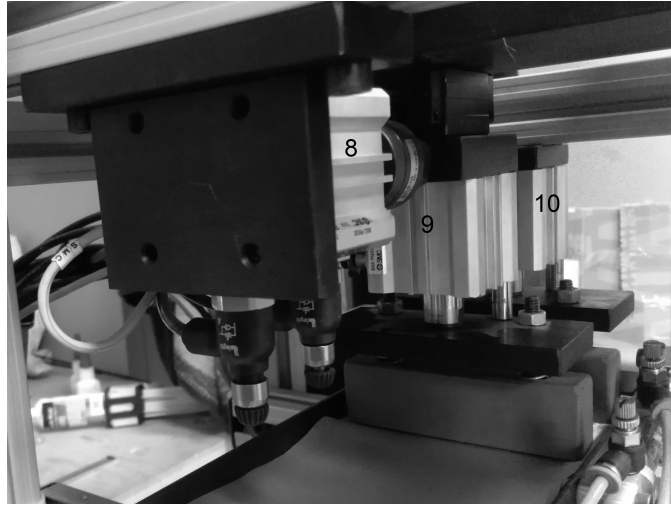


Figure 1.16: Tensioning pneumatic actuators

move the target material: first the cloth is blocked with 9 while 10 is raised (Figure 1.17 a), then 8 moves the entire actuator 9, which drags along the cloth of a distance equal to the stroke of 8 (Figure 1.17 b). At this point 10 is used to block in position the cloth (Figure 1.17 c), and then 9 is raised (Figure 1.17 d) and 8 brings it back in the initial position (Figure 1.17 e and Figure 1.17 f). After a pause to synchronize with the other movements, the procedure is repeated.

Testing operations and known critical issues

The machine can perform the following testing operations:

- Slow closure: the scissors are slowly closed by the actuator with a constant velocity value (a fast acceleration is applied when the moved blade is still far from the cloth, then the movement is kept at constant speed until closure of the scissors). This movement is used both for blank closure and closure on cloth to measure the force required to

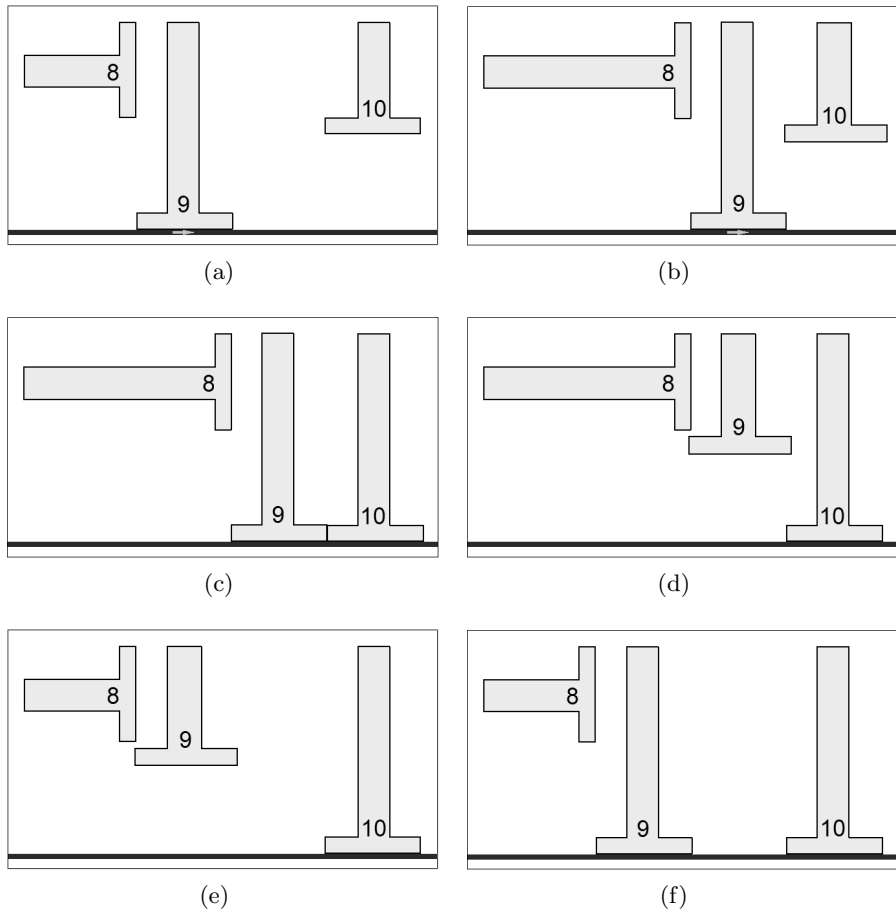


Figure 1.17: Representation of the mechanism moving the cloth

close the scissors.

- Fast closure: always performed without cloth. It is used to check the blank wear of the scissors and loosening of the screw.
- Tear closure: the scissors are closed on the cloth and then unthread from it, keeping the blades closed to check if the cut was performed correctly.

These operations were selected to automatize the operations that are usually done manually to check the critical issues related to scissors. The defects that the operators look usually for and that have been recognized as the troublesome one in the use of scissors are:

- *Hard closure* of the scissors: the screw is too tight or there is too much interference between the blades. This makes the force required to close the scissors higher and so the instrument is hard to use.
- *Soft closure* of the scissors: on the other hand, if the screw is not tightened enough the quality of the cut decreases or only the part of the blades close to the tip cuts.
- Scissors that *jib* or *yield*: there are sudden changes in the force produced by irregularities or nicks on the blades. This phenomenon has also been verified in knives [4].

These qualitative features of the scissors have been related to some quantitative parameters that can be obtained from the results of a test. To detect the *hard closure* problem a limit on the maximum value of the force must be set; conversely, for the *soft closure* problem a limit on the lower force. Finally, to account for problem of *jib* and *yield* a control on maximum and minimum value of the derivative of the force must be imposed.

All these parameters are controlled in postprocessing by realizing graphs

like the ones in Figure 1.18 to Figure 1.22.

The limits on the forces and on the maximum derivative of the force must

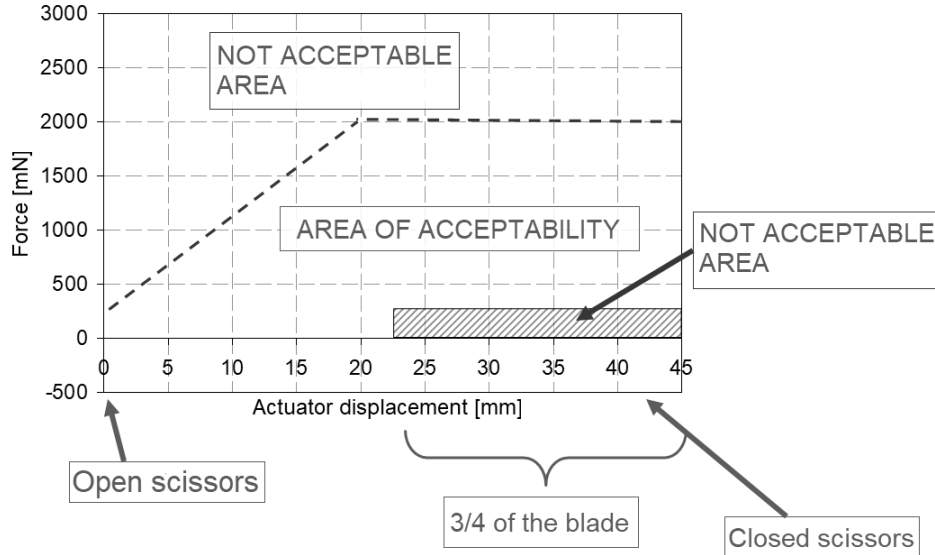


Figure 1.18: Example of limits of acceptability

be defined for each category of product: the one in the picture are limits that have successfully been used in testing scissors for manicure (scissors with geometry similar to the one in Figure 1.11 and Figure 1.12).

Testing procedure

This machine has been used for some tests, especially on small scissors. The test procedure is changed slightly depending on the geometry, dimensions and characteristic of the class of tools under analysis, but the structure of the test is always the same.

First the motor is turned off so that the rod that will connect it to the scissors is free to move and the mechanical jig is set in the positioning stance so that the scissors can be properly arranged (Figure 1.12). After that, the initial position of the screw is marked on the scissors with a marking pen, so that eventual loosening can be detected. Then the scissors are set in position by clamping one bow on the frame of the machine thanks to a screw

(Figure 1.11). During this positioning, the fixed blade must be aligned with the jig without touching it (otherwise the blade edge would be damaged and the test results altered). At this point the mechanical jig can be moved from the positioning stance and set in the testing position.

The following step is the setting of the actuator: the rod must be aligned with the center of the two bows in the open position, and the moved bow must touch the ball bearing in its middle point. The position of the actuator is then regulated as a function of the length of the blades. These last two operations must be repeated iteratively until a satisfactory positioning is obtained.

At this point a manual closure of the scissors connected to the actuator is performed to register the closed position. If the movement is satisfactory, the rod can be connected to the bow with a rubber band.

The value of the closed position must be insert manually in the control program: first the one for the slow closure (as the one read in the previous manual closure of the scissors) and then the one for the fast closure (the distance between the bow must be increased to avoid shocks).

First an opening movement is performed and then three slow closure operations: the results of these closures must be manually copied and saved.

To verify the efficiency of the scissors, a cut operation is performed on the cloth.

At this point the longest automated part of the test is performed, by doing several fast closures (the number varies depending on the class of scissors, for instance in the case of manicure scissors was equal to 800 cycles). The frequency of the process should be equal or lower to 1 Hz to avoid overheating of the screw.

After this, once again three slow closures are performed, manually saving the results and a cut on the cloth is performed to verify the cut efficiency.

Finally, eventual rotations of the screw must be checked either by eye or with the help of magnifying glasses.

Other configuration of the test that have been designed and presented a higher number of cycles (over 20000) or the use of an abrasive material (P600 abrasive paper) instead of a standard cloth.

Results examples

In Figure 1.19 to Figure 1.22 there are examples of results of tests performed with the previously described procedure on manicure scissors. The first two picture (Figure 1.19 and Figure 1.20) present two cases where the scissors did not pass the test. For the A scissors, there are problems of *hard closure* (Figure 1.19), *scratching* and *yielding* (Figure 1.20), while scissors B present *soft closure* problems (Figure 1.19).

Also, two examples of successful tests are reported in Figure 1.21 and

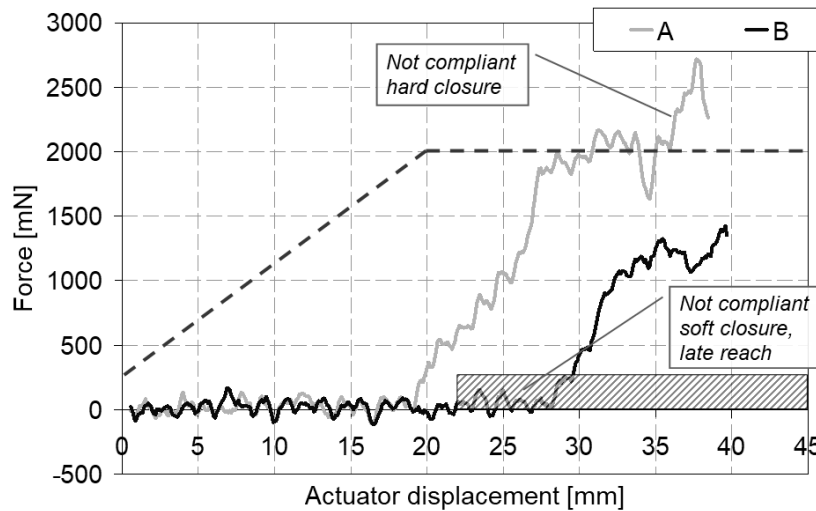


Figure 1.19: Two not compliant tests, force against actuator displacement

Figure 1.22. Here the value of the forces is always inside the area of acceptability during the whole cutting operation for both scissors C and D (Figure 1.21), and also the derivative of the force does not exceed the set limits (Figure 1.22).

To obtain a quantification of the wearing effect of the test on the scissors a comparison between the two set of charts obtained on the slow closures before and after the 800 blank fast closures must be performed: a test is passed if the scissors pass the controls on force and derivative of the force in both sets of figures.

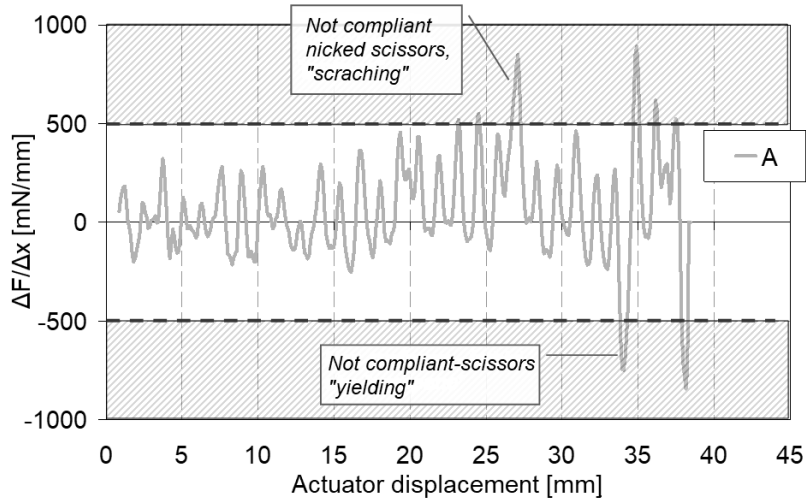


Figure 1.20: Not compliant test, derivative of the force against actuator displacement

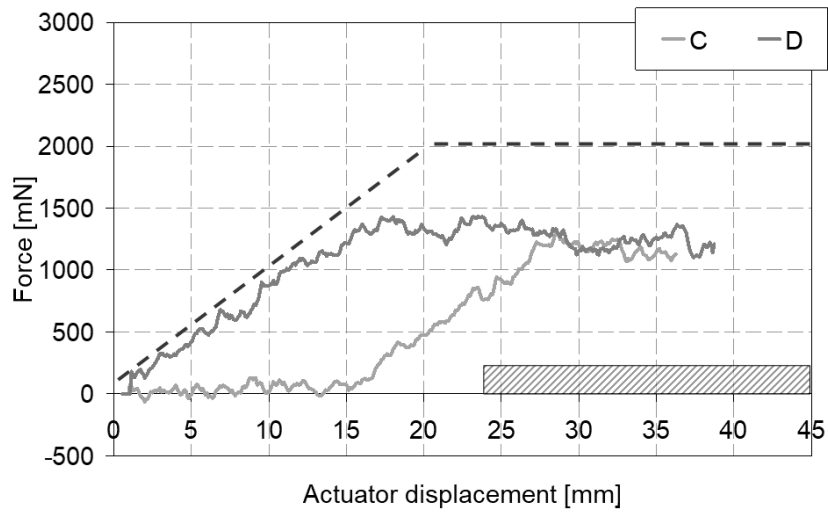


Figure 1.21: Two compliant tests, force against actuator displacement

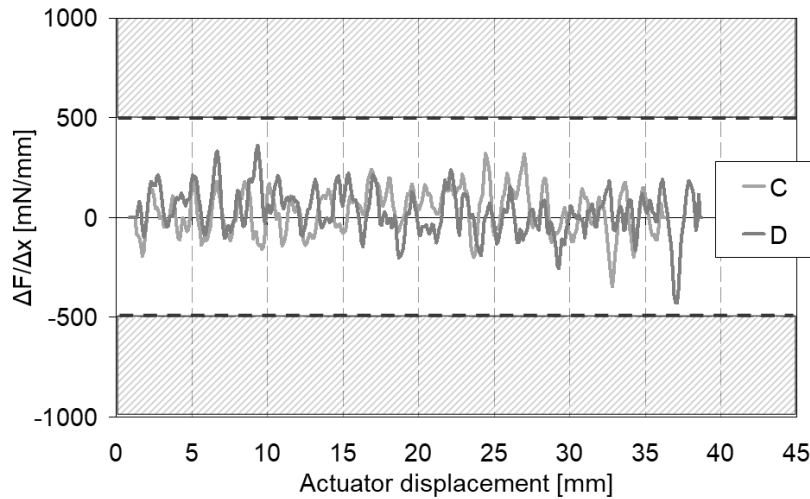


Figure 1.22: Compliant tests, derivative of the force against actuator displacement

1.4 Literature review

Many useful information can be obtained by analyzing the literature about knife life and testing, that can be reasonably transferred to scissors. These field has been studied quite thoroughly and many different machines and test are present on the market to analyze the performances of knives [1][2], such as the one describe in 1.2 and 1.2.1.

A first interesting concept that shall be clarified is the one of bluntness. According to Balevi (1996) [6] there are two different definitions of bluntness:

- Burr edge: formed when unsuitable sharpening processes are adopted that do not allow complete burr removal at the cutting edge, or when uncompleted cutting surfaces are not polished, by fine grinding, honing or polishing abrasives following primary formation.
- Blunt edge: the cutting-edge brakes down because of excessive use and exhibits more than one cutting surface interface, cratering excessive rounding and lack of evidence of distinct cutting surface intersection.

Both cases could be exploited in the case under analysis: the first definition could be used to find the best sharpening procedure; by creating different control groups of the same model of scissors, each group sharpened with one of the procedures and then tests are performed on all the groups. The results of each group are then compared with the others to find the sharpening process that grants the desired response (either low torque in the initial part of the history, or longest life of the cut quality).

In case a comparison of different scissors must be performed there is no need for a rigid distinction between the two definitions: both parameters enter the problem in the same way and no distinction is required.

Still an absolute definition of sharpness is difficult to obtain: while on knives it was partially possible by normalizing the force applied on the cut material starting from a fixed reference tool [1][2] and stating the main characteristics of boundary conditions and blade edge, in the scissors case the influence of the geometry of each single object (and thus its inertial contribution) would prevent the comparison of tools with different size. In fact, even for knives the behavior would change depending on the boundary conditions (such as target material to be cut and pre-tensioning of the material) and the characteristics of the blade, making impossible the design of a universal classification [2]. Thus, always a comparative analysis between similar scissors or different characteristics of a single tool would be advisable.

When comparing different scissors, it is important to keep in mind that the quality of the cutting edge prior to use has a significant effect on the durability of the cutting edge itself and the quality of the cut on the target material [15][16][17][18]. This suggests that not only the comparison between just one scissors of each type is not enough to grant a definitive indication on the tool (a larger number of tests would be advisable for statistical reasons), but also that a correct and careful handling of the objects prior to the test is required not to influence the results. Blade degradation starts even if very soft materials, such as neoprene, are cut [3], thus always newly sharpened tools should be used in the tests, as it is required from [10].

Even some parameters that characterize the blade and influence the cut in knives should be mentioned, because the relative behavior is expected to be similar, or at the very least worth of analysis, for scissors too. In fact, between the two types of tools there is a significant difference in the cutting process: while scissors cut the material under a tensile-shear mechanism,

knives usually apply a compressive-shear action. On the other hand, if the target material is subject to a pre-tension during the cut with a knife, the cutting process is characterized by a shear-tensile behavior, and thus the results are much more relatable to the scissors case [19].

According to Kalder et al. (1997) [7], the parameters that affect a cutting process are: tool geometry, tool material, work material and cutting conditions. The magnitude of the interaction is greatest between the first three factors while cutting conditions only marginally affect the cutting process [7].

Of the tool geometry, the effect of single parameters could be isolated and analyzed one by one.

The first geometrical parameter worth mentioning is the edge roundness (Figure 1.23): this parameter has been proved to affect the depth of cut of a knife under the same force applied.

In particular, the depth of cut is linearly proportional to the reciprocal

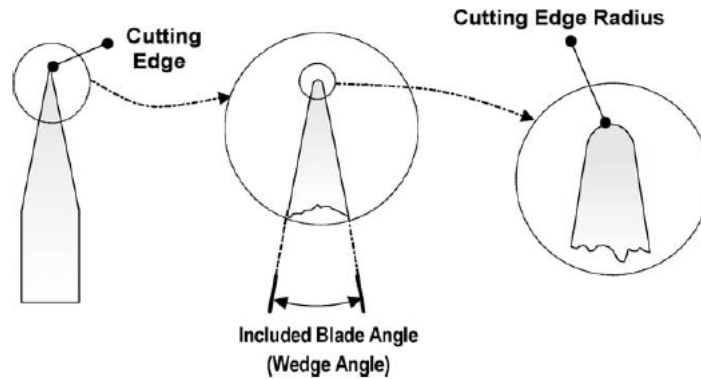


Figure 1.23: Edge radius and edge angle

of the edge radius [8]. This could also be read oppositely in the case of scissors: the lower is the edge roundness, the lower is the torque required to perform the cut to obtain the same depth of cut. This reciprocal behavior has been experimentally proved for knives by Komanduri et al. (1998) [8] and Shin et al. (2003) [19]. Figure 1.24 is extracted from the second article and graphically shows this behavior.

A second interesting parameter is the edge (or wedge) angle (Figure 1.23):

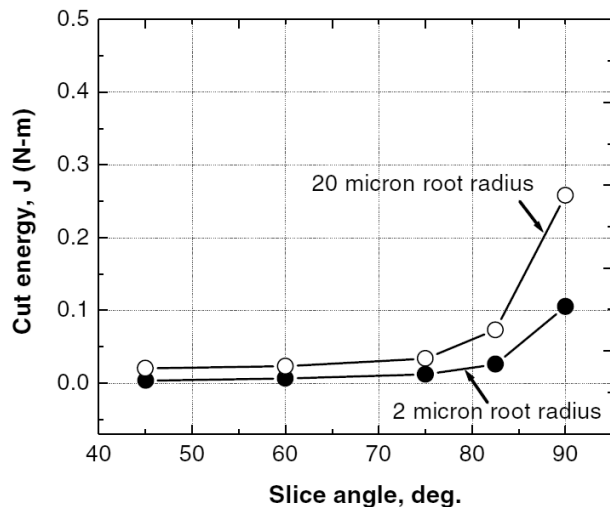


Figure 1.24: Effect of edge roundness on cut energy

it has already been demonstrated for knives that an acute edge angle grants a better initial cutting capacity but a lower retention of the sharpness characteristic. Oppositely, an obtuse angle allows a higher retention of sharpness, paid with a lower initial cutting capacity [1].

Another interesting observation is given by McGorry et al. (2005) [4]: it states that the presence of small nicks on the blade edge could be detected in the testing of knives, by observing oscillations of the force in the time history, concentrated at every cycle of the test in the same area of the time history (as it can be seen from Figure 1.25). It is also specified that the size of the nicks is not necessary visible and their influence is already non-negligible when they can be only felt by running the fingernail over the blade edge [4].

Finally, an overview of the main parameters that influence the testing procedure is given in the case of machines that work on knives.

As it can be intuitively supposed, the level of tangential force required to obtain the same depth of the cut with a knife increases with the dulling of the blade [3]. In particular, it has been proved that the increase of this force is less than linear with the progressing of the dulling of the blade [3] (in Figure 1.26 there is a graphical representation of this effect). The same

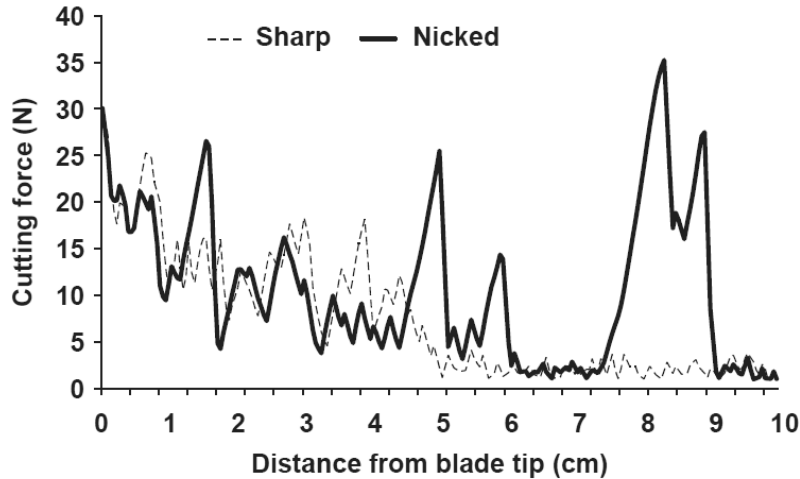


Figure 1.25: Effect of nicks on the force history

behavior is expected for scissors between the applied torque and the dullness of the blade.

Regarding the velocity of the cut, it has been stated that the quality of the cut is not a function of the velocity of the cutting tool itself [3]. For this parameter, a quantitative analysis should be done to verify this trend, by testing motion lows with different maximum velocity in the same boundary conditions of the test and with the same kind of scissors (see 5.4.2).

Finally, the pre-tension force applied to the material to be cut affects the result of tests performed on knives [3].

The pre-tension effect for a tensile-shear cutting mechanism is analyzed by Shin et al. (2003) [19]: they found out that adding pre-tension to the cut material, the energy for the cut decreases. This behavior can be clearly seen in Figure 1.27: the energy (integral of the stress-strain curve, thus area underneath each curve) decreases with the increase of the pre-tension. Also this phenomenon will be tested in the scissors case 5.4.1.

The selection of the material is the last parameter to be discussed. A classification of suitable materials could be performed according to [20]. On the other hand, the material described into Table 1.3 and Table 1.4 has been proven effective in the dulling of blades and was selected both for knives

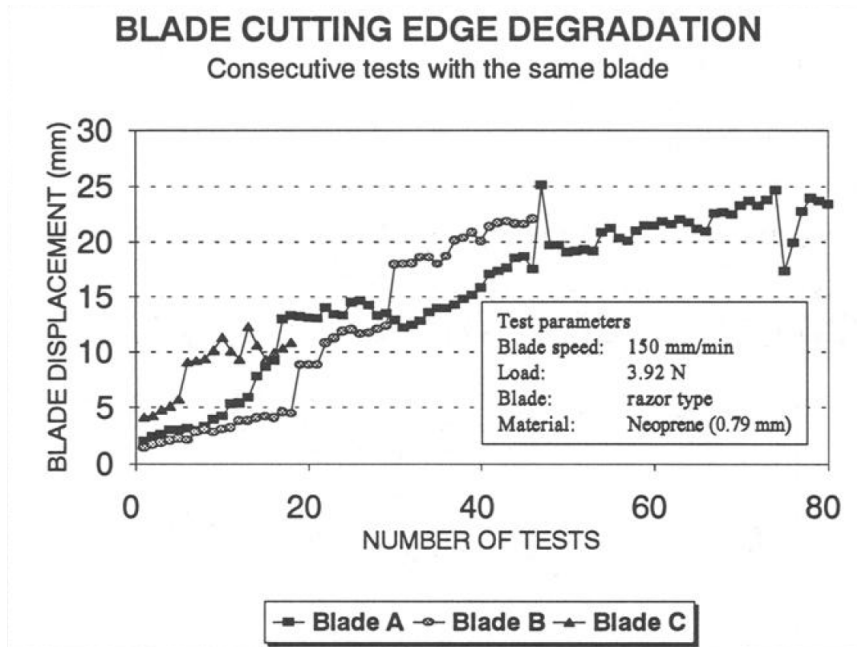


Figure 1.26: Dulling behavior for different number of passages

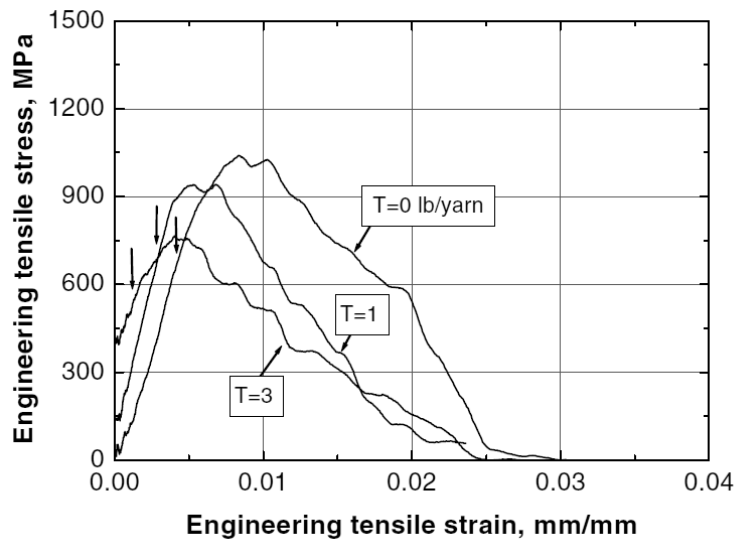


Figure 1.27: Effect of pre-tension on the cut yarn

([10]) and for scissors ([14]). Thus, this material could be a valid option. On the other hand, in the case of 1.3.2 a standard cloth was selected like the one that is commonly used when manually testing scissors. Since it is already spread in the field, this material is the one that is selected as standard testing material in this paper.

1.5 Aim of the project

Aim of this project is the development of the prototype of a machine for the testing of scissors and its experimental validation.

To validate the prototype, a series of test will be performed first assessing the performances of the machine in terms of resolution and reliability, then checking the dependency of the cutting force from various parameters (similarly to the one analyzed in the knife case) and finally performing some wear tests in different condition.

The results will be statistically analyzed and their validity will be assessed.

1.6 Scheme of the thesis

This thesis is structured as follows: chapter 2 describes the design of the functional group that actuates the scissors, both from a hardware point of view (with the selection and design of the physical parts) and a software one (with the set up and tuning of the electrical part and an outline of the control software).

Chapter 3 describes the design of the group moving the target material, still dividing the hardware from the software part for clarity. Then chapter 4 deals with other functional groups that would improve the quality of test or the data, but that have not been developed on this machine.

Chapter 5 deals with the experimental results obtained in the measurement campaign performed to validate the machine set-up.

Finally, chapter 6 contains the conclusions and further possible developments.

Chapter 2

Scissors actuation functional group

In this chapter, the procedure for the design of the functional group used to actuate the scissors is described. This design is started from scratch being the actuation principle, that will be described in 2.1.1, completely different from the one available on the old machine of 1.3.2.

The design can be divided into two main steps: the hardware design, consisting in the development of an initial generic kinematic idea, completed by the selection of parts that must be bought and the actual design of the parts that must be realized; the second step is the software design, so that the machine can perform the wanted motion and can be easily controlled by the operator.

2.1 Hardware development

In this section, first a detailed overview of the kinematic scheme of this group is given, so that advantages of this configuration could be specified. Then the focus is set on the selection of motor and speed reducer, joined by the matching with compatible encoder and control unit. Finally, the selection and calibration of the torque transducer and the design and selection of the remaining parts of the chain that connects the motor to the scissors and their inter-connection is described.

An additional paragraph deals with the design of the positioning system

that will be realized for the final configuration of the prototype.

2.1.1 Overview of the solution

The first and most important decision in this phase is how the scissors should be actuated: a brushless electric motor (1 in Figure 2.1) is selected. It is rigidly connected to one blade (2 in Figure 2.1) so that the axis of the motor is coincident with the pivot of the scissors. The other blade (3 in Figure 2.1) is fixed so that the relative motion is coincident with the movement of just one blade. The following decision regards the realization of the rigid connection: a coupling using a common glue (for example super Attak produced by Loctite¹) is chosen (4 in Figure 2.1), so that a high rigidity of the connection can be granted even for small areas available, such as in the case of manicure or ring lock scissors.

Between the two parts a series of additional elements are added each one

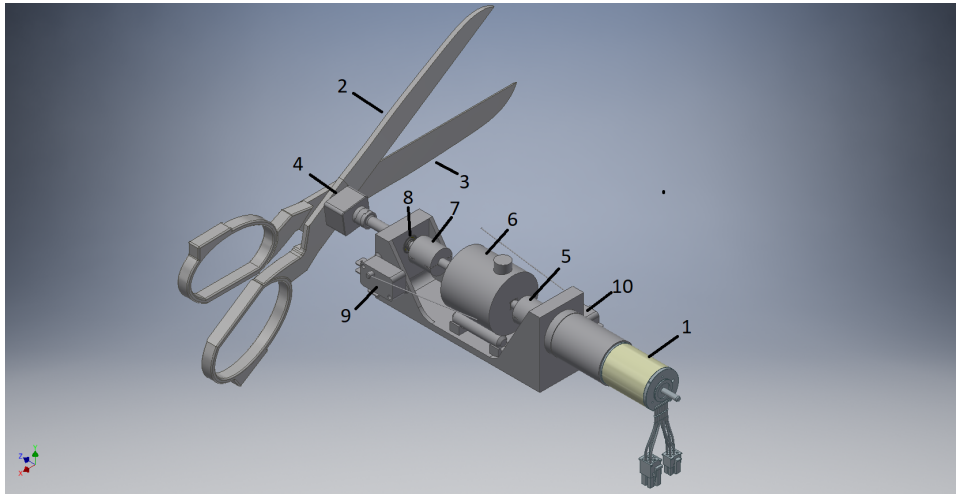


Figure 2.1: CAD model of the scissors actuation functional group

with a specific function: the motor is connected through a beam coupling (5 in Figure 2.1 and extensively described into 2.1.5) to the torque-meter

¹Henkel Italia Srl, via C. Amoretti, 78, 20157 Milano
<http://www.loctite-consumer.it/it.html>

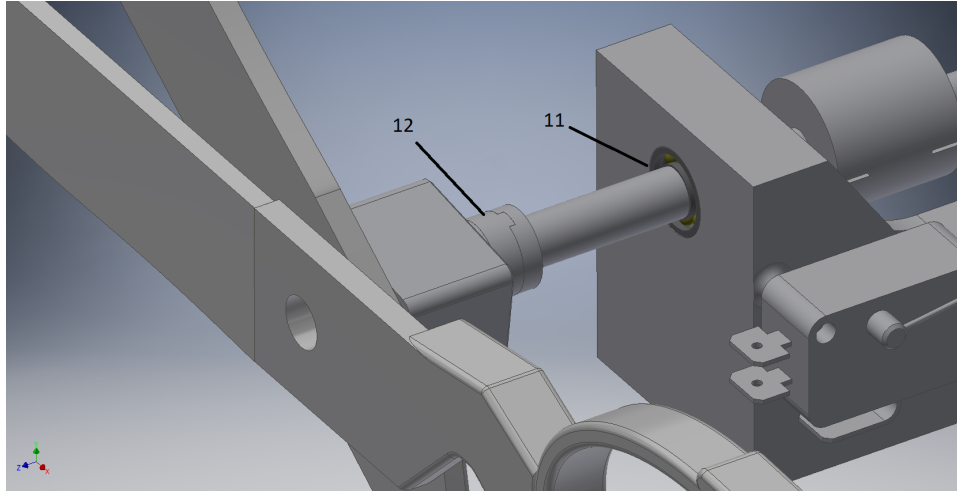


Figure 2.2: CAD model of the scissors actuation functional group, detail

(6 in Figure 2.1), that measures the necessary torque to comply with the imposed motion law. Another beam coupling (7 in Figure 2.1) isolates the torque-meter from tangential displacements and misalignment coming from the following shaft on scissors side that could cause unwanted disturbance forces. This following shaft is supported by two deep groove ball bearings (8 in Figure 2.1 and 11 in Figure 2.2), that can cope with axial forces, and it supports on the free end an Oldham coupling (12 in Figure 2.2). This coupling can compensate small misalignments between the shaft and the pivot of the scissors, transmitting only the torque required by the application and not unwanted tangential forces. The third element of the Oldham coupling can present different geometries each one designed to be compatible with a group of scissors with similar dimensions (see drawings in Appendix A). Finally, the two switches (9 and 10 in Figure 2.1) are needed to stop the movement in case the cable of the torque-meter is near the end of the available space, being a static torque-meter and thus rotating with the shafts.

2.1.2 Motor-reducer unit selection

The procedure for the selection of the motor-reducer group is based on the paper written by Giberti et al. (2011)[21]. In this article, it is developed a practical procedure that allows the selection of the motor and speed-reducer able to impose a pre-defined motion law to a load.

The symbols that are used are reported in Table 2.1 and Table 2.2.

Table 2.1: Motion law parameters

Dimension	Symbol	Value
Total rise	h	40°
Forward motion time	t_1	0.8 s
Backward motion time	t_2	0.8 s
Resting time	t_r	1.25 s

Motion law definition

At first the motion law must be defined. Since the selection of amplitude of motion, speed and acceleration of the movement will be chosen by the final user of the machine, a first guess law is selected then, once the selection of the motor is done, a harsher one is tried to check if the motor is able to comply also with that: the dimensioning is done considering the largest possible scissors and thus the harshest possible load.

As an initial motion law, two anti-symmetrical cycloidal are selected with the parameters reported in Table 2.1. The resulting motion law is depicted into Figure 2.3.

Load modelization

The load is modelled starting from the inertial one given by the largest possible actuated blade of the scissors. This inertia is computed from a CAD model of it. This contribution is then over-estimated to consider the inertia of the additional elements between the motor and the scissors and the resistance of the cloth.

Table 2.2: Symbols used

Dimension	Symbol	Value
Accelerating factor	α	818.18 W/s
Load factor	β	5.75 W/s
Transmission moment of inertia	J_T	0.7 gcm^2
Motor moment of inertia	J_M	11 gcm^2
Cycle time	t_a	2.85 s
Generalized load torque	T_L^*	Function of time
Generalized load root mean square torque	$T_{L,rms}^*$	588.8 mNm
Motor nominal torque	$T_{M,N}$	30 mNm
Motor root mean square torque	$T_{M,rms}$	3.3 mNm
Transmission mechanical efficiency	η	0.6
Transmission ratio of the speed reducer	τ	0.0041
Maximum acceptable transmission ratio	τ_{max}	0.068
Minimum acceptable transmission ratio	τ_{min}	0.0001
Minimum kinematic transmission ratio	$\tau_{M,lim}$	0.0025
Optimal transmission ratio	τ_{opt}	0.003
Load angular acceleration	$\dot{\omega}_L$	Function of time
Maximum speed achieved by the load	$\omega_{L,max}$	16.67 rpm
Load root mean square acceleration	$\dot{\omega}_{L,rms}$	34.68 rpm/s
Maximum speed achieved by the motor	$\omega_{M,max}$	6630 rpm

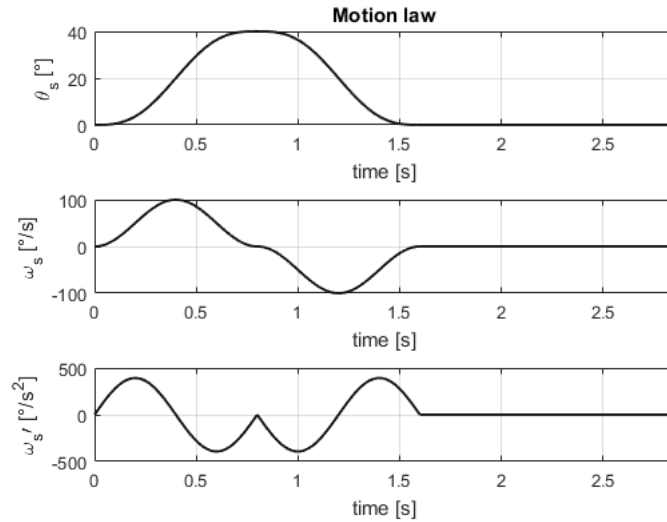


Figure 2.3: First attempt motion law

On the other hand, the friction between the blades gives the largest contribution. This is higher at the start of the movement and reduces once the movement starts. To quantify the static friction a test is performed where an increasing load at constant distance from the pin of the scissors is applied until a value able to start the opening is reached (Figure 2.4). This value is equal to *ca* $0.7 Nm$.

In the dynamic part of the load model this value is then reduced according to the ratio between the dynamic ($\mu_d = 0.5$ [22]) and static ($\mu_s = 0.74$ [22]) friction coefficient of clean and dry steel on steel surfaces.

The resulting load is the one depicted in Figure 2.7, where the step is due to the passage from static to dynamic friction.

First selection of motor-reducer units

For this task, a catalogue of motors and one of speed reducers that seemed appropriate for the application under investigation is developed,



Figure 2.4: Static friction evaluation

based on the catalogue of Maxon motor.² The resulting extract of the catalogue of motors is made by 120 different products: each motor is described by the nominal parameters of Table 2.3 (in which the values corresponding to the selected motor are reported).

On the other hand, the one of speed reducers consists of 110 elements and

Table 2.3: Motor catalogue parameters, values of the selected one

Dimension	Symbol	Value
Maximum speed	$\omega_{M,max}$	6630 rpm
Maximum torque	$T_{M,max}$	34.9 mNm
Nominal torque	$T_{M,nom}$	30 mNm
Inertia of the rotor	J_M	11 gcm ²

each element is described by a different set of parameters (Table 2.4). Both the pre-selection are made performing a qualitative evaluation of the

²Maxon motor ag, Brnigstrasse 220, CH-6072 Sachseln.
<https://www.maxonmotor.it/maxon/view/content/index>

Table 2.4: Speed reducer catalogue parameters, values of the selected one

Dimension	Symbol	Value
Transmission ratio	τ	0.0041
Transmission mechanical efficiency	η	0.6
Inertia of the rotor	J_T	0.7 gcm^2
Maximum continuous-rated torque	$T_{T,max}$	6 Nm
Maximum speed in	$\omega_{T,max}$	8000 rpm

performance of each element.

The article starts by dividing the model of the servo-system into three parts: the motor, the transmission and the load. While the first two are unknown until the final selection is made, the first one is completely known, being function of the task and it has been addressed in the previous paragraph.

It is established [23] that to assess the ability of a motor-reducer unit to perform a specific task, three different controls must be done: one on the rated motor torque, one on the maximum motor speed and the last one on maximum servo-motor torque.

In the paper [21], the procedure is based on a reformulation of this approach. To make the first pre-selection, two parameters are defined, the *accelerating factor*:

$$\alpha = \frac{T_{M,N}^2}{J_M} \quad (2.1)$$

which describes the performance of each motor (being just a function of motor parameters), and the *load factor*:

$$\beta = 2[\dot{\omega}_{L,rms} T_{L,rms}^* + (\dot{\omega}_L T_L^*)_{mean}] \quad (2.2)$$

that defines the performance required by the task.

From a reformulation of the condition on the rated motor torque, the load factor is a lower bound of the load side of the inequality, thus Equation 2.3 must be satisfied with a certain margin.

$$\alpha \geq \beta \quad (2.3)$$

This condition is satisfied ($818.18 \geq 5.75 \text{ W/s}$) and is represented also in Figure 2.5 (only for the motor selected in the end for clarity). The motor

selected, grants a good margin of the accelerating factor with respect to the load factor, but not so high that the motor would be too large (and thus too expensive without reason).

In the following step, the best value of the transmission ratio must be

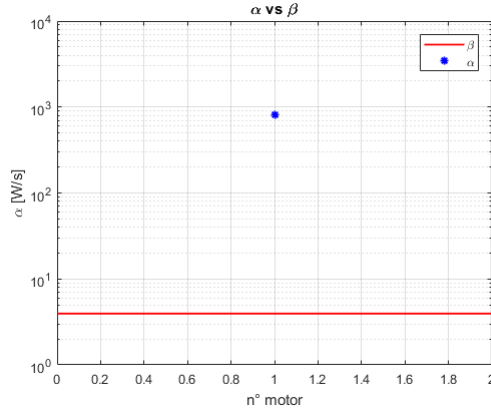


Figure 2.5: α vs β for the final selected motor

selected so that the system is able to comply with the motion law.

The range of acceptable transmission ratios is defined thanks to the calculation of some limits:

$$\tau_{min}, \tau_{max} = \frac{\sqrt{J_M}}{2T_{L,rms}^*} \left[\sqrt{\alpha - \beta + 4\dot{\omega}_{L,rms} T_{L,rms}^*} \mp \sqrt{\alpha - \beta} \right] \quad (2.4)$$

$$\tau_{M,lim} = \frac{\omega_{L,max}}{\omega_{M,max}} \quad (2.5)$$

and the resulting condition is:

$$\tau_{max} \geq \tau \geq \max(\tau_{min}; \tau_{M,lim}) \quad (2.6)$$

This condition is satisfied ($0.068 \geq 0.0041 \geq \max(0.0001; 0.0025)$) and is represented in the case of the system finally selected in Figure 2.6. The transmission ratio selected (represented with a horizontal line in correspondence of the relative transmission ratio) is the closest one to the optimum value present in the catalogue.

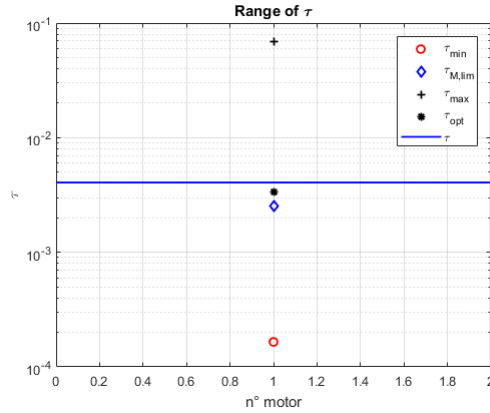


Figure 2.6: Range of τ admissible and final selected transmission

Final checks

Since some approximation were made in the development of the procedure adopted, some additional checks should be performed to grant the compliance of the motor-reducer group with the required performances. These checks take into account the inertial contribution of the transmission and its efficiency.

- Maximum torque supplied by the servo-motor for each angular velocity. This check is done by superimposing the motor torque curve with the torque/speed curve, as in Figure 2.7 (a simplified curve is reproduced but, being the safe margin wide, there is no need for higher refinements).
- Effect of the transmissions mechanical efficiency and moment of inertia:

$$T_{M,N}^2 \geq T_{M,rms}^2 = \int_0^{t_a} \frac{1}{t_a} \left[(J_M + J_T) \frac{\dot{\omega}_L}{\tau} + \frac{\tau T_L^*}{\eta} \right]^2 dt \quad (2.7)$$

And also this check is passed ($900 \geq 10.89 \text{ mN}^2\text{m}^2$).

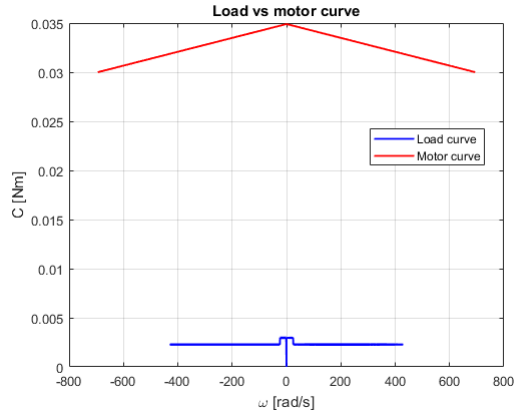


Figure 2.7: Check 1, maximum torque supplied

- The resistance of the transmission as supplied by the manufacturer. The maximum torque is much lower than the maximum value allowed ($0.734 \leq 6 \text{ Nm}$) by the speed-reducer and the rest of the chain will be designed considering this value:

$$T_{L,max} < T_{T,max} \quad (2.8)$$

All these checks are passed with the configuration selected, thus a check with a harsher motion law can be performed.

The second motion law designed is composed by two constant acceleration curves each one with cycle time of 0.5 s (Figure 2.8). This cycle time is selected as the highest possible, since it is already known from tests performed with the old Premax machine that for frequency of the cycle higher than 1 Hz , the screw of the scissors would overheat. The resting time is instead set to zero.

Once again, the procedure is applied to the motor and speed reducer selected and again all tests are passed (all the results related to this case are very similar to the previous case and are thus only reported into Appendix B).

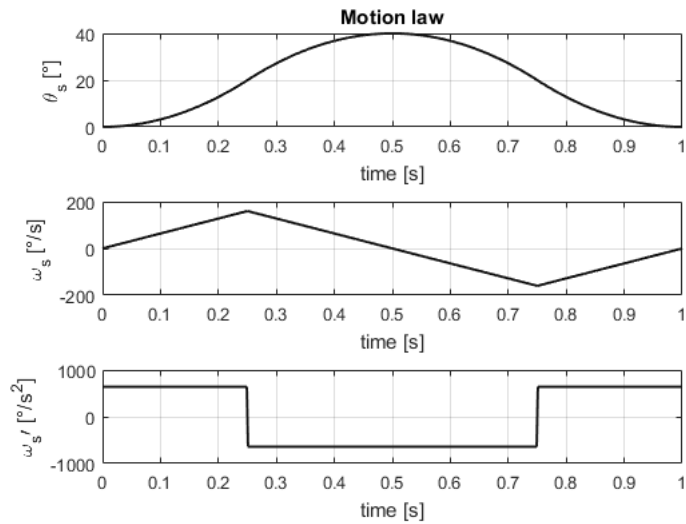


Figure 2.8: Harshhest motion law

Additional elements

Finally, some compatible items are added:

- an encoder with a thousand notch is selected, to have a high resolution on the position;
- an EPOS2 Module 36/2 to be able to control the motor directly from a pc;
- a EPOS2 Module evaluation board, to be able to simply connect the system elements.

2.1.3 Main support of the group

To support the functional group that actuates the scissors, a support is designed (Figure 2.9). The part is realized with a 3D printer, that allows

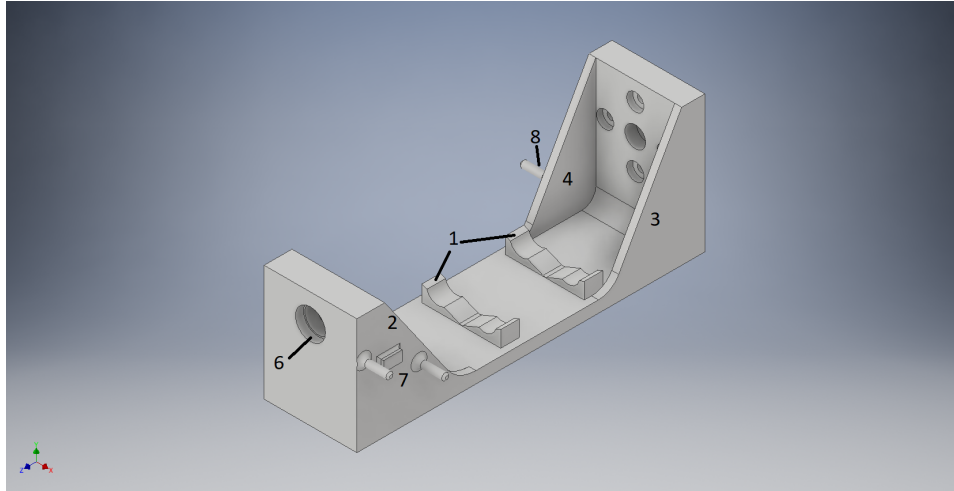


Figure 2.9: Main support of the actuating functional group

the maximum freedom in the selection of the dimensions. On the other hand, once the machine is fully established, it should be replaced with an element made of machined aluminum to increase life time and reduce the deformations and misalignments. The supports of the switches (7 and 8 in Figure 2.9) in the final configuration should be eliminated for technological reasons and the positioning should be done either with screws or by gluing the switches.

Interesting features of the part are the two sets of supports (1 in Figure 2.9) on which two cylindrical elements are placed. These elements, visible in Figure 2.1, have the function of supporting the torque-meter (which otherwise would be suspended between the two beam couplings) without imposing a high friction on it (that would influence the measurement). For this reason, the supports are designed so that they are free to rotate on them.

A possible improvement of the machine could be done if these two cylindrical elements would be supported by ball bearings to further reduce the friction.

There are also four supporting rib (2, 3 and 4 in Figure 2.9, while 5 is not visible, but is symmetric to 2 with respect to the plane marked in the picture as yz), with the function of increasing the stiffness of the structure.

Finally, there are two housing for the two bearings (6 in Figure 2.9 and 8

in Figure 2.1) that have been dimensioned according to the producer suggestion³: the tolerance selected is a J7 for the housings of the two bearings (light to normal loads, axial displacement of outer ring desirable), while the shaft has a tolerance of js5 (value recommended for every kind of load, from light to heavy, for shafts with nominal diameter lower than 10 mm). A technical drawing of this part is reported into Appendix A.

2.1.4 Torque-meter

The torque-meter selected is the MTRS2.5NM produced by Luchsinger srl⁴. The selection of the torque-meter is based on the full scale of the instrument: the maximum analytical value required for the application is equal to 0.75 Nm, which is safely lower than the full scale of the instrument equal to 2.5 Nm.

Calibration

An experimental calibration is performed on the torque-meter. To do so, a series of known torques are applied to it and the related output tension values are measured. The set-up is the one depicted in Figure 2.10.

The procedure starts from the unloaded torque-meter and then an increasing torque is applied in one direction by putting a series of known weights at fixed distances. When the maximum value is reached the load is progressively decreased and the values are measured for the same torque values as before. The same procedure is repeated in the opposite direction. The critical parameters of the test are reported in Table 2.5.

The obtained points are then reported in a voltage-torque graph and a linear regression is performed to obtain the sensitivity of the instrument. The result is depicted in Figure 2.11.

To consider the actual weight of the arm (visible in Figure 2.10) that generates torque, a simplified model of the arm made off just two cylinders is considered and by proportion only the acting contribution is isolated.

³SKF Industrie S.p.A., Via Pinerolo 44, 10060 Airasca (TO).

<http://www.skf.com/it/products/bearings-units-housings/ball-bearings/deep-groove-ball-bearings/deep-groove-ball-bearings/index.html?designation=W%20618/6>

⁴LUCHSINGER S.R.L., Via Bergamo 25, 24035, Curno, (BG).

<https://www.luchsinger.it/>



Figure 2.10: Torque-meter calibration, set up

Table 2.5: Calibration parameters

Parameter	Symbol	Value
Estimated torque generated by the arm	C	0.012 Nm
Arm length	h	$93.05 \pm 0.02 \text{ mm}$
Total arm weight	$M_{t,a}$	44.5 g
Acting arm weight	M_a	20.5 g
Balance pan weight	M_{bp}	51 g
Weighting scale sensitivity	$M_{ws,sen}$	0.5 g

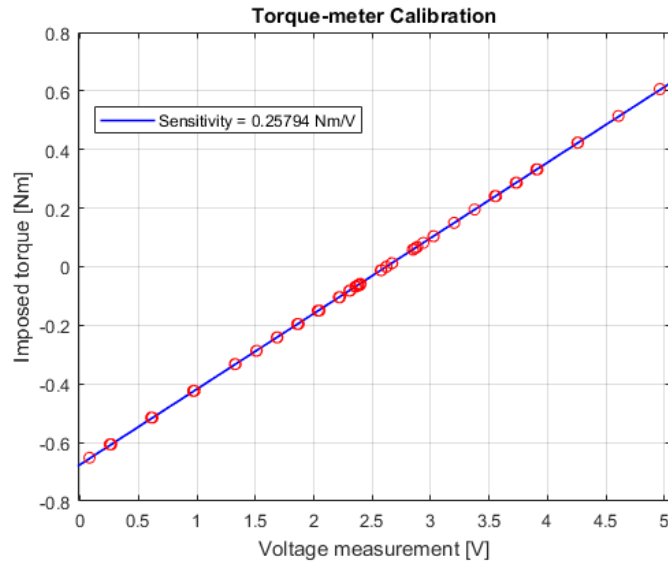


Figure 2.11: Torque-meter calibration, linear regression

Then the torque generated by the gravitational load (schematized as in Figure 2.12) is computed.

Finally, a statistical analysis of the results is performed and the results are

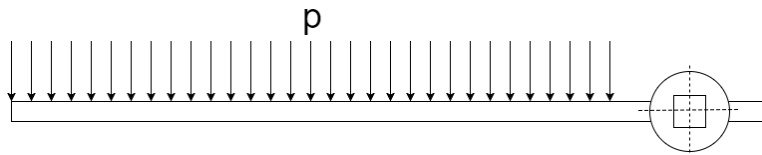


Figure 2.12: Model of the arm

reported in Table 2.6. Having a null P-value and a correlation coefficient very close to one and knowing that the calibration curve of a torque-meter should be linear the regression is successful.

The standard deviation of the data is calculated and will be summed with the uncertainty of each test result.

Table 2.6: Linear regression statistical analysis

Parameter	Symbol	Value
P-value	P	0.00
Correlation coefficient	R	0.999986
Standard deviation	σ	$1.59 * 10^{-3} Nm$
Sensitivity	S	$0.258 Nm/V$
Y-intercept	q	$-0.676 Nm$

2.1.5 Beam couplings

2 beam couplings MWS20-6-6-SS produced by Ruland⁵ are inserted in the kinematic chain before and after the torque-meter.

These elements allow only torque to reach the torque-meter, while angular



Figure 2.13: Helical coupling

misalignment, parallel offset and axial motion are compensated for. The maximum torque value that they can bear is guaranteed as $1.15 Nm$: higher than the estimated maximum torque required by the application, but lower than the dangerous level for the torque-meter ($3.75 Nm$) or the speed reducer ($6 Nm$), so that in case of overloads the couplings would break before the other elements.

⁵Ruland Manufacturing Co., Inc., 6 Hayes Memorial Drive, Marlborough, MA 01752
<https://www.ruland.com/>

2.1.6 Ball bearings

To support the shaft that connects the second beam coupling with the Oldham coupling, two deep groove ball bearings are selected. The chosen model is a W618/6 produced by SKF.

A check on the load applied to the bearings is performed to verify their compliance: since the loads acting on them are very small, but not easily separated from the one going through the support of the scissors and the cylinders supporting the torque-meter, an over-estimation is performed. Both an axial and a radial contribution are present: the axial contribution is due to the pre-load applied during the positioning on the scissors, while the radial contribution comes from the gravitational contribution of the shaft passing through the bearings and part of the beam coupling. The over-estimated values are reported into Table 2.7

The static and dynamic checks are performed according to [24] and the re-

Table 2.7: Linear regression statistical analysis

Parameter	Symbol	Value
Axial force	F_a	50 <i>N</i>
Radial force	F_r	9.81 <i>N</i>
Equivalent static load	P_0	34.9 <i>N</i>
Basic static load rating	C_0	224 <i>N</i>
Static safety coefficient	f_s	6.42
Equivalent dynamic load	P	9.81 <i>N</i>
Basic dynamic load rating	C_0	618 <i>N</i>
Expected life with 10% probability of failure	L_{10}	$2.5 * 10^{11}$

sults are reported into Table 2.7. The static safety coefficient is much higher than one, while the expected life is higher than 4000 *h* of test. Both tests are passed in a satisfactory way, thus the ball bearings are deemed suitable for the application from the load point of view.

The maximum speed is then checked: the limit for this kind of bearing is 67000 *rpm* which is much higher than the maximum velocity reached by the harshest motion law, which is equal to 26.67 *rpm*.

The mounting configuration is the one depicted in Figure 2.14. If the axial action is compressive from the Oldham side it gets to the ground from the

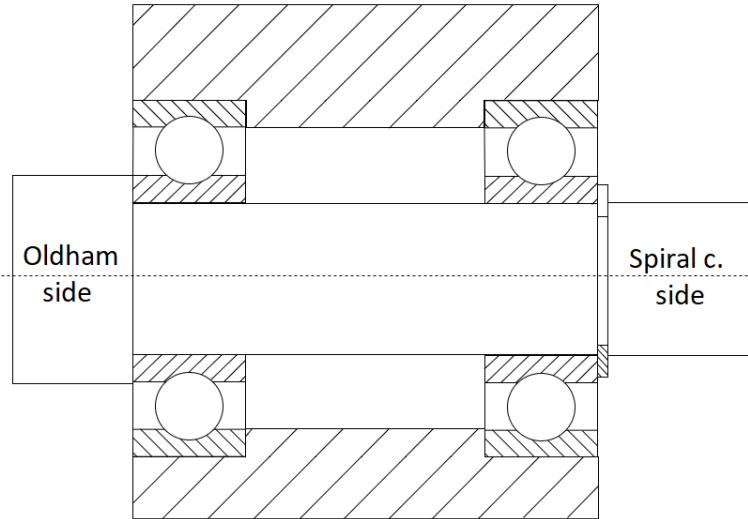


Figure 2.14: Mounting scheme of the ball bearings

shaft shoulder, through the bearing and finally on the housing shoulder. On the other hand, if the action is compressive from the beam coupling side, the action passes from the Seeger ring, through the bearing and finally on the housing shoulder.

2.1.7 Oldham coupling

To allow a quick coupling of the actuation part to the scissors, grant the absence of force perpendicular to the shaft axis and compensate small misalignments an Oldham coupling is inserted. This coupling (depicted in Figure 2.15) is made of three elements: the first element has a rectangular pit in the final disk of the shaft on the vertical direction in the installation position. The last element presents a horizontal pit in the installation position. These pits are required to accommodate the corresponding elements on the floating disk (central element in Figure 2.15). This disk is interposed between the two pits and can slide in them in such a way that small misalignments are compensated without the formation of forces perpendicular to the shaft axis.

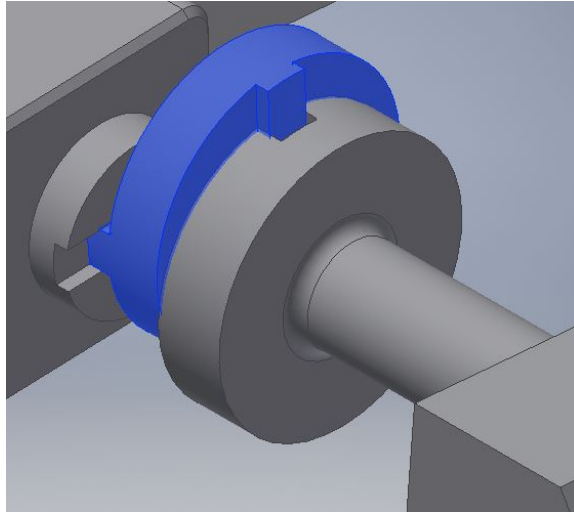


Figure 2.15: Oldham coupling

The optimum working condition for this coupling would be when there is no misalignment between the two shafts, but even in non-optimal condition its influence on the torque has experimentally been proven for this application as a second order effect and thus negligible.

2.1.8 Electrical connection

The electrical connection is designed as in Figure 2.16.

The main power supply is given to the control module through a bench power supply (J1 in Figure 2.16). This converts the grid 220 VAC to a value between 11 VDC and 36 VDC required by the EPOS2 control module.

The EPOS2 module in turn controls and supplies with electrical power the motor, the encoder, the Hall sensors and the two switches (J6, J8, J9 and J11 in Figure 2.16).

On the other hand, the power supply for the torque-meter is granted by the Scout 55, which also amplifies and filters the output signal from the transducer before sending it to the EPOS2 board (J11 in Figure 2.16).

Finally, the board is connected to a pc so that the on-line control can be

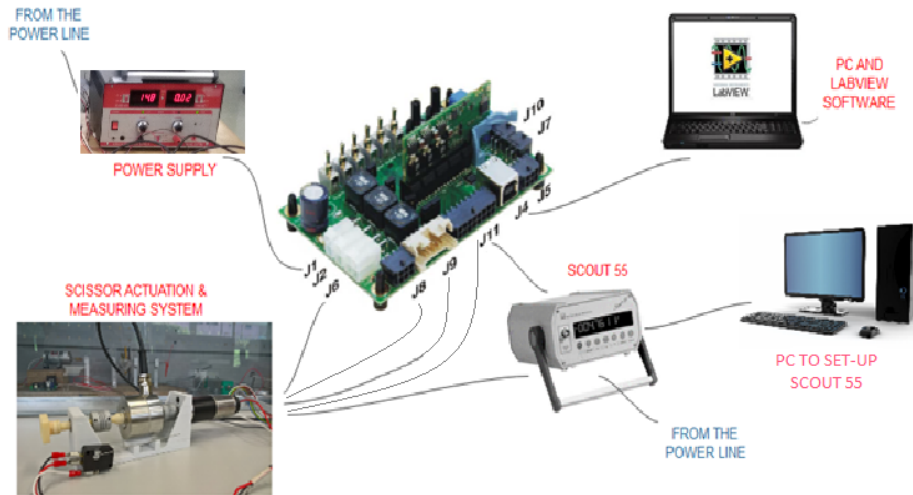


Figure 2.16: Wiring of the system

performed with the use of LabView software (J4 in Figure 2.16). In Table 2.8 are reported the specification of the above-mentioned connections.

Table 2.8: Electrical connection specifications

Connected elements	Electrical signal	Connector type
Grid to bench power supply	220 VAC	Standard IEC C13 Connector
Grid to Scout 55	220 VAC	Standard IEC C13 Connector
Bench power supply to EPOS2	ca15 VDC	Molex Mini-Fit Jr. 2 poles (39-01-2020)
EPOS2 to motor	max12 VDC	Molex Mini-Fit Jr. 4 poles (39-01-2040)
EPOS2 to Hall sensors	ca5 VDC	Molex Micro-Fit 3.0 6 poles (430-25-0600)
EPOS2 to encoder	ca5 VDC	DIN 41651 Plug, pitch 2.54 mm, 10 poles
EPOS2 from switches and Scout 55	0 – 5 VDC	Molex Micro-Fit 3.0 16 poles (430-25-1600)
Scout 55 to EPOS2	±10 VDC	BNC connector
EPOS2 to pc	5 VDC	USB type B, 4 poles

Scout 55 set-up

The connection between the torque-meter and the Scout 55 is performed by soldering the cables of the torque-meter on a VGA-DB15 male connector with the configuration depicted in Figure 2.17 and Figure 2.18.

The set-up of the Scout 55 parameters is initially performed through a pc

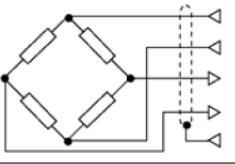
TRANSDUCCERS	OUTPUT	CABLE	CAVO
	EXCITATION+ EXCITATION - OUTPUT+ OUTPUT-	<i>Red</i> <i>Black</i> <i>White</i> <i>Yellow</i> <i>Shield*</i>	Rosso Nero Bianco Giallo Schermo*

Figure 2.17: Torque-meter specification

**S.G. and inductive full bridges
piezoresistive transducers**

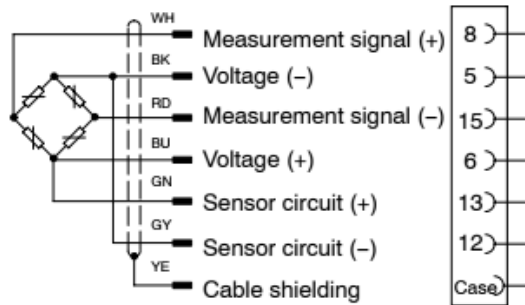


Figure 2.18: Scout 55 specification

connection and then those are stored in its memory for future use, thus the connection to the pc is no longer needed after this first phase (Figure 2.16). The parameters imposed are reported in Table 2.9.

The Butterworth filter is selected to have a flat magnitude in the passband with respect to the Bessel filter (the only other option available)[25].

The selection of the cutoff frequency starts instead by considering the time required for a fast opening of the blade $T = 0.4 s$. This value gives a first significant indication for the cutoff frequency $f_{min} = \frac{1}{T} = 2.5 Hz$. To avoid the filtering of significant oscillations during the positioning the first available cutoff frequency value at least one order of magnitude higher than this one is selected (Table 2.9).

Table 2.9: Scout 55 parameters

Parameter	Setting
Sensor type	Full bridge
Power supply	2.5 V
Input range	4 mV/V
Measurement range	2 mV/V
Type of filter	Butterworth filter
Cutoff frequency	40 Hz
Offset voltage	ca 2.5 V

An offset voltage is imposed because on the output port the Scout 55 gives a signal that varies between $\pm 10 V$, while the EPOS 2 module can accept on its analogue input only signals varying between $0 - 5 V$ (see Table 2.8). Giving this offset and since the used interval in the test performed is contained into the $0 - 5 V$ range, no further modification are required.

A possible improve on the machine could be a system able to convert the output signal from the $\pm 10 V$ to the $0 - 5 V$ range, so that the usable field would increase.

2.1.9 Initial positioning sytem

The scissors actuation functional group must be able to move along two different directions to work on scissors of different geometries: it must be free to move in the horizontal plane (x-z in Figure 2.19).

For this porpuse, the solution in Figure 2.19 is designed. A first slide along direction x (1 in Figure 2.19) allows the system to move in that direction for a distance of 200 mm. Then there is a plate (2 in Figure 2.19) with a series of holes in it and it is used to connect the first element with the one on top of it. In particoular there is a threaded hole for a nylon bolt (3 in Figure 2.19): by tightening this bolt on the base plate the system is fixed in the x direction.

On top of the plate there are two additional slides (4 in Figure 2.19) that allow the system to move along the z direction for a maximum distance of 75 mm. Also here to fix the system in the correct position there is a nylon

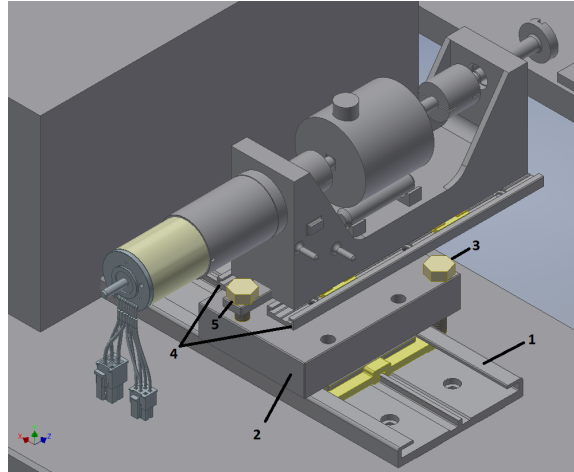


Figure 2.19: Initial positioning system for the scissors actuation functional group

bolt (5 in Figure 2.19).

2.2 Software development

The development of the software for the actuation of the scissors is performed on two different programs: EPOS Studio and LabView⁶. The procedure performed on EPOS Studio is required to set up the EPOS2 module characteristics, which are later used in the LabView program.

2.2.1 EPOS Studio

The procedure performed in EPOS STUDIO is composed by three main steps: the first one is done by using the Startup Wizard, the second by using the Regulator tuning tool and the third is the initialization of the analogue

⁶National Instrumens Corporation, via del Bosco Rinnovato 8, Pal.zo U4, 20090 Assago (MI)
<http://www.ni.com/it-it.html>

and digital ports.

Startup Wizard

In the Startup Wizard the data that characterise the set up are specified. The first required datum is the communication method: a standard USB type B cable with 4 poles plug is selected. Then the transfer rate is asked and it is set at 1 *Mbit/s* (maximum value allowed by the hardware). It is also specified the absence of a velocity auxiliary regulator.

Then the motor and encoder characteristics are specified as in Table 2.10. All the reported values are taken from the data sheet of each machine element.

Table 2.10: Motor-encoder parameters

Parameter	Value
Continuous current	2 <i>A</i>
Peak current	4 <i>A</i>
Pole pairs	1
Thermal time constant of the winding	3.25 <i>s</i>
Encoder counts	1000

Regulation tuning

After the initialization, the Regulator tuning is performed: to have a higher freedom in the selection of the parameters, the Expert Tuning is selected: here both the position and current regulators are set to obtain the wanted response.

This kind of cascade control allows to separate the electric dynamics from the mechanical one [26]. This is possible because the frequency ranges of the two domains are well separated (lower for the mechanical domain and higher for the electrical one by their very own nature [26]).

The tuning on the system must be performed with the full system set because the parameter selection is a function of the load applied to the system. Since the type of scissors tested will have different dimensions, the load will

be different and thus the optimal gain will be different in each case. For these reasons, a medium sized scissors are used in this phase and a robust choice of the gains is performed.

The tuning of the parameter is focused at first on the current loop and only later on the position loop; this is possible because the current loop is completely contained inside the position one and the frequency ranges are well separated. Thus, a tuning of this loop alone can be performed. The current loop is then seen as a simple transfer function by the outer position loop (corresponding to the sensitivity transfer function of the electrical part of the system [26]).

For the current regulator, a proportional integral control is selected. The derivative component is neglected being the current loop dynamics much faster than the mechanical one [26]. Three different gain values are tried: a so called soft regulator, a medium and a hard one. All the values are reported in Table 2.11.

The response of the system to those values are reported in Figure 2.20 a,

Table 2.11: Gain values for the current regulator

Type of regulator	Proportional gain	Integral gain
Soft	106	32
Medium	424	126
Hard	1131	336

2.20 b and 2.20 c. While the difference between Figure 2.20 a and 2.20 b is sensible (the time shift reduces visibly), the improvement deriving from increasing still the gains (Figure 2.20 c) is negligible, while the possibility of saturation in current is increased.

Thus for this loop, the gains are selected as the medium ones.

Then the tuning of the position loop is performed. The regulator chosen in this case is a proportional with integral and derivative action, to have zero steady state error (thanks to the integral contribution) and a fast-dynamic response (thanks to the derivative one)[26]. Again, a similar procedure is followed: three different reasonable group of values are chosen and tried on the full system (Table 2.12).

The response of the system in these conditions are reported in Figure 2.20 d,

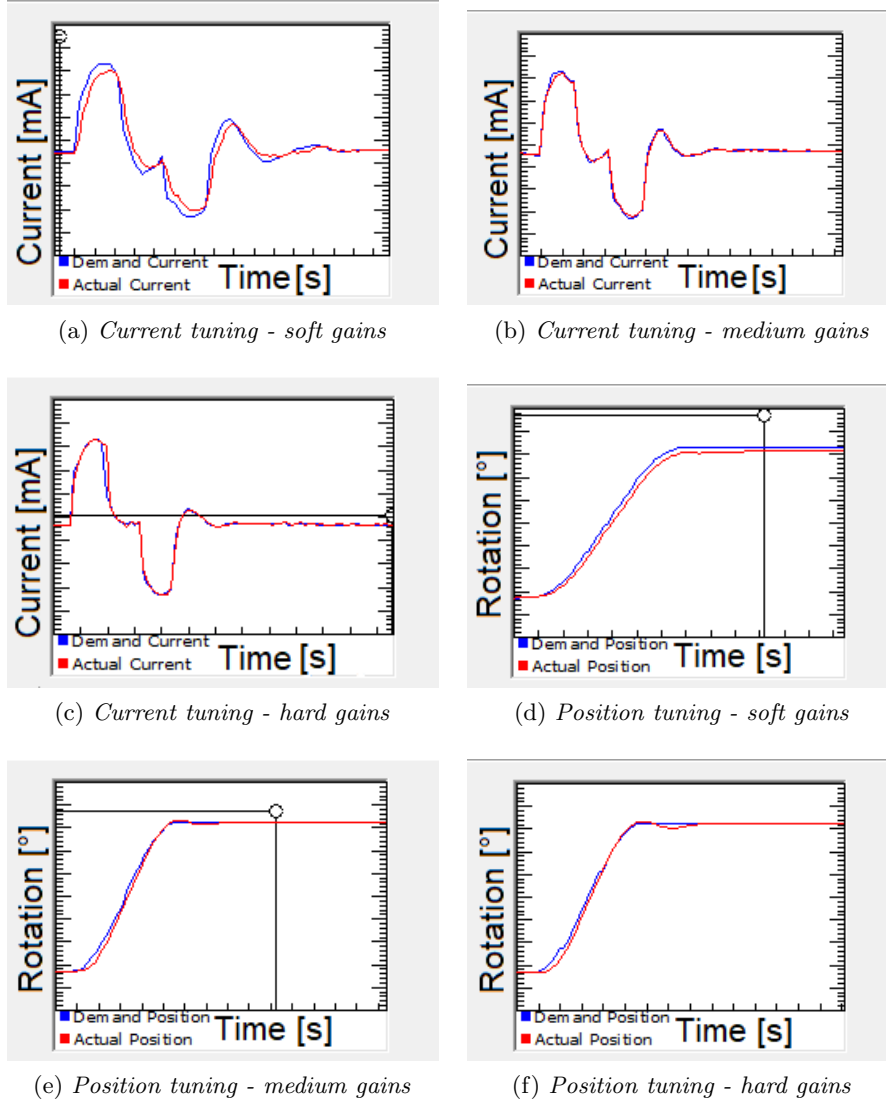


Figure 2.20: Responses of the system to different gain values

Table 2.12: Gain values for the position regulator

Type of regulator	Proportional gain	Integral gain	Derivative gain
Soft	95	114	252
Medium	219	906	282
Hard	309	1787	328

2.20 e and 2.20 f. In Figure 2.20 d it can be seen that the response of the system is significantly slower than the reference signal and the convergence to the steady state value is slow. On the other hand, with the hard gains (Figure 2.20 f) the response is characterized by visible undesired oscillations around the steady state value of the reference signal and an overshoot. So once again, the chosen values are the medium ones.

Port initialization

Finally, the initialization of the port is done with the I/O Configuration Wizard. The signals are in single ended configuration, thus only one port for each signal is required, while the other one is connected to one of the two ground ports (one is used exclusively for the torque-meter to minimize the noise). With this procedure six ports are initialized:

- 1 analogue input, for the signal coming from the torque-meter through the Scout55.
- 2 digital input ports, for the two switches that check that the cable of the torque-meter does not pass the limits on the rotational domain.
- 1 digital output to control the motor moving the cloth. A digital output is used because the EPOS2 board does not have any analogue output and the use of a second board would affect too much the run time of the program. This digital output is used to control the voltage of a power supply unit with suitable gains. No closed loop control is written, but a feedforward action is applied.
- 2 digital output to power the switches. For this application the “logic supply connector” of the board could be used but, since those two ports are not used otherwise, they are switched on at the beginning of the program and kept that way until the end.

With the initialization of the ports, the procedure on EPOS studio is completed and all the value are saved on the EPOS2 board, so that they are available when called by the LabView program.

2.2.2 LabView

Front panel

The front panel is the user interface part of the program and it is depicted in Figure 2.21.

It is composed by three main parts:

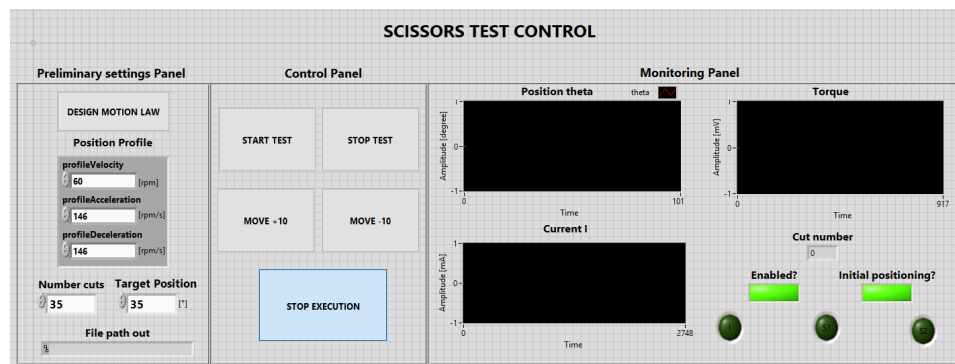


Figure 2.21: Front panel

- The preliminary settings panel, where the user can set the parameters of the motion law (with the limits of Table 2.13 because of motor limitations), the number of cuts that must be performed during the test and the opening angle that the scissors must obtain at each cycle.

In this part it is also visible the path where the output file (containing the position of the motor and the torque applied to the scissors) is saved.

Finally, once the simulation is started, by pushing the DESIGN MOTION LAW button, the parameters of the motion law and the Target Position can be changed. The effect of the changing of the parameters on the motion law can be seen in a graphical representation (the in-

Table 2.13: Limits of the motion law

Parameter	Available interval
profileVelocity	0 – 60 rpm
profileAcceleration	0 – 146 rpm/s
profileDeceleration	0 – 146 rpm/s

terface is visible in Figure 2.22).

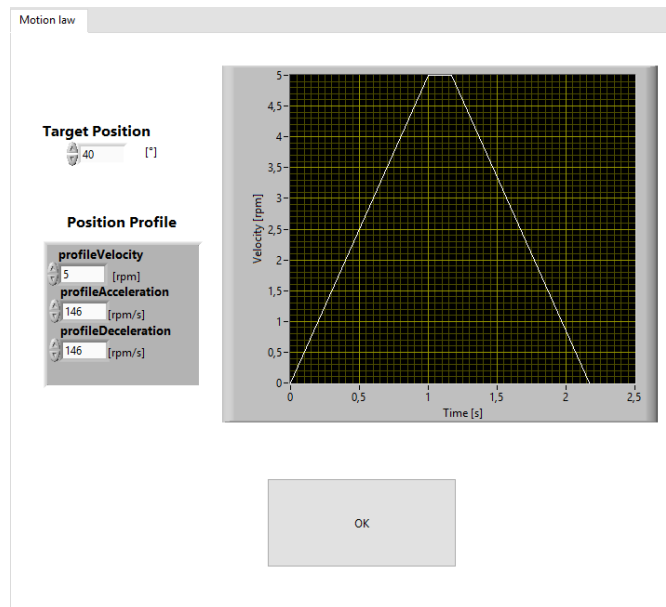


Figure 2.22: User interface of DESIGN MOTION LAW

- The control panel, there the user has five buttons that start the test procedure, stop the test (without interrupting the execution of the program), moves the motor of $\pm 10^\circ$, or stops the execution altogether.
- The monitoring panel, is the only panel where no action can be performed by the operator. Here the position measured by the encoder,

the current flowing in the motor armature and the torque measured by the torque-meter are plotted. Also, two leds signal if the motor is enabled to move and if the Initial positioning procedure has already been performed. Finally, three alarms signal respectively if there is saturation of the current or if one of the two switches is closed (three conditions for which the execution is aborted automatically to avoid damages to the system).

Block diagram

The block diagram is made of a basic list of actions. These actions either react to input from the user or are activated by default from the program at specific instants. A queue of operations is created to performe them in the wanted order.

To communicate with the EPOS2 board a series of LabView functions developed by Maxon motor for this kind of software structure are used.

The possible operations are:

- *Device settings* is always launched as first event at the beginning of the program. It opens a window (Figure 2.23) with the information related to the control board from which the information must be loaded. Once the opening is allowed, it loads all the parameters from the EPOS 2 control module that were set in EPOS studio (motor and encoder characteristics and control gains).

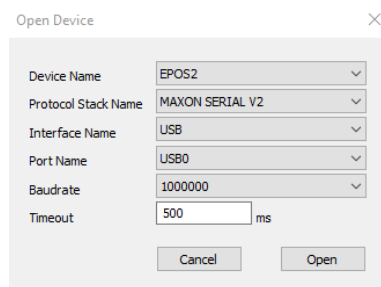


Figure 2.23: Window that opens the communication with the board

- *Enable* is launched right after *Device settings* and it allows the motor movement.
- *Show motion law* is activated every time the user presses the button DESIGN MOTION LAW and starts the routine that plots the motion law corresponding to the data inserted and allows to change the movement parameters (Figure 2.22).
- *Initial positioning* is the third default event and it is the first movement performed by the system. It must be performed before the installation of the scissors. When launched it sets the motor velocity in clockwise direction with a very low velocity (*5 rpm*) until the correspondent switch is closed. At this point the motor is switched off and the position is recorded. Then the same velocity is imposed in counterclockwise direction until the other switch is reached, at which point the movement is once again stopped and the position recorded. Finally, from the two previous known positions, the center point is calculated and this position is reached. This will be the position in which the scissors are closed. This movement is necessary to have the central element always oriented in the same direction regardless of the end position of the previous test performed. Also it places the cable of the torque-meter as far away from the switches as possible.
- *Move position* is the main test operation. It is started by the user clicking the START TEST button. It begins by opening the scissors of the angle indicated into Target Position and then the operation is stopped to allow the positioning of the cloth. During the setup of the cloth the execution is paused until the operator presses the button END OF INSTALLATION (Figure 2.24). Once the button is pressed the system performs as many cuts as specified into Number cuts with the motion law of Position Profile. When the test is finished the program keeps running waiting for further instructions.



Figure 2.24: Pausing program for the installation of the cloth

- *Move +10* is activated when the user presses the button MOVE +10. It imposes a rotation of 10° to the motor with motion law having maximum velocity, acceleration and deceleration as the one specified in Position Profile.
- *Move -10* similar to the previous case except for the direction of rotation.

The values of position and torque are stored in a previously selected folder (visible in File path out) in a *.TDMS* file. These output files are titled as *test_DATE_TIME* and they are automatically closed once the execution is stopped.

The sampling time of the output vectors is set by the hardware characteristics and it is equal to 0.02 s.

Chapter 3

Material feeding functional group

In this chapter, the design of the functional group that feeds the cutting material used on the machine is described. An alternative, more reliable and sophisticated system with the same aim, will be described into chapter 4. As chapter 2, also this one is divided into a hardware and a software development part.

3.1 Hardware development

3.1.1 Overview of the solution

This part of the machine (Figure 3.1) is made by the target material rolled up on a cylindrical element directly connected to an electric motor (1 in Figure 3.1). When the control program gives the order, this motor can unroll the cloth for a pre-defined amount of time. After that the cloth is stopped and the cutting performed.

Since there is not enough space for the cloth to pass parallel to the scissors actuation functional group in case of small scissors, a structure that bends the cloth and direct it toward the ground is added (2 in Figure 3.1).

To grant the pre-tensioning of the cloth and its advancement, a weight (3 in Figure 3.1) is attached to it on the part hanging from the table. The pres-

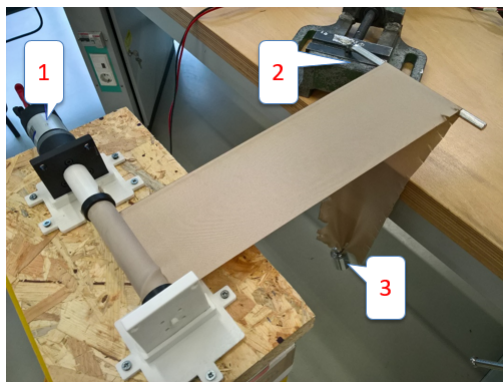


Figure 3.1: Overview of the functional group

ence of this weight prevent the system from doing more than 50 – 80 *cycles* in a row before the weight reaches the ground (this variability depends on the amount of advancement between each cut). At this point the process must be stopped and the weight repositioned closer to the table. Only then the test can start again.

3.1.2 Electric motor

The electric motor is a E192-24-67 produced by Micro Motors¹ and is the one that was used on the Premax machine to unroll the cloth. The main characteristics of this element are reported in Table 3.1.

The motor is experimentally tested in the working condition and the performances complied with the requirements for the application, thus it is adopted.

Advancement

The advancement of the cloth is a function of the speed of rotation of the motor and of the distance of the cloth from the axis of the motor itself. This distance is not constant but it is the sum of the base cylinder and the

¹Micro motors s.r.l, viale Piave 80/82, 23879 Verderio (LC).
<http://www.micromotors.eu/>

Table 3.1: Electric motor parameters

Parameter	Symbol	Value
Nominal voltage	V	24 V
Transmission ratio	τ	0.0149
Nominal torque	T_N	2200 mNm
Speed without load	ω_{max}	61.5 rpm
Speed at nominal torque	ω_{T_N}	45 rpm

quantity of cloth that is actually rolled up on it (Figure 3.2). Thus, if the same voltage is applied to the motor for the same amount of time with a different quantity of cloth rolled up, the advancement will be different.

This difference could be compensated by adding a transducer able to mea-

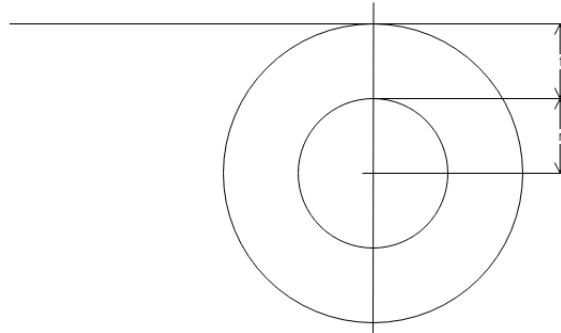


Figure 3.2: Influence of the thickness of the rolled cloth on the advancement

sure the thickness of the rolled-up cloth and computing the time to obtain the wanted advancement of the cloth for that particular thickness but, since such a precise advancement would not improve significantly the accuracy of the system, such a device is not introduced in this phase.

Still, to have a relationship between the time of application of the voltage to the motor and the advancement of the cloth, two different calibrations are performed:

- One with as few cloth as possible rolled up to have an indication of the most critical situation (where for the same time of application of the voltage, the advancement will be the least).

Table 3.2: Parameters influencing the advancement

Parameter	Simbol	Value
Cylinder radius	r	10 mm
Maximum thickness of the cloth	t	8.5 mm
Voltage applied	V	6.4 V

- And one with the maximum amount of cloth rolled up, to have the most distant condition from the previous one.

To test these two situations, the voltage is applied to the motor for different periods (spanning from 0 s to 2 s) in a random order and the relative advancement is measured. The results of these tests are depicted into Figure 3.3 and the parameters referring to the linear regression are reported into Table 3.3. Both linear regressions are satisfactory so the linear model can

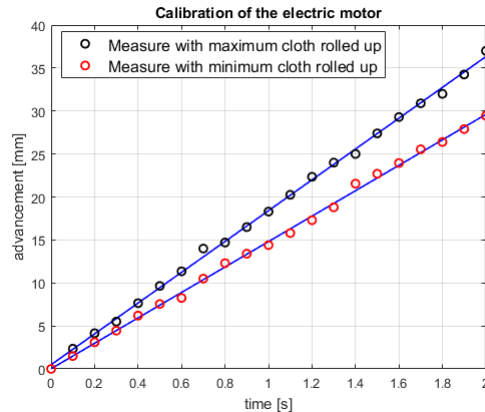


Figure 3.3: Electric motor calibration

safely be used. The sensibility selected will be very close to the safest condition (so the one with the minimum amount of cloth) and will be selected as equal to 15 mm/s.

If for example one wants to impose an advancement of 20 mm to the cloth an error due to the model will occur of -0.28 mm in the case of minimum cloth rolled on and 3.98 mm in case of maximum cloth rolled on. In any

Table 3.3: Calibration results

Parameter	Symbol	Value
Sensibility with minimum cloth	s_{min}	14.79 mm/s
Correlation coefficient minimum cloth	R_{min}	0.999
P-value minimum cloth	P_{min}	0.000
Sensibility with maximum cloth	s_{max}	17.92 mm/s
Correlation coefficient maximum cloth	R_{max}	0.999
P-value maximum cloth	P_{max}	0.000

other condition the error will be in this interval.

The error in the minimum case is negligible (being just the 1.4% of the wanted value), while in the maximum case it is significant (19.9%), but it increases the advancement, so it is considered acceptable.

3.1.3 Electric connection

The electric connection is made by two new elements with respect to the one that was already presented in 2.1.8 one is the electric motor and the other one is an additional bench power supply (Figure 3.4). This second

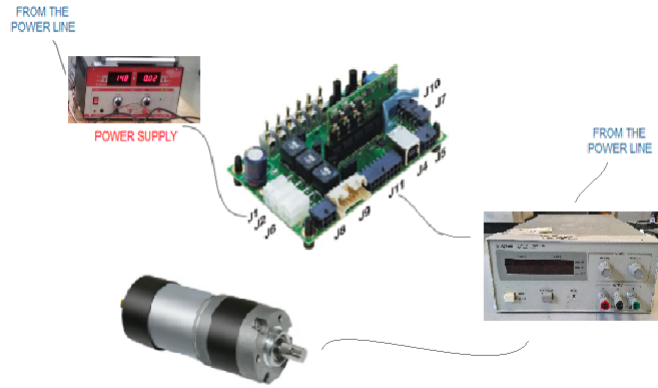


Figure 3.4: Electric connection of the material feeding functional group

element is required because a digital output is used to control the motor. The digital output gives a satisfactory voltage but a very low current. This signal is thus used to control the bench power supply which in turn amplifies the signal and gives an output suitable for the application.

The connectors used in the application are reported in Table 3.4

Table 3.4: Electrical connection specifications

Connected elements	Electrical signal	Connector type
Grid to bench power supply	220 <i>VAC</i>	Standard IEC C13 Connector
EPOS2 to bench power supply	0 – 5 <i>VDC</i>	Molex Micro-Fit 3.0 16 poles (430-25-1600)
Bench power supply to electric motor	6.4 <i>VDC</i>	Testing cables with hooked connector, 60 <i>V</i> , 2 <i>A</i>

3.1.4 Final designs

The design of the group used for the testing campaign was just a temporary solution. Both the structure supporting the motor and the one bending the cloth toward the ground are re-designed still with the same functionalities, but making the set-up operation easier for the operator.

The new design is depicted into Figure 3.5. The structure that supports

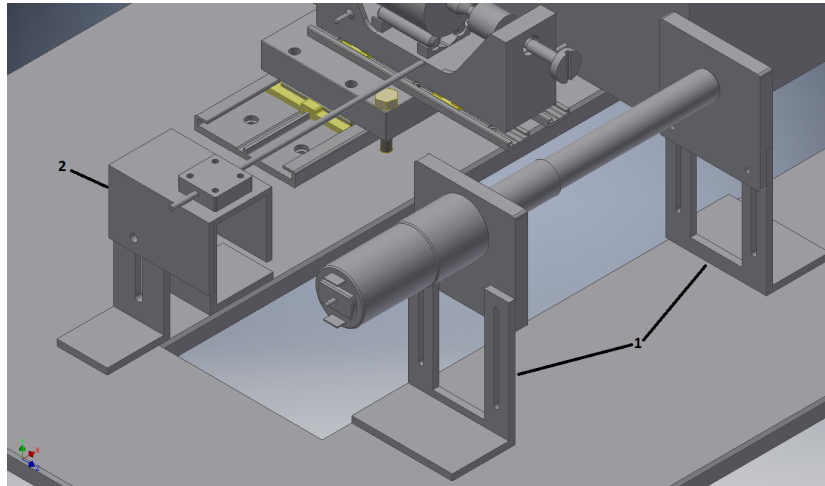


Figure 3.5: Final design of the material feeding functional group

the motor (1 in Figure 3.5) can be regulated along the vertical direction thanks to the grooves in which the bolt can slide when it is not tightened.

The structure can also be moved in the plane being the bottom part of the structure coated with Teflon. To block the movement some clamps are used. The structure that bends the cloth toward the floor (2 in Figure 3.5) has similar feature as the previous one: it can be regulated in the y direction and can be moved in the horizontal plane thanks to the Teflon coating.

3.2 Software development

The software is incorporated in the LabView program described into 2.2.2. Here, during the *Move position* operation there is an instance to move the cloth just after the installation (after the operator has pressed END OF INSTALLATION) before the first cut is performed (in case the cloth was still in the same position as at the end of a previous succesfull test) and another one in the main loop of the test after every cut operation.

Chapter 4

Improvements and additional functional groups

In this chapter the concept for three functional groups are described. These groups are either improvement of an existing one or a reproduction of a force acting on the scissors in real applications. These systems have not been implemented on the prototype, but they have been conceptually designed to be integrated in the existing machine and would be advisable as a future development of the project.

4.1 Improved material feeding functional group

The material feeding functional group could be improved because, as stated into 3.1.1, every 50 – 80 *cycles* the weight has to be repositioned to avoid touching the ground.

A layout that could solve this problem and would also grant control of the pre-load of the cloth is depicted in Figure 4.1.

This configuration is made of two motors: one controlled in force (1 in Figure 4.1) and one controlled in position (2 in Figure 4.1). The first one would set the pre-load on the cloth by pulling it with a C_t able to grant the wanted pre-load. The second motor instead would impose the wanted advancement of the cloth by moving it with a trapezoidal velocity trajectory that minimizes the time and keeps it still when the cutting operation

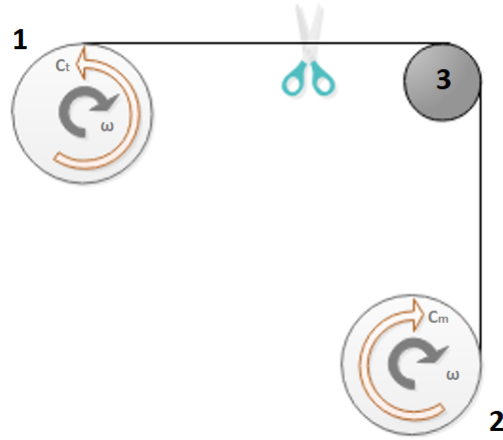


Figure 4.1: Layout of the improved material feeding functional group

is performed.

To implement this solution, some additional elements should be purchased: at least one brushless motor (to simply apply the control and the motion law on it, assuming that the old electric motor could be used for the force control) and a new control board able to control the three motors of the system. In fact a simple control as the one applied into 3.2 would not be sufficient for this application: at least two analogue outputs are required. Also, the new board should be able to control the motor that actuates the scissors, since the use of two boards in the same program would affect the run time of the program and reduce its reliability in term of punctuality of each cycle.

If a check on the actual value of the pre-load is wanted, a load cell could be added on the structure that changes direction to the cloth (3 in Figure 4.1). With the addition of this group the machine would be completely automatic: once the installation of the scissors and of the cloth (after the first opening of the blades) are done, the machine could operate cuts on cloth for an undetermined amount of time without need of any human intervention.

4.2 Tear cut functional group

An altogether new functional group could be developed to increase the information collectable by the machine. This group is the so-called tear cut functional group and its layout is depicted in Figure 4.2. This group would

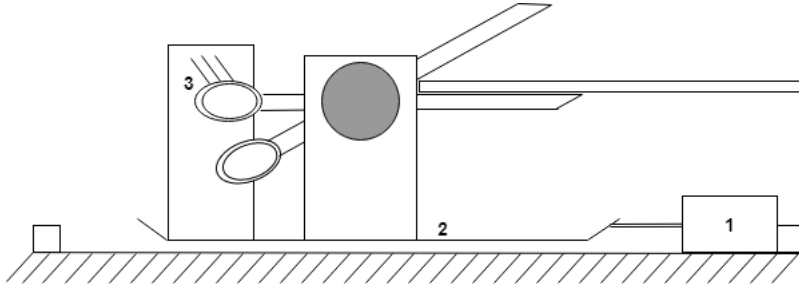


Figure 4.2: Layout of the tear cut functional group

reproduce a movement that is typically performed during the manual testing of the scissors: with the scissors blade closed on the cloth after a cut the whole scissors is pulled out of the cloth. If the cut was performed correctly the blade can disengage the cloth without any problem. On the other hand, if the cloth was not properly cut, with this movement the uncut part of the cloth that is pinched between the blades will be torn. This would in turn generate an increase in the force required to perform the movement.

The actuation would be performed with an electric motor using a transmission belt to pass from the rotational to the alternated movement. Also a stepper motor could be used for the application and would grant good performances with just a small investment.

To check for the increase in the force required for the performing of the motion a load cell could be mounted in parallel with the actuating group (motor plus transmission). On the other hand, if an electric motor is used, the increase in current alone could be used to check for the increase in the force [26] (this would not be possible with a stepper since the current absorbed is not a function of the load [27]).

To perform this motion and be able to continue the test, not only the scissors must be moved away from the target material, but also the scissors actuation functional group and the part that maintains still the other blade.

So, this whole part of the machine should be mounted on the transmission belt, thanks to a mechanical slide that allows the motion in the wanted direction. Once the tear cut movement has been performed the cloth could be advanced, the scissors opened and the slide with the scissors, the support and the actuation group put back in the original position to resume the test.

This movement would be performed only after a set amount of cuts as a check and not at every cut to avoid excessive increase in the test time.

4.3 Hand pressure functional group

Another functional group that could increase the quality and flexibility of the test would be the so-called hand pressure functional group. This system is made so that the lateral pressure applied with the palm of the hand on the scissors during the normal use is reproduced during the motion.

The force would be applied with the use of a helical traction spring connected to the ground on one side and, through a rope, to the scissors moved bow on the other (1 in Figure 4.3). To make the length of the rope move

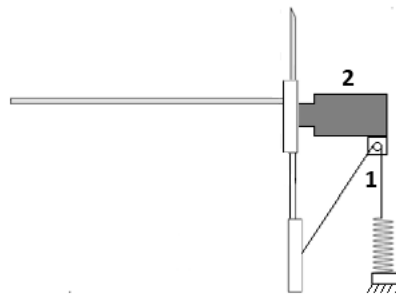


Figure 4.3: Layout of the hand pressure functional group

approximately on a circumference (and thus the force transmitted constant in magnitude even if not in direction), it should be directed thanks to a pulley mounted on the side of the scissors actuation functional group (2 in

Figure 4.3).

To make the value of the lateral force controllable, a set of springs with different stiffness should be available to the final user.

If left handed scissor are tested, the system would still apply the force in the appropriate direction with the same layout of the functional group by still attaching the rope to the moved blade.

Chapter 5

Experimental results

In this chapter the experimental campaign is described. To validate the system and perform an analysis on the influence of some parameters around 125000 cuts are performed.

This experimental campaign is not intended to fully characterize the scissors (a much higher number of tests would be required), but it is finalized to validate the design of the machine and show its potential.

This chapter describes at first the development of the software for the data analysis; then it deals with the selection of the parameters best suited for the characterization of the cut. A third part describes the performance of the system in terms of repeatability and reproducibility. The fourth and final part deals with the influence that different parameters have on the ability of the scissors to cut.

5.1 Analysis software development

To analyse the data obtained with the set-up described in chapter 2 and chapter 3 a software is developed with Matlab¹. This software has a basic structure which is later customized to extract the results of interest of each single test.

¹The MathWorks Inc, 1 Apple Hill Drive, Natick, MA 01760-2098, USA
<https://it.mathworks.com/>

5.1.1 Loading of the data

At first the loading of the data is performed: a loop with as many cycles as the number of file that must be loaded is used. Each time this cycle loads the .TDMS file of interest (whose name must be written before starting the program depending on the target data) into two structs. These structs contain all the information that are present in the .TDMS file (such as name, channel number, etc.), but for this analysis only the recording of position and torque are of interest. Thus, from the struct finalOutput the third and fourth set of data are extracted.

From the data, the part of the recording referring to before the starting of the actual test is eliminated and the sensibility of the torque-meter, that was obtained in 2.1.4, is applied to the torque value.

At this point the instant where the opening and closing operations start are searched: for this purpose, the position array is used since it is much cleaner than the torque one. The search can be divided into two phases: search for the first opening and closing and search for all the remaining one. The first element looked for is an opening.

The first opening is identified as the point right before the position passes the 0.5° . Then the first closure is looked for: it is identified as the point before the first one where the position is lower than the opening angle decremented of 0.5° and the difference between the position point and the previous one is negative. This operation works because the position signal cannot present a sign of the derivative different from the actual one, being it measured with an encoder.

The remaining openings and closings are searched at the same time by checking the position vector in its full length just one time (differently from the first two operations where the first vector was checked in all its length for each operation found) and the position recoded are:

- A point used to identify an opening must have three characteristics:
 - 1 A part of the slope is selected big enough to have a point for any possible value of velocity and far from the limit to account for eventual changing in the maximum and minimum position value during the test (Figure 5.1 around 18000 s).

$$\theta \in \left[\frac{\theta_{max}}{2}; \frac{\theta_{max}}{3} \right] \quad (5.1)$$

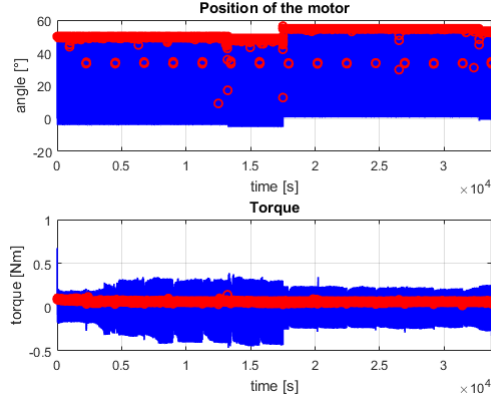


Figure 5.1: Step in the position due to a problem in the test, the software still finds the start of the operations correctly

- 2 The variation of the position with respect to the previous point must be positive to have an opening and not a closing movement.

$$\theta_i - \theta_{i-1} > 0 \quad (5.2)$$

- 3 The difference on the index of the opening must be safely distant from the previous one. This check is necessary to recognize each opening as just one in case there are more than one point in the part of the slope used to identify the operation (the slower the operation, the more points there will be). The difference between the index of two successive opening is function of the velocity of opening and must be regulated accordingly. The time required to perform the cut is known from the LabView software described into 2.2.2, which always compute this value to set the delay time in the execution to synchronize with the physical system. This value is used to set the minimum required distance between two operation of the same kind as the samples required to do an opening and a closing operation:

$$n_j - n_{j-1} > 2 \frac{T_{cut,calculated}}{t_{ris}} \quad (5.3)$$

- A point used to identify a closing must have three characteristics:

- 1 The slope is found with the same first check as before (5.1).
- 2 The slope must be negative.

$$\theta_i - \theta_{i-1} < 0 \quad (5.4)$$

- 3 The same third check as before is performed to recognize each closure as only one (5.3).

Each one of the points that have been identified is not the actual start of the operation, but a generic point on the slope because of the first check. So, to find the actual starting point of each operation a backward time shift must be applied. This time shift, like the minimum distance between two operations of the same kind (5.3), is a function of the speed of cut and must be regulated accordingly before the execution of the program.

To check the previous searching operations, the time vector is built (knowing the sampling frequency, $t_s = 0.02 \text{ s}$) and a plot like the one of Figure 5.2 is produce for each record.

There the green points are the points recognized as the start of the opening

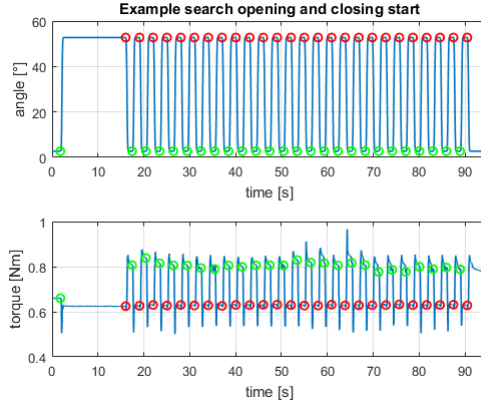


Figure 5.2: Example of search of the opening and closing cycle

operation, while the red ones are the starts of the closing cycles. Finally, to fully identify the position of each cut, the number of sample belonging to each cut must be computed: this parameter is function of the velocity of cut. Known the calculated cut time, the number of points that

must be considered as part of the cut can be computed as:

$$n_{pt,cut} = \frac{T_{cut,calculated}}{t_{ris}} \quad (5.5)$$

5.1.2 Analysis and plot of the results

Now that the position of each cut has been identified, in the second part of the script the parameters relevant for the analysis are computed and plotted. First the maximum torque and the RMS (root mean square, 5.6) of each j^{th} cut are computed.

$$RMS(T_{j^{th}cut}) = \sqrt{\frac{1}{N} \sum_{i=n_j}^{n_j+n_{pt,cut}} T_i^2} \quad (5.6)$$

Some interesting parameters are then plotted:

- The full history of each cut is plotted as a function of the cut angle and superimposed with all the other cuts histories, to check if there is anyone acting in a significantly different way (Figure 5.3).

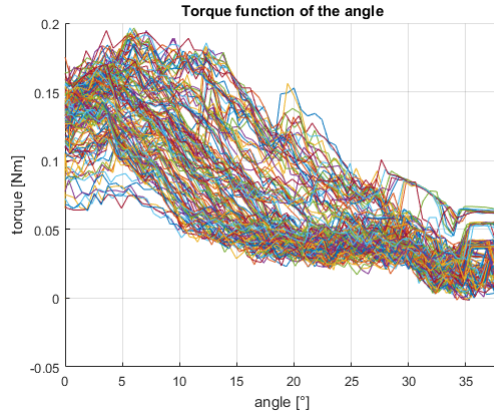


Figure 5.3: Example of superimposed torques as function of the scissors' angle

- The maximum torque value applied at each cut as a function of the cut order, to visually check if there is for this value a significant trend.
- RMS for each cut in the cut order, to check if there is a sensible variation or a significant trend in the measure of the mean power of the cut.

5.2 Characterizing parameters

To analyze the cutting torque three alternatives are considered: use the complete time history of the torque generated, use exclusively the peak values (maxima) of the cutting torque or use the RMS of the torque history at each cut. The first alternative is burdensome in terms of computational power and, most importantly, is hard to implement a constant and quantitative analysis at least for the purpose of interest of this paper; the second one could generate errors since the maximum value of the torque is a punctual parameter and thus it is deeply affected by localized noise. So, the best alternative is to use the RMS value which can describe the entire time history with the use of one single parameter. The RMS value of discrete time systems was defined into 5.6.

In Figure 5.4 the time history of two cuts are displayed with the relative

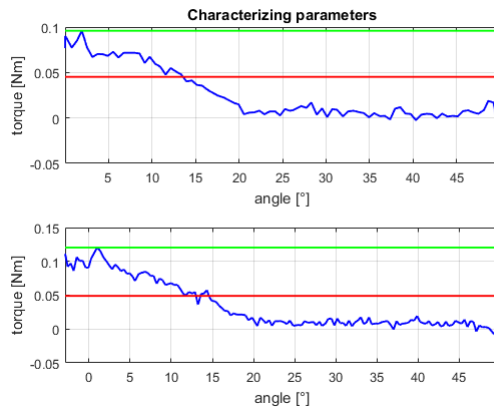


Figure 5.4: Example of characterizing parameters

maximum value (green line) and the RMS value (red line). Between the two cuts only 26 cuts were performed. Even though the two torques histories are similar, the maximum values are significantly different (Table 5.1). On the other hand the RMS values are very similar. This example shows how the RMS can describe the time history much better than the maximum torque.

Table 5.1: Comparison between similar cuts

Parameter	Symbol	Value
First maximum torque	$T_{max,1}$	0.093 Nm
Second maximum torque	$T_{max,2}$	0.118 Nm
First RMS value	$RMS(T_1)$	0.047 Nm
Second RMS value	$RMS(T_2)$	0.051 Nm

5.3 Repeatability and reproducibility

The first two analysis have the goal of testing the effectiveness of the mechanical system and of the control software by analyzing the repeatability and reproducibility of the cut results of consecutive cuts in two different test conditions:

- Repeatability of consecutive cuts.
- Repeatability of consecutive cuts with re-positioning of the target material.

5.3.1 Repeatability of consecutive cuts

Aim of the test is to perform consecutive cuts and monitoring the evolution of the RMS value. It can be reasonably assumed that for a low number of cuts the RMS value of the torque should exhibit negligible variations and thus the cuts can be considered as nominally equivalent. The tests are carried on using two different options to unwind the material object of the cut: unwinding using an electric motor and unwinding by hands. Two tests for both cases have been performed.

The first test is characterized by the following parameters:

- Partially worn scissors (few cuts performed before the test).
- Unwinding operation performed firstly using the electric motor and then by hand.
- 20 cuts performed for each test (number near enough to the statistical meaning for the identification of mean and standard deviation parameters, since it is reasonably a random Gaussian noise).
- Pre-tension applied to the material of 1.96 N .
- Trapezoidal (symmetric) motion law for scissors opening and closure ($\theta = 50^\circ$, $v = 60\text{ rpm}$, $a = 164\text{ rpm/s}$, $d = -164\text{ rpm/s}$).

In Figure 5.5 and Figure 5.6 are shown the RMS value of each cut operation to show that no relevant trend is detectable.

The results of the two acquisition are collected in Figure 5.7.

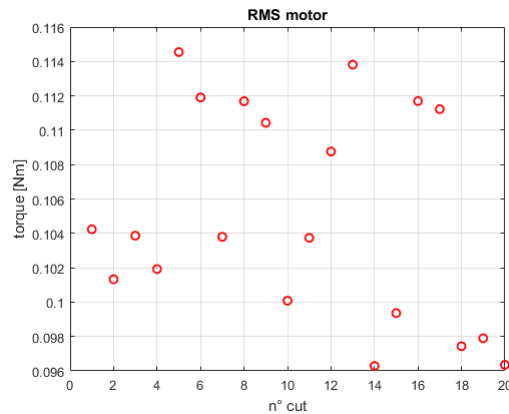


Figure 5.5: Test 1, RMS(T) with motor unwinding

The second test is equal to the previous one, except for the fact that unwinding by hand and motor are switched to isolate any influence of the test order.

This test is characterized by:

- Completely new scissors.

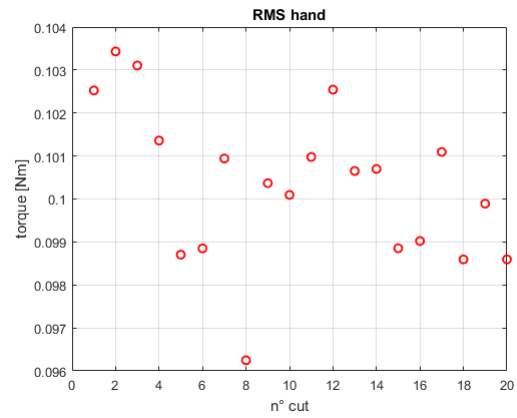


Figure 5.6: Test 1, RMS(T) with hand unwinding

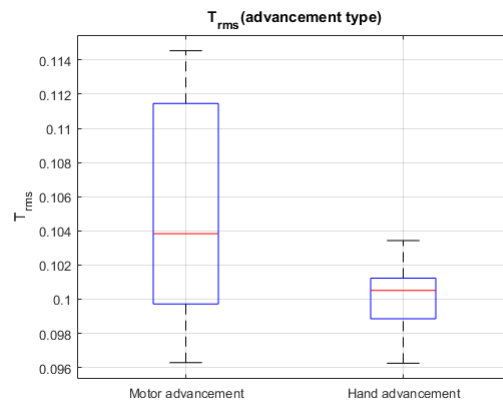


Figure 5.7: Test 1, RMS(T) boxplot comparison

- Unwinding operation performed at first by hand and then using the electric motor.
- 20 cuts performed for each test.
- Tension applied to the material of 1.96 N .
- Trapezoidal (symmetric) motion law for scissors opening and closure ($\theta = 50^\circ$, $v = 60\text{ rpm}$, $a = 164\text{ rpm/s}$, $d = -164\text{ rpm/s}$).

The same plots as in the previous case are reported (Figure 5.8-5.10).

The parameters that describe the dispersions in the two tests are reported

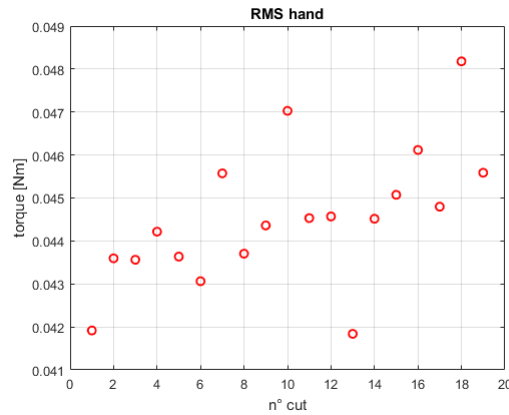


Figure 5.8: Test 2, RMS(T) with hand unwinding

into Table 5.2.

In all four cases the percental error on the RMS value is reasonably acceptable since it is always lower than 6.6%. This is even more true if the resolution of the torque-meter is considered: from the calibration done in 2.1.4 the resolution of the instrument was evaluated as 0.0016 Nm ; considering that the error in the different tests is always of the same order of magnitude of this value, it can be stated that the reproducibility error cannot be significantly improved with this set-up.

By comparing the results of each test, it can be noted that the use of the motor to unwind the target material increases the dispersion of the cuts (test 1 +4.12%, test 2 +2.08% on the standard deviation). Even so, the use of the

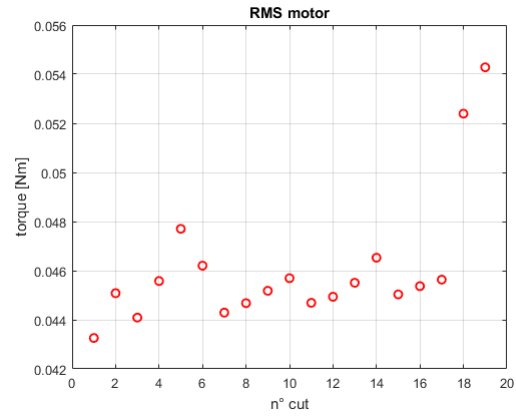


Figure 5.9: Test 2, RMS(T) with motor unwinding

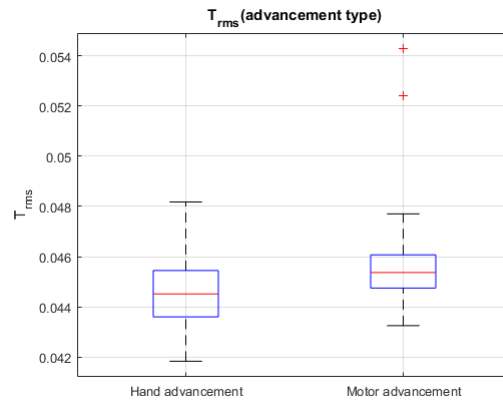


Figure 5.10: Test 2, RMS(T) boxplot comparison

Table 5.2: Repeatability of consecutive cuts

Parameter	Symbol	Value
Mean RMS motor advancement, test 1	$\mu_{RMS,m,1}$	0.105 <i>Nm</i>
Standard deviation of RMS motor advancement, test 1	$\sigma_{RMS,m,1}$	0.006 <i>Nm</i>
Mean RMS hand advancement, test 1	$\mu_{RMS,h,1}$	0.100 <i>Nm</i>
Standard deviation of RMS hand advancement, test 1	$\sigma_{RMS,h,1}$	0.002 <i>Nm</i>
% weight of σ on μ motor advancement, test 1	$\epsilon_{m,1}$	5.91 %
% weight of σ on μ hand advancement, test 1	$\epsilon_{h,1}$	1.79 %
Mean RMS motor advancement, test 2	$\mu_{RMS,m,2}$	0.046 <i>Nm</i>
Standard deviation of RMS motor advancement, test 2	$\sigma_{RMS,m,2}$	0.003 <i>Nm</i>
Mean RMS hand advancement, test 2	$\mu_{RMS,h,2}$	0.045 <i>Nm</i>
Standard deviation of RMS hand advancement, test 2	$\sigma_{RMS,h,2}$	0.002 <i>Nm</i>
% weight of σ on μ motor advancement, test 2	$\epsilon_{m,2}$	6.52 %
% weight of σ on μ hand advancement, test 2	$\epsilon_{h,2}$	4.44 %

Table 5.3: Repeatability of consecutive cuts

Parameter	Symbol	Value
Resolution torque-meter	r	0.002 <i>Nm</i>
Standard deviation of RMS motor advancement	$\sigma_{RMS,m,2}$	0.003 <i>Nm</i>
Standard deviation of RMS hand advancement	$\sigma_{RMS,h,2}$	0.002 <i>Nm</i>
% weight of σ on μ motor advancement	$\epsilon_{m,2}$	6.52 %
% weight of σ on μ hand advancement	$\epsilon_{h,2}$	4.44 %

motor is recommended especially for long tests: the dispersion can be low for a small number of cuts with advancement by hand carefully performed, but when the test time increases it would be hard to keep a constant and reliable advancement in a manual operation.

There seems to be also a slight influence of the type of advancement on the mean value but this effect (whose significance could be checked with and hypothesis test) is negligible since only tests with the same type of advancement will be compared from here on.

5.3.2 Repeatability of consecutive cuts with re-positioning

Another factor that may influence the repeatability of consecutive cuts is the operation of re-positioning of the target material and the weights hung to the material to provide the tensioning. The operation of re-positioning previously mentioned is necessary since, to obtain a nearly constant pre-load on the material, a weight is hung to the free-falling edge of the strip of cloth. During the testing operation, the hung weight gets closer and closer to the ground. To avoid contact between the weight and the floor (that would significantly change the pre-tension value), the cutting operation is stopped before contact occurs and the weight is re-positioned further up on the material. When the re-positioning is done, the test resumes from where it was stopped. To quantify the effects of the re-positioning two tests are performed.

The first test is characterized by:

- Partially worn scissors (few cuts performed before the test).
- Tension applied to the material of 1.96 N .
- Trapezoidal (symmetric) motion law for scissors opening and closure ($\theta = 50^\circ$, $v = 60\text{ rpm}$, $a = 164\text{ rpm/s}$, $d = -164\text{ rpm/s}$).

Firstly 25 consecutive cuts are performed and the relative values of RMS are computed; each RMS is then compared to the next one so to depict only the variation of the cutting power required to perform the cuts.

Then 50 cuts, each couple with re-positioning between them, are analyzed and the relative values of RMS are computed; each value is subtracted from

the next one so the variation of the cutting power between the two cuts before and after the re-positioning operation is isolated. The cut before the re-positioning is the last of a series of 8 consecutive cuts used to stabilize the reading of the system.

The results are shown in Figure 5.11. The populations are so low that the

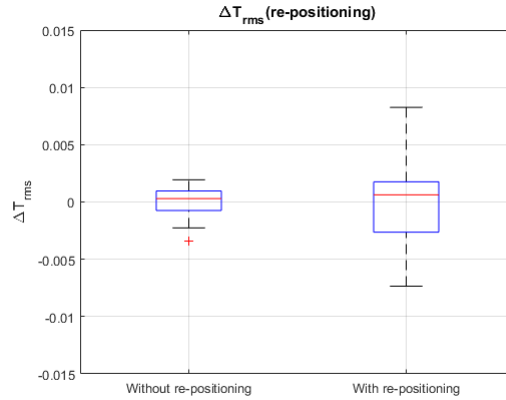


Figure 5.11: Test 1, RMS(T) boxplot comparison

probability density function can hardly be identified, but an higher number of test would further increase the influence of the dulling of the blade. Still a variation on the mean value between the two distributions and, more importantly, an increase of the standard deviation are observed. To assess the statistical relevance of these two differences, two hypothesis tests are performed:

- a two samples t-test (23 degrees of freedom, with different standard deviation) to check if the difference between the mean values is significant, where the null and alternative hypothesis are:

$$H_0 : \mu_1 - \mu_2 = 0 \quad (5.7)$$

$$H_1 : \mu_1 - \mu_2 \neq 0 \quad (5.8)$$

The p-value obtained (reported in Table 5.3) is higher than the highest used level of statistical significance, $25.6\% > 10\%$, thus the null hypothesis is accepted and the two distributions have statistically the

same mean value.

- a test for two variances (with both Bonett and Levene method), where the null and alternative hypothesis are:

$$H_0 : \frac{\sigma_1}{\sigma_2} = 1 \quad (5.9)$$

$$H_1 : \frac{\sigma_1}{\sigma_2} \neq 1 \quad (5.10)$$

Since in both cases the p-value is lower than the significance level, $0.8\% < 5\%$ and $1.1\% < 5\%$, the null hypothesis is rejected and, thus, the ratio of the standard deviations is statistically different from 1. The ratio is in the confidence intervals reported in Table 5.3 with a confidence level of 95%.

A second similar test is performed to verify the consistency of the results, but the order of consecutive cuts and cuts with re-positioning operation is exchanged to isolate influences of the test order.

The second test is characterized by:

- Completely new scissors.
- Tension applied to the material of 1.96 *N*.
- Trapezoidal (symmetric) motion law for scissors opening and closure ($\theta = 50^\circ$, $v = 60 \text{ rpm}$, $a = 164 \text{ rpm/s}$, $d = -164 \text{ rpm/s}$).

The results of this second series of tests (Figure 5.12) are once again analyzed with the same two tests and similar results are obtained ($p_\mu = 17.6\% > 10\%$, $p_{\sigma,B} = 2.2\% < 5\%$ and $p_{\sigma,L} = 0.9\% < 5\%$).

The results are in accordance with what theoretically expected: although the mean value changes the changing is so low that is not statistically relevant; on the other hand, the changing in the standard deviation is significant and it is generated by the extensive changing in the boundary conditions of the problem (such as pre-load, orientation of the cloth, etc.).

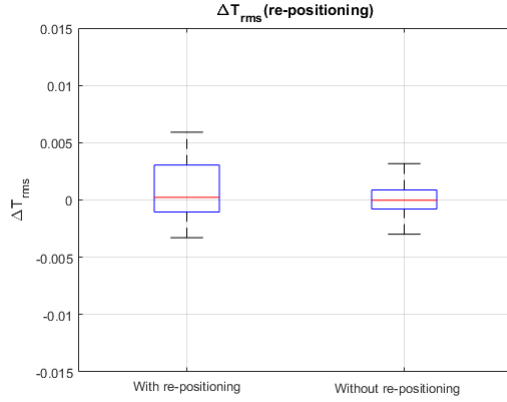


Figure 5.12: Test 2, RMS(T) boxplot comparison

Table 5.4: Effect of the re-positioning

Parameter	Symbol	$1^{st} test$	$2^{nd} test$
Mean value without re-positioning	$\mu_{no,rep}$	$-9.1 * 10^{-5} Nm$	$9.1 * 10^{-5} Nm$
Mean value with re-positioning	μ_{rep}	$0.0012 Nm$	$0.0017 Nm$
P-value two samples t-test on mean	p_{μ}	0.256	0.176
Standard deviation without re-positioning	$\sigma_{no,rep}$	$0.0014 Nm$	$0.0018 Nm$
Standard deviation with re-positioning	σ_{rep}	$0.0050 Nm$	$0.0050 Nm$
Estimated ratio of the standard deviations	α	3.55	2.72
95% confidence interval for ratio using Bonett	$\alpha_{95,B}$	(1.488; 7.296)	(1.196; 5.461)
P-value Bonett	$p_{\sigma,B}$	0.008	0.022
95% confidence interval for ratio using Levene	$\alpha_{95,L}$	(1.563; 9.777)	(1.380; 4.968)
P-value Levene	$p_{\sigma,L}$	0.011	0.009

5.4 Influence of process parameters on the cutting torque

After the validation of the system and identification of its reliability, in the second part of the testing campaign the influence of some test parameters on the cutting torque is analyzed. These parameters are the one that have been studied in the knife case in 1.4.

5.4.1 Influence of pre-tensioning of the material

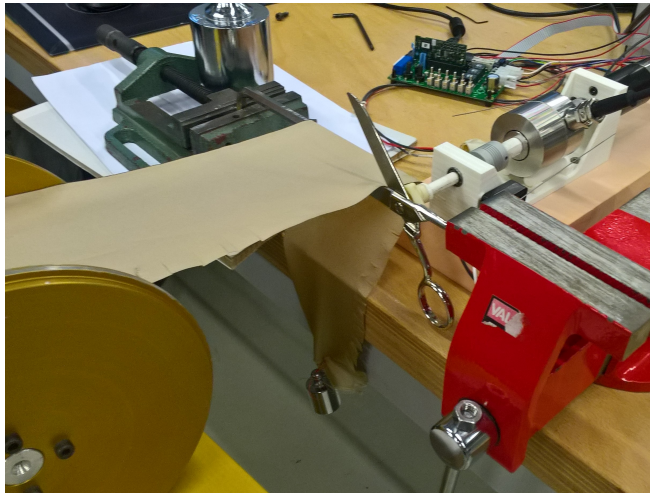


Figure 5.13: Set-up used to analyze the pre-tensioning influence

The effect of the pre-tensioning of the target material on the RMS of the torque is analyzed. In Figure 5.13 the set-up used to perform the experiments is shown.

The tension on the strip of material is generated hanging to the free-falling end of the strip of cloth a calibrated weight. The weights vary from very low values (50 g) up to higher ones (500 g in the first three tests and 1000 g in the last one). These tests are once again performed under the assumption that, for a low number of cuts, the dulling of the blade has negligible influence on the cutting capability.

The first test characteristics are:

- Completely new scissors.
- 1 acquisition for each pre-load value.
- 10 cuts for each value of the pre-load.
- Random order of application of the pre-tension.
- Trapezoidal (symmetric) motion law for scissors opening and closure operation ($\theta = 50^\circ$, $a = 164 \text{ rpm/s}$, $d = -164 \text{ rpm/s}$).

The second test characteristics are:

- Partially used scissors .
- 1 acquisition for each pre-load value.
- 5 cuts for each value of the pre-load.
- Random order of application of the pre-tension.
- Trapezoidal (symmetric) motion law for scissors opening and closure operation ($\theta = 50^\circ$, $a = 164 \text{ rpm/s}$, $d = -164 \text{ rpm/s}$).

The third test characteristics are:

- Complitley new scissors.
- 1 acquisition for each pre-load value.
- 10 cuts for each value of the pre-load.
- Random order of application of the pre-tension.
- Trapezoidal (symmetric) motion law for scissors opening and closure operation ($\theta = 50^\circ$, $a = 164 \text{ rpm/s}$, $d = -164 \text{ rpm/s}$).

The results of these tests are depicted in Figure 5.14 - 5.16. By visually analyzing them it can clearly be seen that there is no trend detectable neither as a function of the pre-load applied to the target material nor as a function of the number of test.

At this point a further analysis is tried: the previous test are repeated once

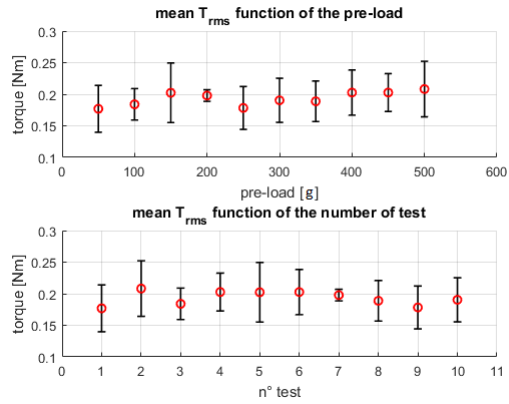


Figure 5.14: Test 1, influence of the pre-tensioning

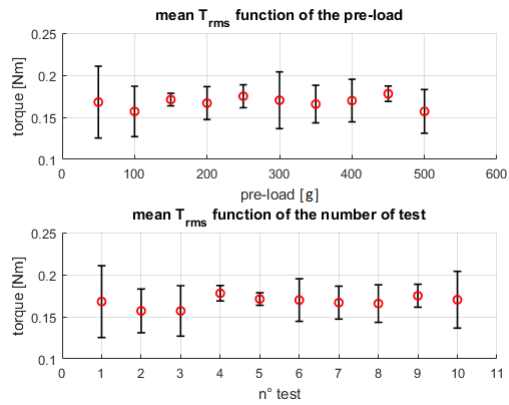


Figure 5.15: Test 2, influence of the pre-tensioning

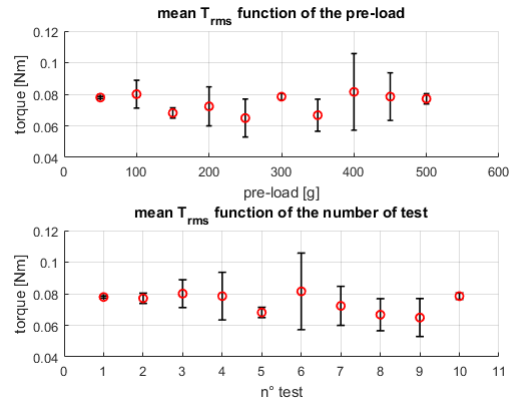


Figure 5.16: Test 3, influence of the pre-tensioning

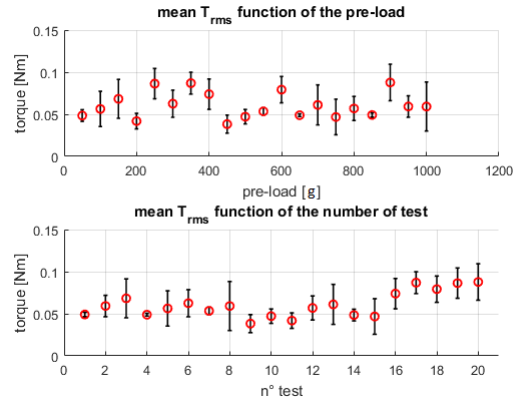


Figure 5.17: Test 4, test with higher pre-load

more with new scissors and with a pre-load that reaches 1 kg in order to verify if there is a threshold value for which an appreciable influence of the pre-load is detected. As can be observed in Figure 5.17, even in this case the results lead to the same conclusion as the previous tests.

5.4.2 Velocity influence

In this section the influence of the maximum velocity reached during the cut on the RMS value is analyzed. Two different tests are performed.

The first test characteristics are:

- Partially worn scissors (few cuts performed before the test).
- One single acquisition containing all the velocity ranges.
- 4 cuts performed for each value of the velocity.
- Before each changing of the velocity parameter, a re-positioning action is performed.
- Tension applied to the material of 1.96 N .
- Trapezoidal (symmetric) motion law for scissors opening and closure ($\theta = 50^\circ$, $a = 164\text{ rpm/s}$, $d = -164\text{ rpm/s}$).
- Random order of the different velocities.

The tests results (shown in Figure 5.18) may present a cubic or tangential trend of the RMS as a function of the maximum velocity. To confirm this trend a second test is performed, characterized by:

- Completely new scissors
- 1 acquisition for each velocity value.
- 4 cuts performed for each value of the velocity.
- No re-positioning actions performed.
- Tension applied to the material of 1.96 N .

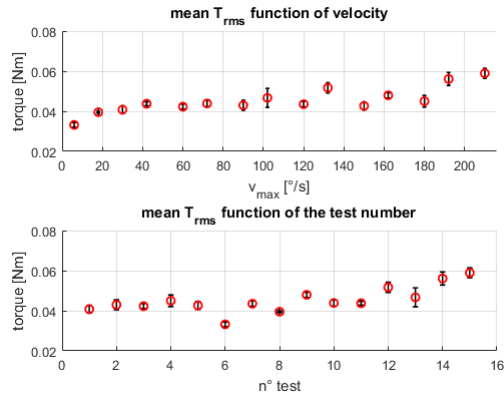


Figure 5.18: Test 1, influence of the velocity

- Trapezoidal (symmetric) motion law for scissors opening and closure ($\theta = 50^\circ$, $a = 164 \text{ rpm/s}$, $d = -164 \text{ rpm/s}$).
- Random order of the different velocities.

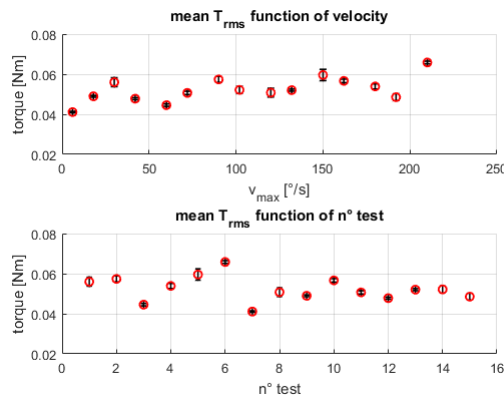


Figure 5.19: Test 2, influence of the velocity

The results are depicted into Figure 5.19. This second test disproves the possible trend of the previous one, in fact no trend can be detected neither as a function of the maximum velocity, nor as a function of the number of

test.

This result is further validated by the comparison with the knife case: as already stated into 1.4 the influence of the cutting velocity on the cut ability is negligible.

5.4.3 Influence of the resistance of the cut material

The effect of the cut material resistance on the RMS of the cutting torque is analyzed in this section. It is supposed that more or less resistant materials will affect differently the cutting torque generated by the scissors. To carry out the tests it was decided to use sheets of paper with different weights (ranging from no material at all to 300 *g*) and this value is used as measurement of the resistance of the material. Two tests are performed.

The first test characteristics are:

- Partially worn scissors (few cuts performed before the test).
- 10 cuts performed on each sheet of paper (or no paper).
- No tension applied to the material.
- Trapezoidal (symmetric) motion law for scissors opening and closure ($\theta = 40^\circ$, $v = 60 \text{ rpm}$, $a = 164 \text{ rpm/s}$, $d = -164 \text{ rpm/s}$).
- Radom order of the sheets.

The second test characteristics are the same as the previous one except for the use of a different model of scissors.

The results obtained from these two tests are shown in Figure 5.20 and Figure 5.21.

From the results it can be observed that a linear increasing trend is detectable and it is proportional to the weight of the paper.

The results of the linear regression are reported in Table 5.4. Since in both cases the P-value is lower than 5% the linear regression is successful and the linear trend as a function of the material resistance is verified.

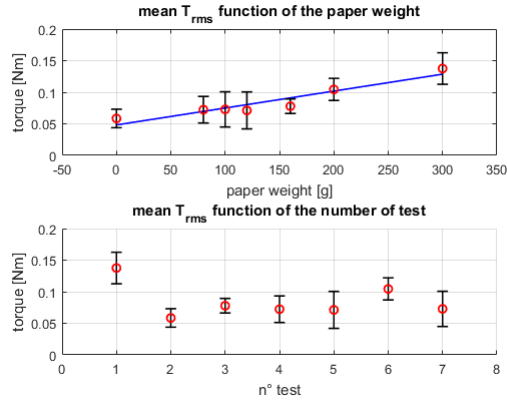


Figure 5.20: Test 1, influence of the resistance of the cut material

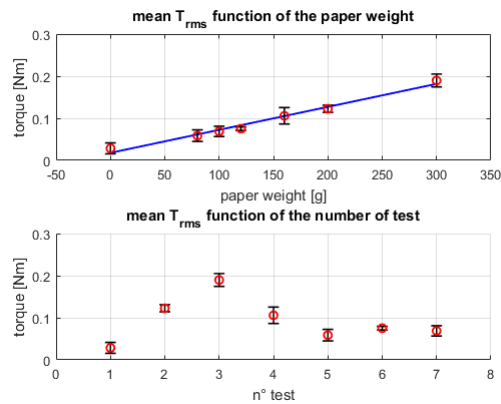


Figure 5.21: Test 2, influence of the resistance of the cut material

Table 5.5: Linear regression, influence of resistance of the material

Parameter	Symbol	Value
P-value, test 1	P	0.001
Correlation coefficient, test 1	R	0.946
P-value, test 2	P	0.000
Correlation coefficient, test 2	R	0.991



Figure 5.22: Nicked blade

5.4.4 Influence of nicks on the blade

The effect of a nick on the blade has already been studied in the literature dedicated to knives and blades. The idea of this test is to verify if those results may be translated to the scissors case. The test showed that when a blade of the scissors is nicked (even if the damage is hardly visible as showed in Figure 5.22) a peak in the torque value between a cut and the subsequent one can be detected. The peak occurs for a value of the closing angle equal to the value of the angle at which the nick is located (Figure 5.23).

Another interesting aspect can be observed by looking at the torque history of some cuts before and after the presence of the nick: the pick in the torque is localized only on the cut immediately after the application of such a small nick (red curve in the second plot of Figure 5.24), while for successive cuts it is much less distinguishable. On the other hand, it can clearly be seen that the presence of the nick causes an increase in the maximum torque value. All these results confirm the one already obtained in the case of knives (see 1.4).

5.4.5 Wear of the scissors, test on cloth

Aim of this test is to analyze the duration of scissors and if they can maintain their cutting capability after having performed several cutting cy-

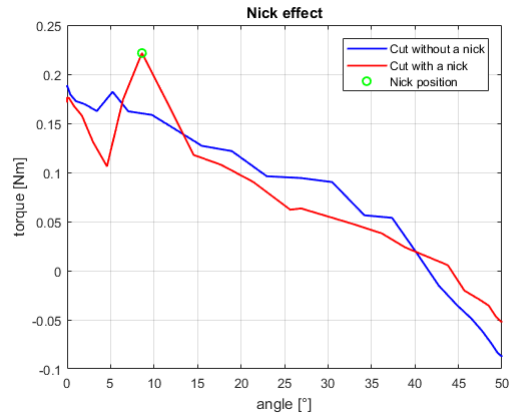


Figure 5.23: Effect of a nick on the blade

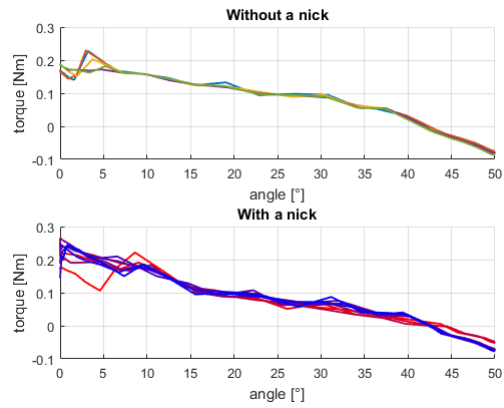


Figure 5.24: Effect of a nick on more than two cuts

cles on a target material.

The test characteristics are:

- Completely new scissors.
- 3000 cutting cycle analyzed.
- Tension applied to the material of 1.96 N .
- Trapezoidal (symmetric) motion law for scissors opening and closure ($\theta = 50^\circ$, $v = 60\text{ rpm}$, $a = 164\text{ rpm/s}$, $d = -164\text{ rpm/s}$).

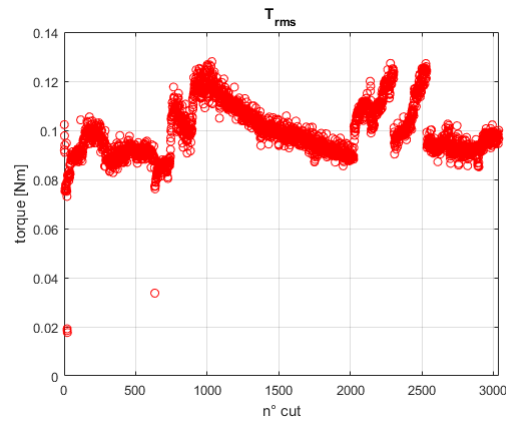


Figure 5.25: Test fully on cloth

The idea is to verify if after 3000 cycles the scissors exhibit symptoms of wear by analyzing the evolution of the RMS of each cutting operation.

As it can be observed in Figure 5.25 the test results are affected by many steps on the history that tend to hide any useful information. Anyhow, the variation of the RMS for 3000 cycles is of the order of 0.03 Nm and the scissors do not present any sign of wear at a manual testing operation.

It was already established by experience of workers of the field that scissors can be considered as new after they have performed 3000 cycles cuts and they start showing wear much closer to the order of 10000 cycles. So, the next step is to greatly increase the number of cycles by doing many blank closures alternated with groups of cuts on cloth that are used as a control parameter.

5.4.6 Wear of the scissors, test alternated blank/cloth cuts

As previously mentioned the idea of this section is to analyze if largely increasing the number of cycles allows the system to observe any significant wearing phenomena. For this reason, the number of cycles is raised from 3000 to 30000. In detail, the procedure for the test is performing 10 cuts on cloth and analyze the RMS (mean value and standard deviation), then performing 2000 blank cuts and repeat this procedure for 15 times.

Traditional scissors for nails

The first test parameters are:

- Completely new scissors.
- 30000 cutting cycle analyzed.
- Tension applied to the material of $1.96 N$.
- Trapezoidal (symmetric) motion law for scissors opening and closure ($\theta = 50^\circ$, $v = 10 rpm$, $a = 164 rpm/s$, $d = -164 rpm/s$) for the cuts on cloth.
- ($\theta = 50^\circ$, $v = 60 rpm$, $a = 164 rpm/s$, $d = -164 rpm/s$) for the blank cuts.

The maximum velocity value during the cutting operation on cloth is set so low to have many sampling points and thus an higher resolution on the torque curve (the sampling frequency is the same, but the temporal length of the curve is increased). On the other hand, in the blank cuts the velocity is maximised to decrease the test time.

The results obtained clearly exhibit a decreasing trend of the cutting torque as the number of cycles increases (Figure 5.26). A decrease of about 40% of the maximum RMS value is clearly visible after 22000 cycles of work. The reason of such behavior could be a gradual loosening of the pivot-bolt of the scissors. Since this possibility was accounted for before the test, a picture of the scissors' screw was taken before performing each test on cloth (and also after the end of the test). Three relevant picture are depicted in Figure 5.27. A variation in the angle in the three cases is found and the

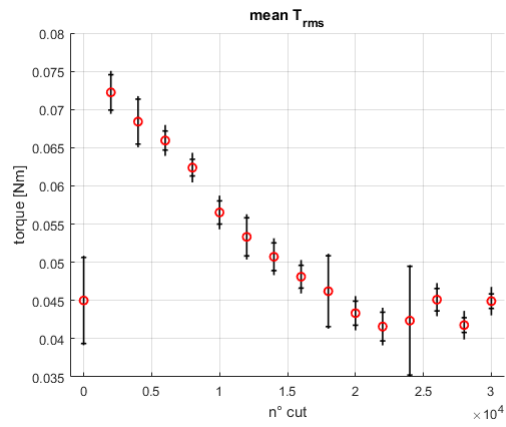
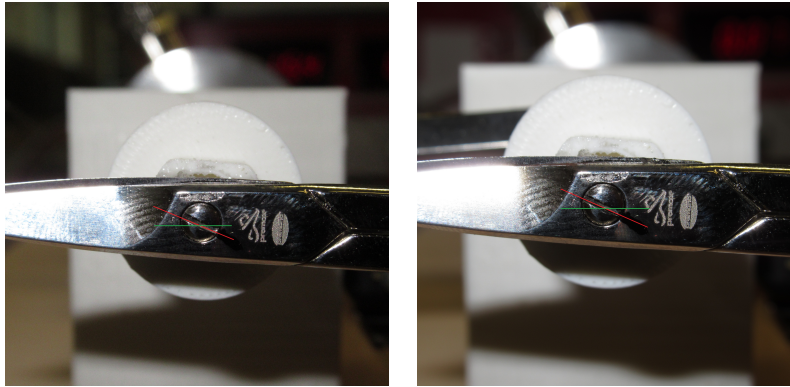


Figure 5.26: Test 1, type of closure alternated

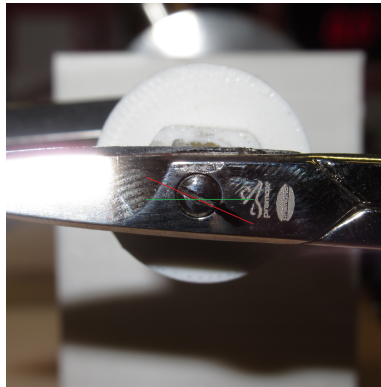
Table 5.6: Linear regression, influence of resistance of the material

Parameter	Symbol	Value
Screw angle before the test	α_{before}	22.6°
Screw angle after 22000 blank cuts	α_{22000}	23.8°
Screw angle after the test	α_{after}	23.5°



(a) *Screw before the test*

(b) *Screw after 22000 cuts*



(c) *Screw after the test*

Figure 5.27: Loosening of the screw during the wear test

values are reported in Table 5.5. There is a significant variation of the angle between the start and the end of the test ($\Delta\alpha = 0.9^\circ$). Also, the angle value after 22000 cuts is even larger than in the final case, but any variation lower than half a degree does not seem significative for the procedure followed to measure the angle.

So, in conclusion of this test, a wearing phenomenon is found after 30000 blank cuts and it is connected to a loosening of the scissors screw. Even so, when manually operated the scissors still presented a very good behavior and thus a longer test would be required to reach its limit.

Ring lock scissors for nails

A second test is performed on a different type of scissors: this one does not have a screw to keep the two blades together, instead there is the so-called Ring Lock[®] system, patented by Premax and depicted in Figure 5.28. This system was designed to replace the screw that connects the two blades



Figure 5.28: Ring lock system

and eliminate its influence. The characteristics of this test are the same as the previous case:

- Completely new scissors.
- 30000 cutting cycle analyzed.
- Tension applied to the material of $1.96 N$.
- Trapezoidal (symmetric) motion law for scissors opening and closure ($\theta = 50^\circ$, $v = 10 rpm$, $a = 164 rpm/s$, $d = -164 rpm/s$) for the cuts on cloth.

- ($\theta = 50^\circ$, $v = 60 \text{ rpm}$, $a = 164 \text{ rpm/s}$, $d = -164 \text{ rpm/s}$) for the blank cuts.

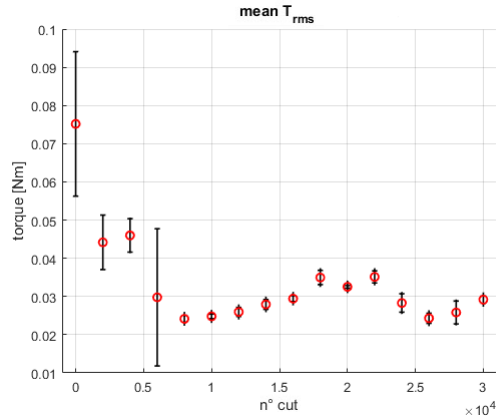


Figure 5.29: Test 2, type of closure alternated

In Figure 5.29 the results of this test are depicted. The first three distribution should not be considered since for two times there the pc crashed during the execution and the second time the third element of the Oldham coupling was broken.

Analyzing the remaining part of the test, an oscillation is found. This oscillation may be caused by the progressive deterioration of the surface of the blades close to their edge (Figure 5.30²).

These oscillations do not present a deterministic trend. Furthermore their magnitude in the considerable part of the history ($0.012 \text{ Nm} < 0.030 \text{ Nm}$) and the percental relevance on the maximum value of the acquisition ($30\% < 42.3\%$) are much smaller than in the previous case.

So it can be concluded that in this second case, no appreciable wearing effect is found after 30000 cycles.

²The two blades are of different scissors since there is no picture of the tested blades before the test. The picture have just an explicative intent.

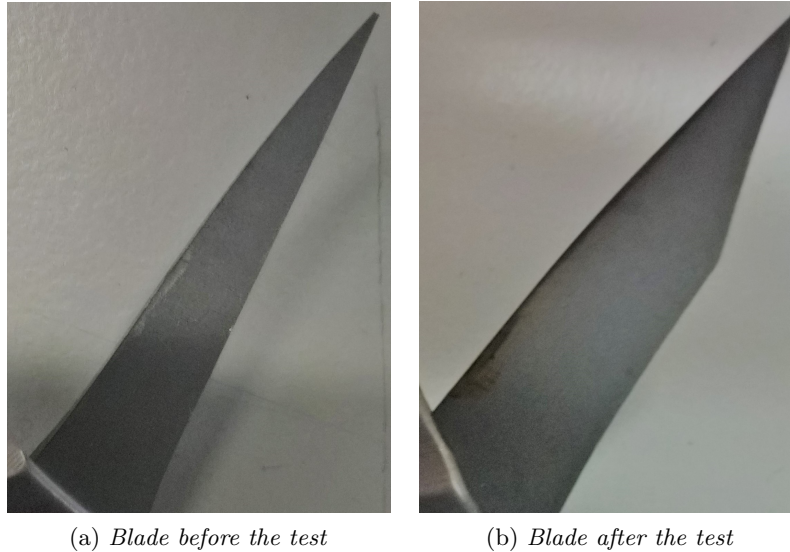


Figure 5.30: Variation of the surface of the blade during the test

Traditional scissors for paper

The same test as before is repeated on two pair of scissors for paper. If in the past two tests scissors of high quality were used, this time much cheaper one are adopted: lowering the quality a shorter life is expected and thus an higher influence of the wear.

The test characteristics remains the same of the previous test:

- Completely new scissors.
- 30000 cutting cycle analyzed.
- Tension applied to the material of 1.96 N .
- Trapezoidal (symmetric) motion law for scissors opening and closure ($\theta = 50^\circ$, $v = 10\text{ rpm}$, $a = 164\text{ rpm/s}$, $d = -164\text{ rpm/s}$) cuts on cloth.
- ($\theta = 50^\circ$, $v = 60\text{ rpm}$, $a = 164\text{ rpm/s}$, $d = -164\text{ rpm/s}$) blank cuts.

The results obtained are shown in Figure 5.31. There is an initial step between the first series of cuts on cloth and the series after 2000 cuts. This

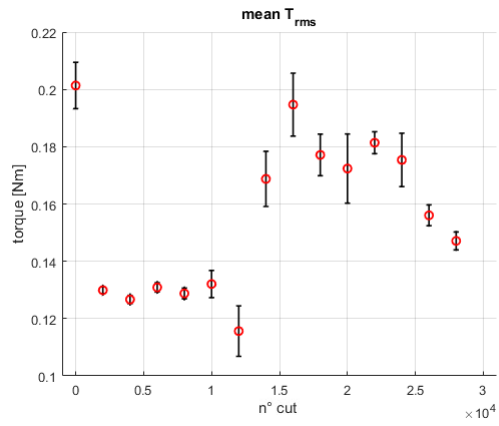


Figure 5.31: Test 3, type of closure alternated

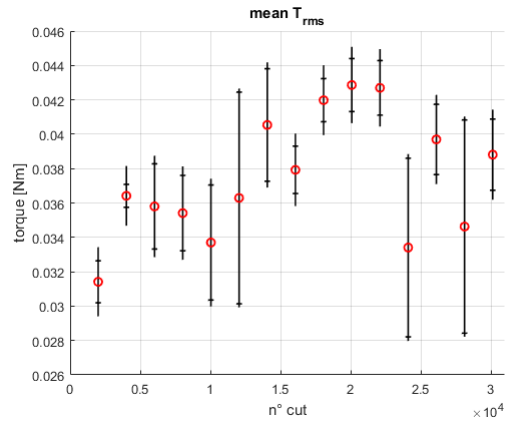


Figure 5.32: Test 4, type of closure alternated

can reasonably be associated to an initial stabilization of the scissors performances.

Then it can be observed an increase of the cutting torque until 22000-24000 cuts. The increasing of about $0.07 Nm$ can be justified by the aging of the scissors which could cause in this case not a problem of loosening of the pivot-bolt, but a reduction in the cutting capability with the subsequent generation of a hard closure and blocking phenomenon (this kind of problem was already introduced in 1.3.2).

Then the torque starts to decrease: this may be caused by a predominance of the process of loosening of the screw.

The same kind of analysis could be done for the similar case of Figure 5.32. The test is performed under the same conditions and gives the same indication. The main difference is the size of the scissors in the two cases: in the second case the torque values are much lower and thus the noise on the distribution is percentually much higher.

At the end of these tests it can be stated that for scissors of lower quality the two known aging mechanism acting on scissors are superimposed and they dominate visibly only in turn: at first there is a predominance of the hard closure mechanism that is replaced by the soft closure as predominant phenomenon at around 22000 cuts.

Chapter 6

Conclusion

As conclusion of this project a brief recap of the work done and described in the previous chapters is added. Also, a series of possible future developments are stated.

6.1 Recap of the work

This project started from the need of an investigation of the behavior of a widely spread tool like the scissors. This tool has everyday applications in many fields and working environments, but there is not a systematic analysis of its characteristics or a recognized way of comparing similar tools.

For this reason, this project started with the analysis of the knife case where this analysis has been done and it converged in the redaction of a norm. This norm, testing machines for knives and a literature review were analyzed. Also, the machines able to test scissors present on the market were analyzed and their limitations investigated.

At this point the actual project started with the design of a system able to overcome the limitations found in the existing machines and exploiting some knowledge already established on the field by the Premax union. The system was designed to be as flexible as possible with respect to the geometry of the tested tool and, at the same time, as reliable as possible.

For the design of the machine scientific literature and analytical tools were used to make the set-up as functional and apt to the task as possible, trying

at the same time to avoid any useless over-complication that would not have increased the performances of the machine.

In the development of the software, a trade-off between easiness of use for the final operator and completeness of the tool has been looked for.

In the second phase of the project, an experimental campaign was performed to validate the system and analyze the influence of process parameters on the cutting torque.

In the validation phase the repeatability and reproducibility of the system were quantified in different operative condition (consecutive cuts and cuts with re-positioning of the target material) and the results were satisfactory for a prototype.

The influence of process parameters was investigated both for assessing similarities between scissors and knives, but also for further testing the machine performances. The parameters analyzed and the synthetic results were:

- Pre-tension of the target material, its influence on the cutting torque was proved to be negligible in the scissors case.
- Maximum velocity reached during the cutting operation, whose influence was once again negligible with a result in accordance with the knife case.
- Influence of a nick on the blade, that generates a pick in the cutting torque in the cuts immediately after its generation and causes an increase of the maximum force over the following cutting cycles. This result was in accordance with tests performed on knives too.
- Wear of high quality scissors, it turned out that traditional scissors tend to deteriorate following the “Soft closure” mechanism exclusively, while on scissors with the Ring Lock[®] system neither “Soft closure” nor “Hard closure” is appreciable in the first 30000 cuts.
- Wear of low quality scissors, here both deteriorating phenomena have been observed, in particular until around 22000 cycles the “Hard closure mechanism dominates, while between 22000 and 30000 “Soft closure is more important.

6.2 Future development

This project was a first step in the systematic analysis of the characteristics and behavior of scissors. The experimental campaign was only aimed at validating the system and at making a first analysis of relevant process parameters. This could be seen as a first step for the creation of a norm for the testing of scissors not so different from the knife case. To reach this objective a larger experimental campaign should be performed to fully characterize the dulling mechanism of scissors for any geometry of the tool and for longer testing procedures.

Also, the prototype could be improved by adding some functional groups, starting from the concept delineated in this paper: the realization of the improved material feeding functional group and the realization of the tear cut and hand pressure mechanisms could increase the performances and flexibility of the system.

Bibliography

- [1] Jacques Marsot, Laurent Claudon, and Marc Jacqmin. Assessment of knife sharpness by means of a cutting force measuring system. *Applied Ergonomics*, 38(1):83–89, 2007.
- [2] G.A. Reilly, B.A.O. McCormack, and D. Taylor. Cutting sharpness measurement: a critical review. *Journal of Materials Processing Technology*, 153-154(Supplement C):261–267, 2004. Proceedings of the International Conference in Advances in Materials and Processing Technologies.
- [3] Turcot D. Daigle R. Lara, J. and J. Boutin. A new test method to evaluate the cut resistance of glove materials. *Performance of Protective Clothing*, V(1):23–31, 1996.
- [4] Raymond W. McGorry, Peter C. Dowd, and Patrick G. Dempsey. A technique for field measurement of knife sharpness. *Applied Ergonomics*, 36(5):635–640, 2005.
- [5] RR Bishu, C Calkins, X Lei, and A Chin. Effect of knife type and sharpness on cutting forces. *Adv Occupat Ergon Safety*, 2:479–83, 1996.
- [6] Ben Balevi. Engineering specifics of the periodontal curet’s cutting edge. *Journal of periodontology*, 67(4):374–378, 1996.
- [7] S Kaldor and PK Venuvinod. Macro-level optimization of cutting tool geometry. *Journal of manufacturing science and engineering*, 119:1, 1997.

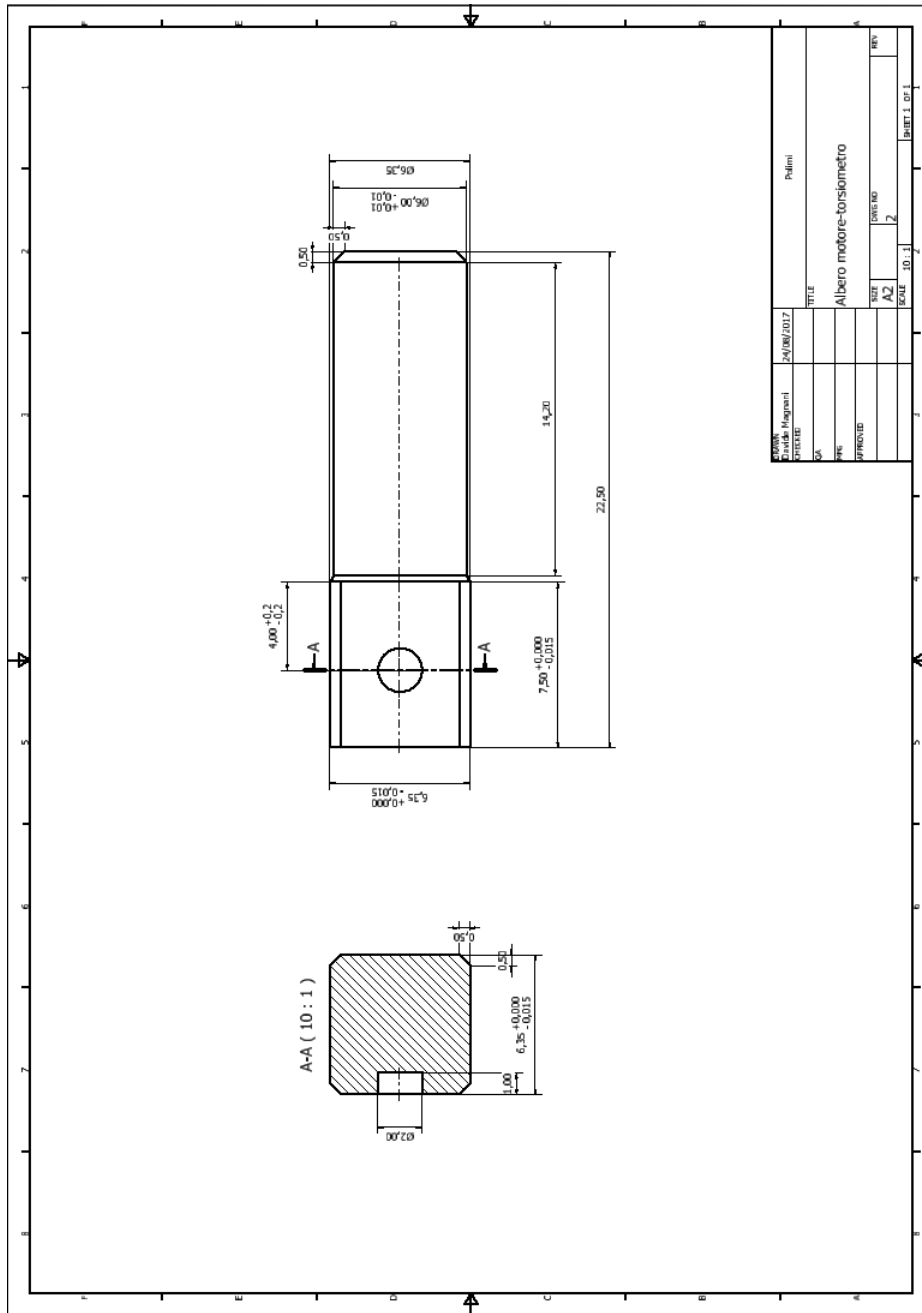
- [8] R Komanduri, N Chandrasekaran, and LM Raff. Effect of tool geometry in nanometric cutting: a molecular dynamics simulation approach. *Wear*, 219(1):84–97, 1998.
- [9] Raymond W McGorry, Peter C Dowd, and Patrick G Dempsey. Cutting moments and grip forces in meat cutting operations and the effect of knife sharpness. *Applied ergonomics*, 34(4):375–382, 2003.
- [10] International Organization for Standardization. *ISO 8442: Materials and articles in contact with foodstuffs Cutlery and hollowware part 5: specification for sharpness and edge retention test of cutlery*, 2004.
- [11] CATRA (Cutlery & Allied Trades Research Association). [27] knife and blade cutting test machine, <http://www.catra.org/pages/products/kniveslevel1/slt.htm>, 2017.
- [12] Haida International Equipment CO. Knife sharpness performance test machine, <http://www.haidatestequipment.com/products/knives-sharpness-test-equipment.htm>, 2017.
- [13] W. NEWELL and D.S. Vogel. Testing device and method for testing scissors, <https://www.google.com/patents/us20130186190>, July 25 2013. US Patent App. 13/742,642.
- [14] CATRA (Cutlery & Allied Trades Research Association). Scissors cutting performance test machine, <http://www.catra.org/pages/products/sissors/stm.htm>, 2017.
- [15] GE Smith and NP Clark. Evaluation of hand instruments used in operative dentistry: hardness and sharpness. *Operative dentistry*, 14(1):12–19, 1989.
- [16] JG Vincent and J Doting. From flintstone to diamond blade: a new multifunctional instrument for use in coronary surgery. *European journal of cardio-thoracic surgery*, 3(4):373–375, 1989.
- [17] Junsuke Akura, Taisaku Funakoshi, Kazuaki Kadonosono, and Masahiko Saito. Differences in incision shape based on the keratome bevel. *Journal of Cataract & Refractive Surgery*, 27(5):761–765, 2001.

- [18] H Tal, A Kozlovsky, E Green, and M Gabbay. Scanning electron microscope evaluation of wear of stainless steel and high carbon steel currettes. *Journal of periodontology*, 60(6):320–324, 1989.
- [19] Hyung-Seop Shin, DC Erlich, and DA Shockey. Test for measuring cut resistance of yarns. *Journal of materials science*, 38(17):3603–3610, 2003.
- [20] British Standard Insitute. *EN ISO 13997 Protective Gloves Against Mechanical Risks*, 1999.
- [21] Hermes Giberti, Simone Cinquemani, and Giovanni Legnani. A practical approach to the selection of the motor-reducer unit in electric drive systems. *Mechanics based design of structures and machines*, 39(3):303–319, 2011.
- [22] Serope Kalpakjian, Steven R Schmid, and Stefania Bruschi. *Tecnologia meccanica*. Pearson, 2014.
- [23] Herman J Van de Straete, Pascal Degezelle, Joris De Schutter, and Ronnie JM Belmans. Servo motor selection criterion for mechatronic applications. *IEEE/ASME Transactions on mechatronics*, 3(1):43–50, 1998.
- [24] Gustav Niemann, Hans Winter, and Bernd-Robert Höhn. *Manuale degli organi delle macchine*. Tecniche Nuove, 2006.
- [25] Ernest O Doebelin, Alfredo Cigada, Alfredo Cigala, and Michele Gasparetto. *Strumenti e metodi di misura*. McGraw-Hill, 2008.
- [26] Paolo Bolzern, Riccardo Scattolini, and Nicola Schiavoni. *Fondamenti di controlli automatici*. McGraw-Hill Libri Italia, 1998.
- [27] LAM technologies electric equipments. Stepper motors, <http://www.motoripassopasso.it/motoripassopassocosasono.aspx>, 2018.

Appendix A

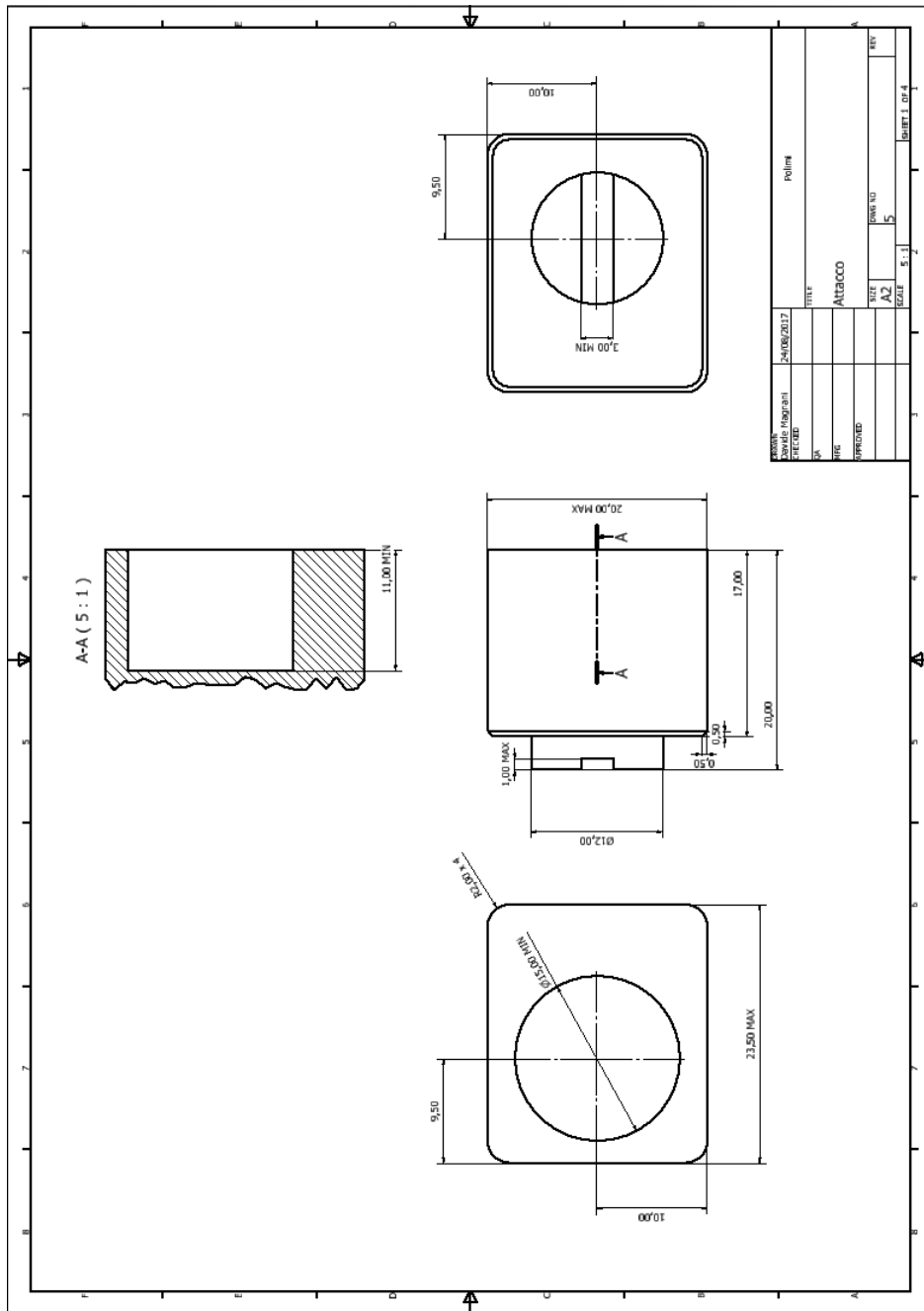
Drawings

In this Appendix, the technical drawings of the parts designed for the realization of the machine are reported. The picture were realized to be show in an A2 paper, thus the scale there reported is not the actual one.

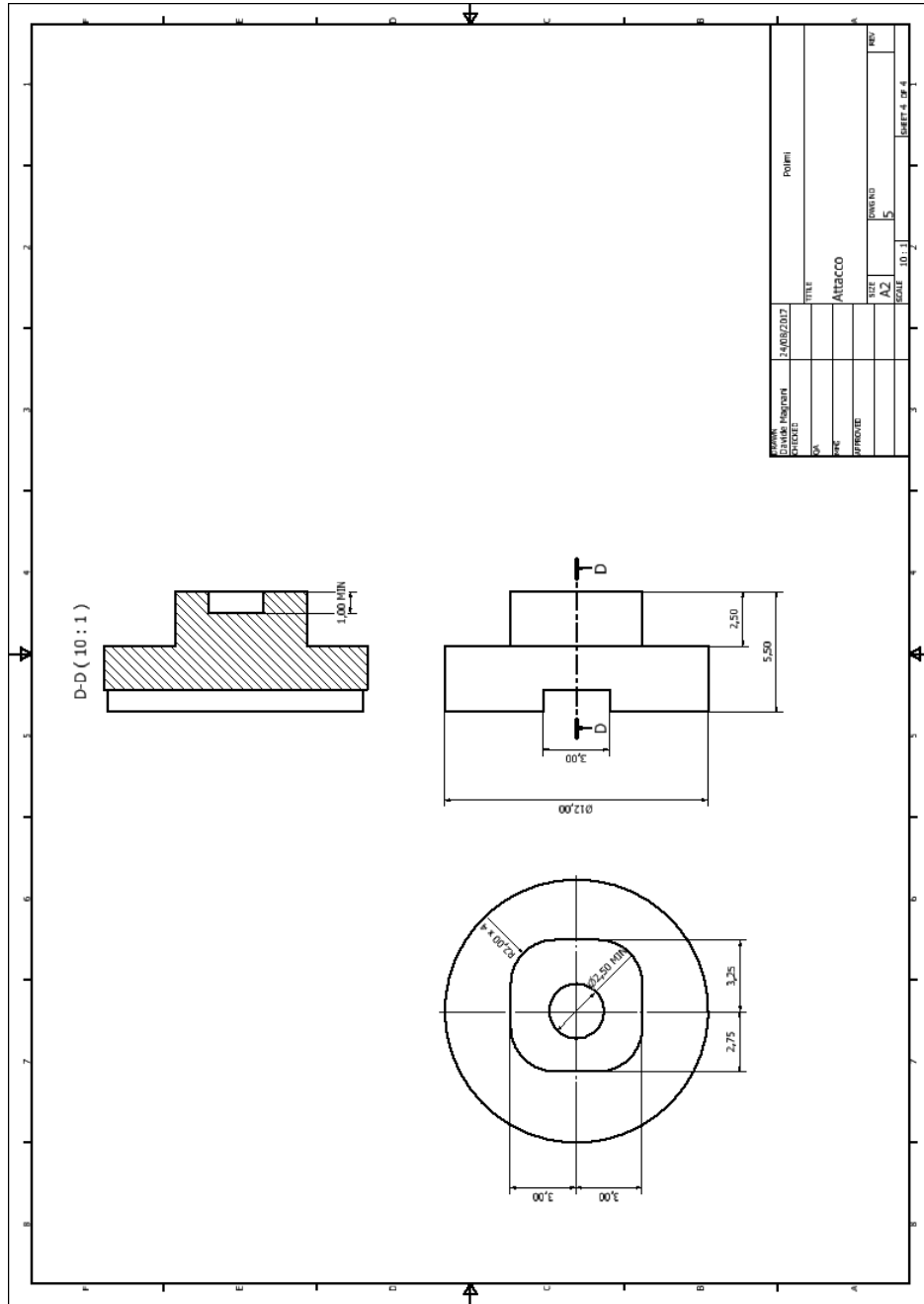


DATE	24/06/2017	TITLE	Palini
DESIGNER	Enrico Reggiani	PROJ. NO.	
CHK.	SA	APP. NO.	Albero motore-torsiometro
APPROVED		SCALE	1:1
		REV.	2
		REV.	

Shaft connecting the motor to the torsionmeter



Final element of the Oldham coupling: 1



Final element of the Oldham coupling: 4

Appendix B

Check with second motion law

In this Appendix, the data of the harsher law used during the selection of the motor is described (in the two tables) and the same graphs as in section 2.1.2 are reported. All the checks are passed and all the graphs are compliant with the performance required.

Harsher motion law parameters

Dimension	Symbol	Value
Total rise	h	40°
Forward motion time	t_1	0.5 s
Backward motion time	t_2	0.5 s
Resting time	t_r	0 s

$$\alpha = 818.18 \geq \beta = 13.02 \text{ W/s}$$

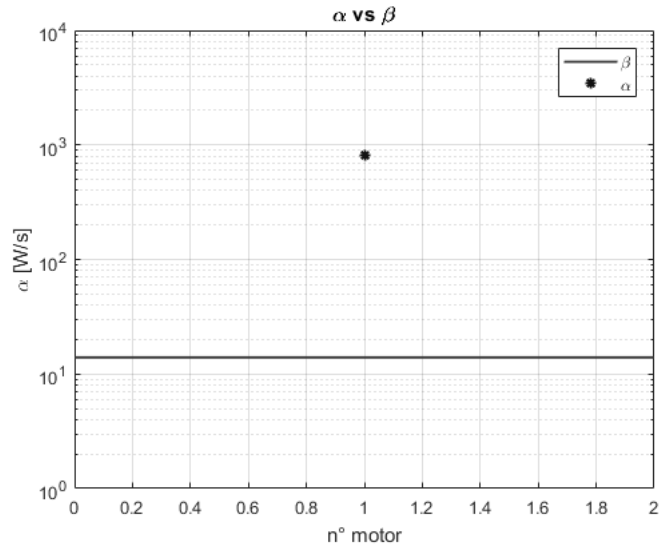
$$\tau_{max} = 0.053 \geq \tau = 0.0041 \geq \max(\tau_{min} = 0.0004; \tau_{M,lim} = 0.004)$$

Final checks

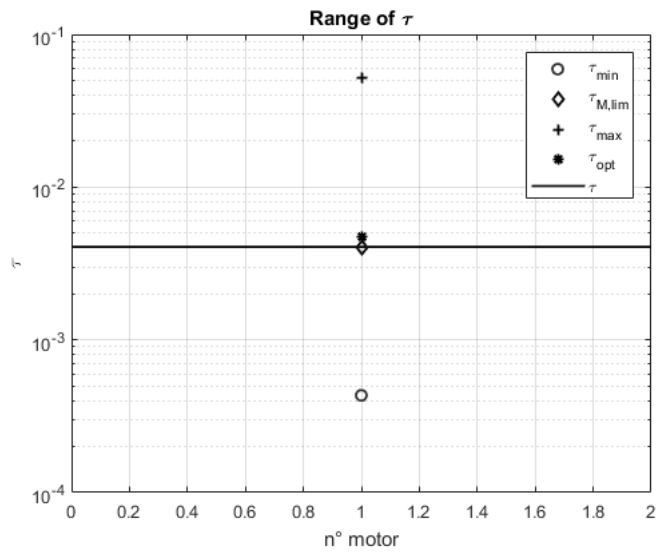
$$T_{M,N}^2 = 900 \geq T_{M,rms}^2 = 19.36 \text{ mN}^2\text{m}^2$$

Harsher motion law, symbols used

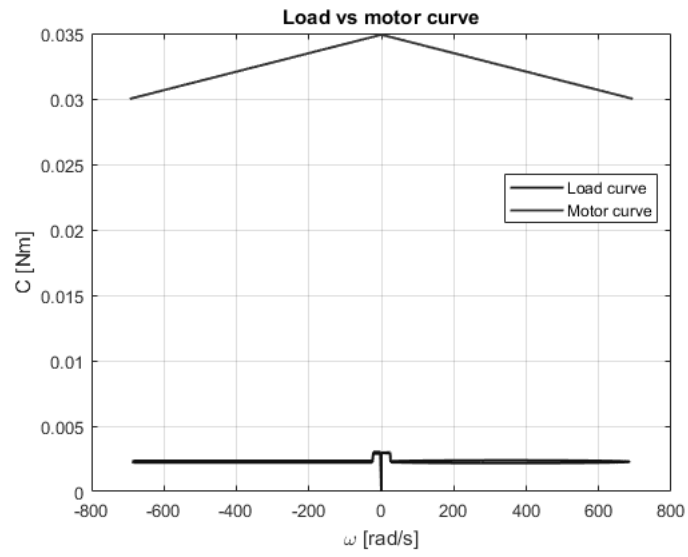
Dimension	Symbol	Value
Accelerating factor	α	818.18 W/s
Load factor	β	13.02 W/s
Transmission moment of inertia	J_T	0.7 gcm^2
Motor moment of inertia	J_M	11 gcm^2
Cycle time	t_a	1 s
Generalized load torque	T_L^*	Function of time
Generalized load root mean square torque	$T_{L,rms}^*$	566.6 mNm
Motor nominal torque	$T_{M,N}$	30 mNm
Motor root mean square torque	$T_{M,rms}$	4.4 mNm
Transmission mechanical efficiency	η	0.6
Transmission ratio of the speed reducer	τ	0.0041
Maximum acceptable transmission ratio	τ_{max}	0.053
Minimum acceptable transmission ratio	τ_{min}	0.0004
Minimum kinematic transmission ratio	$\tau_{M,lim}$	0.004
Optimal transmission ratio	τ_{opt}	0.005
Load angular acceleration	$\dot{\omega}_L$	Function of time
Maximum speed achieved by the load	$\omega_{L,max}$	26.67 rpm
Load root mean square acceleration	$\dot{\omega}_{L,rms}$	106.61 rpm/s
Maximum speed achieved by the motor	$\omega_{M,max}$	6630 rpm



α vs β for the final selected motor



Range of τ admissible and final selected transmission



Check 1, maximum torque supplied

$$T_{L,max} = 0.745 < T_{T,max} = 6 Nm$$